

UC Santa Barbara

UC Santa Barbara Electronic Theses and Dissertations

Title

Unraveling the causes and consequences of dynamic species interactions in California kelp forests

Permalink

<https://escholarship.org/uc/item/9tc5n7fv>

Author

DiFiore, Bartholomew P

Publication Date

2023

Peer reviewed|Thesis/dissertation

UNIVERSITY OF CALIFORNIA

Santa Barbara

Unraveling the causes and consequences of dynamic species interactions in California kelp
forests

A dissertation submitted in partial satisfaction of the
requirements for the degree Doctor of Philosophy
in Ecology, Evolution, and Marine Biology

by

Bartholomew Paul DiFiore

Committee in charge:

Professor Adrian Stier, Chair

Professor Holly Moeller

Professor Erika Eliason

Dr. Daniel Reed, Research Biologist

Dr. Jameal Samhuri, NOAA NWFS

December, 2023

The dissertation of Bartholomew Paul DiFiore is approved.

Holly Moeller

Erika Eliason

Daniel Reed

Jameal Samhuri

Adrian Stier, Committee Chair

September, 2023

Unraveling the causes and consequences of dynamic species interactions in California kelp
forests

Copyright © 2023

by

Bartholomew Paul DiFiore

ACKNOWLEDGMENTS

I feel incredibly lucky to have so many mentors, friends, and family who have supporting me during my dissertation and beyond. Completing this undertaking wouldn't have been possible without all of you, and I will be forever grateful for your love, support, critiques, and guidance.

For research I've conducted at UCSB I am deeply indebted to my committee and to my advisor, Adrian Stier. Each of you, in your own way, has changed who I am as a scientist, and I can only hope to carry those lessons forward into the future.

Holly, I can't thank you enough for always getting excited about ideas, for the white board sessions, for always lending a supporting ear, and for always dragging me into the math despite my best protestations. You, more than anyone, have convinced the naïve field ecologist in me to appreciate the value of an equation.

Dan, I can't thank you enough for always reminding me that at its core any question in science, regardless of how general or theoretical, is a question about a critter and the system it lives in. You taught me the value of using precise language and avoiding vague generalities (Judging by a few parts of this dissertation...it's still a work in progress)—of paying close attention to my writing to ensure that what I'm saying is actually what I mean.

Erika, when I initially interviewed at UCSB I naively told you that I "wasn't into physiology". I'll always be grateful that you convinced me physiology was cool. You always kept me on my toes, and some of the most thought-provoking moments during my dissertation have come from working with you to reconcile why animals eat as much as they eat.

Jameal, I can't thank you enough for your patience, guidance, and help navigating my career after UCSB. I know that joining as an outside committee member was a huge challenge on your time. I'm so grateful for your astute edits, insightful questions, and for always reminding me of the big picture.

None of this work would have been possible without you, Adrian. You have served as a mentor, a friend, and have opened my mind to the science and art of ecology. I will always appreciate your support during the birth of my daughters, without it I would likely not have finished this dissertation. And I will always remember switching back and forth between discussing size-scaling relationships and changing diapers.

I have a very special place in my heart for all of my lab mates, including Kurt Ingeman, Megsie Siple, Emily Donham, Sam Csik, Joe Curis, An Bui, Kai Kopecky, Lily Zhao, and Nina Munk—and so many other graduate students at USCB (Emily Hardison, Sevan Esian, Krista Kraskura, Joey Peters, Raine Detmer, Ana Miller-ter Kuile, Kelly Speare, just to name a few). Over the years, each of you has supported me in more ways than you could know. You were always there to listen when I needed to vent, to entertain my crazy ideas, to smile and nod when I started ranting about Bayesian models, and to drink too much coffee (Kai...) or too much beer. Nothing about my decision to finish remotely made me more sad than not being able to spend more time with you all in person. I never would have finished this dissertation without your support.

I'm also indebted to so many mentors from outside of UCSB. Simon Queenborough and Liza Comita, thank you for entertaining my marine science dreams in a tropical forest ecology lab. Mary Beth Decker so many thanks for giving me a chance and sending me to Bering Sea to study jellyfish. Scootch Albers and Chugey Sepulveda, you sparked my

interest in being a marine ecologist so many years ago, and I'll be forever jealous of the positions you have down at PIER. Molly Lutcavage, your passion for bluefin tuna and determination to study them will always be an inspiration to me. Dan Brayton, you gave me the confidence to write, and always encouraged me to follow my heart, regardless of how winding the path. For that I will be forever grateful.

To Luke Schoel, Robert Porter, Nat Moody, Joe Sanfilippo, Bill Brown, Drew Dominick, Kyle Grant, Bob Morris, and all the other commercial fishermen who have taken me under their wing: You're some of the most astute scientists I've ever encountered, and I can't thank you enough for always reminding me why I'm doing this.

To McNiff: for always reminding me to not take life too seriously. While you can't be her to bring me a donut on that first day out of school, I'll be having one with you.

Finally, I can't express how thankful I am for my family. To my parents and my brother: you gave me roots and you gave me wings. You trusted me enough to let me mess about on boats since I was 4, to plant two acres of tomatoes and an acre of hot peppers without a clue what I was doing. You taught me to work, you taught me what grit was, and you taught me the capacity of bottomless love.

To my daughters: Marin and Thea, nothing has given me more joy than watching you come into this world and grow—watching you pick up seaweed, run through the sand, dig clams, and pick tomatoes from the garden naked. I have had a picture of you on the beach at Cross Creek next to the skiff while I wrote this dissertation to remind me why I'm doing it.

To my wife: Alison, you always joked that you were the least supportive academic partner. I beg to differ. No one has been more supportive. Thanks for sticking through this with me. It's been a long journey, but there is no one who I'd rather have at my side.

VITA OF BARTHOLOMEW PAUL DIFIORE
September, 2023

EDUCATION

- 2023 Ph.D. – Ecology, Evolution, and Marine Biology
 University of California, Santa Barbara
- 2017 M.E.Sc. – Yale School of the Environment
 Yale University
- 2010 B.A. – Biology and English (Double Major)
 Middlebury College

PUBLICATIONS

9. **DiFiore, B.P.** and A.C. Stier. 2023. Variation in body size drives spatial and temporal variation in lobster-urchin interaction strength. *Journal of Animal Ecology* 92: 1075-1088.
8. Csik, S., **B.P. DiFiore**, K. Kraskura, E. Hardison, J. Curtis, E. Eliason, and A.C. Stier. 2023. The metabolic underpinnings of temperature-dependent predation in a key marine predator. *Frontiers in Marine Science* 10:114.
7. Decker, M.B., R.D. Brodeur, L. Ciannelli, L.L. Britt, N.A. Bond, **B.P. DiFiore**, and G.L. Hunt. 2023. Cyclic variability of eastern Bering Sea jellyfish relates to regional physical conditions. *Progress in Oceanography* 210:102923.
6. Miller-ter Kuile, A., A. Apigo, A. Bui, K. Butner, J.N. Childress, S. Copeland, **B.P. DiFiore**, E.S. Forbes, M. Klope, C.I. Motta, D. Orr, K. A. Plummer, D.L. Preston, and H.S. Young. 2022. Changes in invertebrate food web structure between high- and low-productivity environments are driven by intermediate but not top predator diet shifts. *Biology Letters* 18:20220364.
5. Ingeman, K.E., L. Zhao, C. Wolf, D.R. Williams, A.L. Ritger, W.J. Ripple, K.L. Kopecky, E.M. Dillon, **B.P. DiFiore**, J.S. Curtis, S.R. Csik, A. Bui, A.C. Stier. 2022. Glimmers of hope in global apex predator recoveries. *Scientific Reports* 12:1-13.
4. Rennick, M.* †, **B. P. DiFiore***, J. Curtis, D. C. Reed, and A. C. Stier. 2022. Detrital supply suppresses deforestation to maintain healthy kelp forest ecosystems. *Ecology* 103:e3673. *co-lead author, †undergraduate mentee
3. Miller-ter Kuile, A., A. Apigo, A. Bui, **B. DiFiore**, E. S. Forbes, M. Lee, D. Orr, D. L. Preston, R. Behm, T. Bogar, J. Childress, R. Dirzo, M. Klope, K. D. Lafferty, J. McLaughlin, M. Morse, C. Motta, K. Park, K. Plummer, D. Weber, R. Young, and H. Young. 2022. Predator–prey interactions of terrestrial invertebrates are determined by

predator body size and species identity. *Ecology* e3634.

2. **DiFiore B.P.**, S. Queenborough, E. Madin, V. Paul, M. Decker, A. Stier. 2019. Grazing halos on coral reefs: predation risk, herbivore density, and habitat size influence grazing patterns that are visible from space. *Marine Ecology Progress Series* 627:71-81.
1. Heberer C., S.A. Aalbers, D. Bernal, S. Kohin, **B.P. DiFiore**, and C.A. Sepulveda. 2010. Insights into catch-and-release survivorship and stress-induced blood biochemistry of common thresher sharks (*Alopias vulpinus*) captured in the southern California recreational fishery. *Fisheries Research* 106:495-500.

Manuscripts in Submission/Review/Preparation (Drafts available upon request)

Cooper, S.D., S.W. Wiseman, **B.P. DiFiore**, and K. Klose. *In Revision*. Trout and invertebrate assemblages in stream pools through wildfire and drought. *Freshwater Biology*.

Bui, A., M. C. N. Castorani, **B.P. DiFiore**, L. Kui, R.J. Miller, J.C. Nelson, D.C. Reed, and A.C. Stier. *In prep*. Foundation species recovery does not necessarily lead to recovery of associated communities: results from long-term experimental manipulation. *Target journal: Ecology*.

Peters, J.R., **B.P. DiFore**, D.C. Reed, and D.E. Burkepile. *In prep*. Fishing spiny lobsters disrupts important hotspots of nitrogen for benthic macroalgae. *Target journal: Ecosystems*.

Esaian, S., A. Bui, K. Husted, **B.P. DiFore**, J.R. Peters, L. Wilbanks, and H. Moeller. *In prep*. Giant kelp microbiome community compositions shift from stochastic to depth specialized as host blades mature. *Target journal: Environmental Microbiology*.

FELLOWSHIPS AND AWARDS

2023	Charles A. Storke Graduate Fellowship
2017	National Science Foundation Graduate Research Fellowship Chancellor's Fellowship – University of California, Santa Barbara
2015	Yale School of Forestry and Environmental Studies Tuition Award
2011	Middlebury Fellowship in Environmental Journalism
2009	Ronald H. Brown '62 Award

Grants in Support of Research

2023	UCSB EEMB Block Grant (\$1650)
2018	Lerner-Gray Award (\$2451) – American Museum of Natural History UCSB EEMB Block Grant (\$900)
2016	Link Foundation / Smithsonian Graduate Research Fellowship (\$6500) Tropical Resources Institute Fellowship (\$6000) – Yale F&ES

2015 Carpenter Sperry Fund (\$1500) – Yale F&ES
DigitalGlobe Foundation Imagery Grant – DigitalGlobe Foundation
David Schiff Fund (\$6000) – Yale

PROFESSIONAL EMPLOYMENT

2017 – 2023 Graduate student researcher. National Science Foundation, GRFP Fellow.
University of California, Santa Barbara

2018 – 2023 Graduate student researcher. Santa Barbara Coastal Long-term Ecological
Monitoring program

2022 – 2023 Research contractor. University of Massachusetts, Amherst. Gloucester
Marine Station

2020 Teaching assistant. Field methods in aquatic ecology & Macroevolution.
University of California, Santa Barbara

2019 – 2023 Captain and scientific diver. University of California, Santa Barbara

2016 Teaching assistant. Biological Oceanography. Yale University

2016 Research assistant. Yale University w/ Dr. Mary Beth Decker

2012 Researcher/Crew. Plastics at SEA: North Pacific Expedition. Sea Education
Association

2012 Lab technician. Large Pelagics Research Center. University of Massachusetts,
Boston

2009 Intern. Pflieger Institute of Environmental Research. San Diego, CA

ABSTRACT

Unraveling the causes and consequences of dynamic species interactions in California kelp forests

by

Bartholomew Paul DiFiore

The strength of species interactions shapes the structure and function of ecological communities, with profound implications on the ecosystem services these communities provide, such as maintenance of biodiversity, carbon sequestration, cultural heritage, and viable food production. However, we, as humans, are altering the strength, direction, and variability in species interactions through global climate change, habitat loss, and harvest. By altering how species interact, these anthropogenic impacts are shifting both consumptive and non-consumptive ecosystem services. Therefore, understanding why species interactions are changing and what the consequences of these changes are on ecological communities is an important component of effectively managing ecosystems in a dynamic future. In this dissertation, I explore two different mechanisms that underscore variation in species interactions across space and through time: variability in body size among individual predators and their prey and contingencies associated with historic population fluctuations in a marine foundation species.

In **Chapter 1**, I combined mesocosm experiments and long-term ecological data to test to what extent individual variation in predator body size, prey body size, and prey density drove spatiotemporal variation in interaction strength. I then tested the efficacy of established body size-scaling relationships at predicting variation in interaction strength. My

results demonstrate that the majority of variation in how strongly California spiny lobster (*Panulirus interruptus*) interact with their purple sea urchin (*Strongylocentrotus purpuratus*) prey can be attributed to variation in body size. Furthermore, utilizing established size-scaling relationships from the literature failed to accurately predict our experimental estimates of interaction strength by more than an order of magnitude.

In **Chapter 2**, I sought to uncover the physiological mechanisms driving the relation between a predator's body size and its consumption rate. Specifically, I tested between alternative theoretical hypotheses for the relationship between an animal's size, metabolism, and consumption rate to better understand the connection between a predator's ecology and physiology. Contrary to prevailing theoretical expectations, I demonstrate that larger lobster can consume disproportionately more than smaller conspecifics, despite declining metabolic requirements, which could have implications on how body size is incorporating into models of community and ecosystem dynamics.

Finally, in **Chapter 3**, I examine how historic variability in the foundation species, *Macrocystis pyrifera*, alters non-trophic interactions between functional groups on the seafloor. My results suggest that, while the current biomass of *M. pyrifera* has the strongest impact, metrics of historic variability in the foundation species have strong effects on benthic community structure that ameliorate with time.

A pressing issue in managing ecosystems is understanding what causes variation in how strongly species interact, what the implications of this variation are for communities, and how to predict shift in species interactions in the future. My research suggests that incorporating historical contingencies and individual variation in body size could bolster

management and restoration efforts that aim to increase the resilience of marine communities in a dynamic future.

TABLE OF CONTENTS

1. INTRODUCTION	1
1.1. Motivation and Objectives.....	1
1.2. The role of body size in driving variation in interaction strength.....	3
1.3. References.....	8
2. Chapter 1	15
2.1. Abstract.....	15
2.2. Introduction.....	16
2.3. Methods.....	19
2.4. Results.....	26
2.5. Discussion.....	29
2.6. References.....	36
2.7. Figures and Figure Captions.....	44
3. Chapter 2	49
3.1. Abstract.....	49
3.2. Introduction.....	50
3.3. Methods.....	54
3.4. Results.....	60
3.5. Discussion.....	61
3.6. References.....	67
3.7. Figures and Figure Captions.....	73
4. Chapter 3	78
4.1. Abstract.....	78
4.2. Introduction.....	79
4.3. Methods.....	82
4.4. Results.....	88
4.5. Discussion.....	92
4.6. References.....	98
4.7. Figures and Figure Captions.....	105
5. Conclusions	110
6. Appendices	112
6.1. Chapter 1 – Appendix.....	112
6.2. Chapter 2 – Appendix.....	131
6.3. Chapter 3 – Appendix.....	139

LIST OF FIGURES

Chapter 1

Figure 1.1. Conceptual diagram.....	44
Figure 1.2. Size-dependent functional response of lobster foraging on urchin.....	45
Figure 1.3. Size-scaling of functional response parameters.....	46
Figure 1.4. Spatiotemporal variation in predicted lobster-urchin interactions.....	47
Figure 1.5. Variance-partitioning and comparison with general estimates.....	48

Chapter 2

Figure 2.1. Conceptual diagram.....	73
Figure 2.2. Size-dependent functional response of lobster foraging on mussel.....	75
Figure 2.3. Scaling of whole-animal metabolism and consumption with body size.....	76
Figure 2.4. Mass-specific scaling of metabolism and consumption.....	77

Chapter 3

Figure 3.1. Conceptual diagram.....	105
Figure 3.2. Theoretical simulation results.....	106
Figure 3.3. Spatiotemporal variation in kelp dynamics.....	107
Figure 3.4. Responses of benthic community.....	108
Figure 3.5. Species-level responses to historic kelp variability metrics.....	109

Appendices

Figure S1.1. Lobster-urchin body mass ratio.....	123
Figure S1.2. Individual functional responses of lobster foraging on urchin.....	124
Figure S1.3. Prior and posterior comparison.....	125
Figure S1.4. Effects of density and body mass ratio on interaction strength.....	126
Figure S1.5. Rank order predictions of interaction strength across sites and years.....	127
Figure S1.6. Simulations with multiple sources of uncertainty.....	128
Figure S2.1. Size-scaling of functional response parameters.....	135
Figure S2.2. Individual functional responses of lobster foraging on mussels.....	136
Figure S2.3. Whole-animal SMR, MMR, FAS, and AAS size scaling.....	137
Figure S3.1. Theoretical simulation of different life-history parameters.....	146

LIST OF TABLES

Table S1.1. Prior distribution summary.....	115
Table S1.2. Summary of literature-based estimates.....	121
Table S1.3. Summary of parameter estimates from the literature.....	122
Table S2.1. Prior distribution summary for functional response model.....	132
Table S2.2. Prior distribution summary for metabolism model.....	133
Table S2.3. Model summary table.....	134
Table S3.1. Theoretical model parameters.....	142
Table S2.3. Summary of supplemental historic variability metrics.....	143-145

1. INTRODUCTION

1.1. Motivation and Objectives

Interactions between species, including trophic (e.g., predatory), competitive, or mutualistic interactions, can have widespread implications on the structure of ecological communities and the services they provide to people and nature (Oksanen et al. 1981, Paine 1992, Albrecht et al. 2014). However, anthropogenic drivers, such as climate change, habitat loss, and the harvest of wild populations, are changing the strength and direction of species interactions (Soudijn et al. 2021, Sandor et al. 2022, Smale et al. 2022), leading to the large-scale restructuring of both terrestrial and marine ecosystems (Frank et al. 2011, Lister and Garcia 2018). For instance, human-driven species introductions (Miller-ter Kuile et al. 2021), changes in species ranges (Urban et al. 2012, Kitchel and Pinsky 2023), shifts in species traits (Lindmark et al. 2019), and increases in disturbance to biogenic habitat (Castorani et al. 2018) can alter the identity of species in a community and how strongly those species interact. Faced with unprecedented environmental change, it can seem that species interactions are entirely context dependent (Lawton 1999, Chamberlain et al. 2014). However, understanding if general mechanisms underlie the seeming context-dependence of species interactions is key to predicting the repercussions of direct (e.g., harvest, species introductions) and indirect (e.g., climate change) human disturbances and implementing flexible management strategies that adapt with shifting environmental conditions (Poisot et al. 2015, Ingeman et al. 2019, Geary et al. 2020).

In this dissertation, I ask, “What are the causes and consequences of variation in species interactions?” using California kelp forests and their associated species as a study

system. Specifically, I explore two mechanisms that could cut through the context-dependency of species interactions.

The first mechanism that I explore is how variation in individual traits, like body size, can be used to predict the strength of interactions between a predator and its prey. Decades of theoretical and empirical research has focused on quantifying how the interaction strength varies across different species pairs (Berlow et al. 1999), leading to seminal advances in the understanding of community stability (Berlow 1999, Downing et al. 2020), the maintenance of biodiversity (Tilman 1994), and the consequence of species loss (Duffy et al. 2007). However, species are not static entities, and interactions occur between individuals that vary in physiological, behavioral, and ecological traits (Bolnick et al. 2011), causing any two species in a community to interact differently in different contexts (Poisot et al. 2015). Body size is a conspicuous trait of individuals that is strongly linked to an organism's metabolism (Brown et al. 2004), and thereby its ecological role as a consumer in an ecosystem (Peters 1983, Yodzis and Innes 1992). Yet, the relationships between an animal's body size, physiology, and ecology remain unclear (e.g., Lindmark et al. 2022). Uncovering the nature of these relationships could reveal physiological drivers of when and where two species interact strongly or weakly.

The second mechanism that I explore is how historical contingencies influence spatial variation in non-trophic interactions. An ecological community is not just the sum of current biotic interactions and abiotic conditions. Rather, interactions in the present can be influenced by historic events such as the previous presence of a competitor (Miller et al. 2009), the timing of species arrivals (Fukami 2015), or historic disturbances (Johnstone et al. 2016). Understanding how history informs species interactions in the present could offer

insight into predicting spatial and temporal variation in community structure and inform management that focuses on the restoration of ecosystem health and services.

To test the roles of body size and historic contingencies in driving variation in species interactions I used a combination of mesocosm experiments, theoretical models, and long-term observational data. Specifically, in **Chapter 1** I explore how prey density and the body size of predator and prey lead to variation in interaction strength across space and time. In **Chapter 2**, I test widely assumed theoretical relationships between a predator's physiology and ecology. The results challenge prevailing notions on the relationships between body size, physiology, and consumption by demonstrating that larger predators can consume disproportionately more than smaller conspecifics despite declining metabolic requirements. Finally, in **Chapter 3**, I explore how historic populations fluctuations in the foundation species, Giant kelp (*Macrocystis pyrifera*), alter competitive and facilitative interactions between benthic guilds long into the future.

1.2. The role of body size in driving variation in interaction strength

Ecologists have long understood that an animal's size is a critical driver of its role in an ecosystem (Brooks and Dodson 1965, Lindmark et al. 2019). After almost a century of research, it is clear that body size is linked to numerous ecological processes (Peters 1983). For instance, body size is correlated with how fast an animal grows (West et al. 2001), how far an animal migrates (Hein et al. 2012), how biomass is distributed across size classes in ecosystems (Sheldon et al. 1972, Heather et al. 2021), and the rate that populations grow (Savage et al. 2004) or decline (McCoy and Gillooly 2008). Critically, body size is correlated with the foraging ecology of consumers, providing a link between individual traits and community dynamics. Across taxa and ecosystems, predators tend to consume relatively

smaller prey (Barnes et al. 2010, Gravel et al. 2013, Brose et al. 2019), and the amount of prey that a predator consumes at a given prey density (e.g., the functional response; (Holling 1959) increases with the size of the predator (Rall et al. 2012). Understanding what underlies this powerful connection between body size and foraging ecology is critical to predicting the community-scale consequences of dynamic interactions caused by variation in body size.

The leading hypothesis for why predator foraging ecology scales with body size is grounded in the evidence that larger organisms have higher metabolic rates. While the exact exponent is widely debated (White et al. 2007), metabolic rate (b) increases as a power-law function of body mass (m)

$$b \propto m^\beta \quad (1)$$

where the scaling exponent (β) is remarkably consistent across taxa ($\beta \cong 0.6 - 0.8$; (Kleiber 1932, West et al. 1997, White and Seymour 2003, Glazier 2010). The metabolic theory of ecology (MTE) contends that most biological processes scale with body size at the same rate that metabolism scales with body size (Brown et al. 2004). In regard to foraging ecology, MTE suggests that the mechanism behind why larger animals eat more than smaller animals is larger animals have higher total metabolic rates and require more food to fuel basal metabolic requirements (Rall et al. 2012). Specifically, MTE predicts that because animals must balance energy acquisition (i.e., consumption, C) with demand (i.e., metabolism), how much an animal consumes scales with body size at the same rate that metabolism scales with body size:

$$C \propto m^\beta \quad (2)$$

The theory that body size can be used to approximate how much a predator eats has led to the development of dynamic food webs models grounded in the bioenergetic

requirements of individual consumers (e.g., Yodzis and Innes 1992, Weitz and Levin 2006, Kalinkat et al. 2013). In a foundational paper, Yodzis and Innes (1992) constructed a consumer-resource model, where they assumed that a predator's functional response scales with body size according to the metabolic scaling exponent. Yodzis and Innes (1992) and subsequent theoretical research (Andersen 2019), propose that animals allocate energy gained through foraging to cover basal metabolic requirements and the energy lost to foraging (i.e., maintenance costs). When the amount of energy acquired exceeds maintenance costs, surplus energy is converted to somatic (i.e., an increase in body size) or reproductive (i.e., higher fecundity) biomass, providing a link between individual bioenergetics, population demographic rates (i.e., per-capita growth/reproduction), and consumer-resource dynamics (i.e., the functional and numerical response). Therefore, there is a strong theoretical foundation for predicting how interacting populations will change through time based on the body size of individuals (Persson et al. 1998) or the average body size of species (DeLong et al. 2015).

The ability to estimate community dynamics based on metabolic-scaling relationships is a compelling strategy due to the challenges associated with estimating interaction strength in nature (Abrams 2001, Wootton and Emmerson 2005). The classic approach to estimate how strongly predator and prey interact involves mesocosm foraging experiments, where researchers manipulate the density of prey and other covariates. But mesocosm experiments are limited to small species due to logistical constraints (i.e., enclosure size) and may fail to approximate ecologically relevant estimates of interaction strength due to the complexity of natural systems (Bergström and Englund 2004, Bergström et al. 2006, Englund and Leonardsson 2008). Alternatively, researchers use intensive field observations to estimate

how predators' consumption rates change with prey availability, predator density, and environmental conditions (Novak 2010, 2013, Stier and White 2014, Preston et al. 2018, 2019), but such an approach may not be feasible for species of management or conservation concern if those species are highly migratory, or interactions cannot be directly observed. Finally, the effect of predator populations on their prey can be estimated through statistical analysis of time series data (Essington and Hansson 2004, Moustahfid et al. 2010), but this technique requires considerable data which may be costly to collect or not exist for species of interest.

Body size, one of the most commonly measured traits, offers a means of overcoming the challenges of estimating interaction strength, by allowing ecologists to predict predator consumption rates and, therefore, model community dynamics with few parameters (Pope et al. 2006). However, the power of using body size to predict interactions based on metabolic scaling exponents is dependent on the assumed relationships between consumption, metabolism and body size.

Recent syntheses of empirical studies reveal that the relationship between predators' functional responses and body size is far more complicated than would be predicted by simple metabolic scaling arguments (Rall et al. 2012, Uiterwaal and DeLong 2020). Across empirical studies, maximum consumption rates (i.e., consumption at saturating prey densities) increase with predator size and decrease with prey size, consistent with metabolic expectations, but the rate that consumption scales with body size varies considerably between taxa. For example, in what is likely one of the most comprehensive assessments, Uiterwaal and DeLong (2020) find that maximum consumption rates increase with body size at a rate between $[-1,1]$ for different taxa, after accounting for variation in prey size and other

covariates. Previous work has attributed variation in the consumption-size scaling relationship to variation in temperature (Englund et al. 2011), habitat dimensionality (i.e., 2-D vs. 3-D foraging environments, (Pawar et al. 2012, Barrios-O’Neill et al. 2016), or predator foraging mode (Barrios-O’Neill et al. 2019). However, no single predictor explains why the rate that consumption increases with body size is so variable, calling in to question the ability to predict consumption based on metabolic constraints.

Considering how challenging it is to estimate species interactions, bioenergetic consumer-resource models that assume metabolic scaling exponents are an appealing means to model the consequences of disturbances, like fisheries harvest, on ecosystems. Broadly, these stage- or size-structured models assume that mortality, growth, and reproduction are functions of body size (Blanchard et al. 2017), and have been used to understand the consequence of harvest on target populations (Andersen et al. 2009), communities (Claessen et al. 2009, Andersen et al. 2015), or whole ecosystems (Fulton et al. 2011, Heymans et al. 2016), a critical step in effectively implementing ecosystem-based management (Persson et al. 2014). However, these models often rely on metabolic exponents to parameterize the rate that consumption scales with body size (*but see* (Reum et al. 2019, Spence et al. 2021). Considering the substantial variation in the rate that consumption scales with body size, it is unclear to what extent size-structured models grounded in metabolic theory provide qualitative versus quantitative predictions for the consequences of harvest on community dynamics. Therefore, to advance ecologists’ capacity to use body size to make quantitative predictions of community dynamics, my dissertation:

- Determines how well consumption-size scaling relationships from the literature predict variation in interactions between a specific predator-prey pair across space and time (**Chapter 1**),
- Tests the widely held assumption that increases in a predator's metabolic demand with body size underlie the relationship between a predator's foraging ecology and body size (**Chapter 2**)

1.3. REFERENCES

- Abrams, P. A. 2001. Describing and Quantifying Interspecific Interactions: A Commentary on Recent Approaches. *Oikos* 94:209–218.
- Albrecht, J., D. Gertrud Berens, B. Jaroszewicz, N. Selva, R. Brandl, and N. Farwig. 2014. Correlated loss of ecosystem services in coupled mutualistic networks. *Nature Communications* 5:3810.
- ANDERSEN, K. H. 2019. Preface. Pages ix–x *Fish Ecology, Evolution, and Exploitation*. Princeton University Press.
- Andersen, K. H., K. D. Farnsworth, M. Pedersen, H. Gislason, and J. E. Beyer. 2009. How community ecology links natural mortality, growth, and production of fish populations. *ICES Journal of Marine Science* 66:1978–1984.
- Andersen, K. H., N. S. Jacobsen, and K. D. Farnsworth. 2015. The theoretical foundations for size spectrum models of fish communities. *Canadian Journal of Fisheries and Aquatic Sciences* 73:575–588.
- Barnes, C., D. Maxwell, D. C. Reuman, and S. Jennings. 2010. Global patterns in predator–prey size relationships reveal size dependency of trophic transfer efficiency. *Ecology* 91:222–232.
- Barrios-O'Neill, D., R. Kelly, J. T. A. Dick, A. Ricciardi, H. J. MacIsaac, and M. C. Emmerson. 2016. On the context-dependent scaling of consumer feeding rates. *Ecology Letters* 19:668–678.
- Barrios-O'Neill, D., R. Kelly, and M. C. Emmerson. 2019. Biomass encounter rates limit the size scaling of feeding interactions. *Ecology Letters* 22:1870–1878.
- Bergström, U., and G. Englund. 2004. Spatial scale, heterogeneity and functional responses. *Journal of Animal Ecology* 73:487–493.

- Bergström, U., G. Englund, and K. Leonardsson. 2006. Plugging space into predator-prey models: an empirical approach. *The American Naturalist* 167:246–259.
- Berlow, E. L. 1999. Strong effects of weak interactions in ecological communities. *Nature* 398:330–334.
- Berlow, E. L., S. A. Navarrete, C. J. Briggs, M. E. Power, and B. A. Menge. 1999. Quantifying Variation in the Strengths of Species Interactions. *Ecology* 80:2206–2224.
- Blanchard, J. L., R. F. Heneghan, J. D. Everett, R. Trebilco, and A. J. Richardson. 2017. From Bacteria to Whales: Using Functional Size Spectra to Model Marine Ecosystems. *Trends in Ecology & Evolution* 32:174–186.
- Bolnick, D. I., P. Amarasekare, M. S. Araújo, R. Bürger, J. M. Levine, M. Novak, V. H. W. Rudolf, S. J. Schreiber, M. C. Urban, and D. A. Vasseur. 2011. Why intraspecific trait variation matters in community ecology. *Trends in Ecology & Evolution* 26:183–192.
- Brooks, J. L., and S. I. Dodson. 1965. Predation, Body Size, and Composition of Plankton. *Science, New Series* 150:28–35.
- Brose, U., P. Archambault, A. D. Barnes, L.-F. Bersier, T. Boy, J. Canning-Clode, E. Conti, M. Dias, C. Digel, A. Dissanayake, A. A. V. Flores, K. Fussmann, B. Gauzens, C. Gray, J. Häussler, M. R. Hirt, U. Jacob, M. Jochum, S. Kéfi, O. McLaughlin, M. M. MacPherson, E. Latz, K. Layer-Dobra, P. Legagneux, Y. Li, C. Madeira, N. D. Martinez, V. Mendonça, C. Mulder, S. A. Navarrete, E. J. O’Gorman, D. Ott, J. Paula, D. Perkins, D. Piechnik, I. Pokrovsky, D. Raffaelli, B. C. Rall, B. Rosenbaum, R. Ryser, A. Silva, E. H. Sohlström, N. Sokolova, M. S. A. Thompson, R. M. Thompson, F. Vermandele, C. Vinagre, S. Wang, J. M. Wefer, R. J. Williams, E. Wieters, G. Woodward, and A. C. Iles. 2019. Predator traits determine food-web architecture across ecosystems. *Nature Ecology & Evolution* 3:919–927.
- Brown, J. H., J. F. Gillooly, A. P. Allen, V. M. Savage, and G. B. West. 2004. Toward a metabolic theory of ecology. *Ecology* 85:1771–1789.
- Castorani, M. C. N., D. C. Reed, and R. J. Miller. 2018. Loss of foundation species: disturbance frequency outweighs severity in structuring kelp forest communities. *Ecology* 99:2442–2454.
- Chamberlain, S. A., J. L. Bronstein, and J. A. Rudgers. 2014. How context dependent are species interactions? *Ecology Letters* 17:881–890.
- Claessen, D., A. S. de Vos, and A. M. de Roos. 2009. Bioenergetics, overcompensation, and the source–sink status of marine reserves. *Canadian Journal of Fisheries and Aquatic Sciences* 66:1059–1071.

- Downing, A. L., C. Jackson, C. Plunkett, J. A. Lockhart, S. M. Schlater, and M. A. Leibold. 2020. Temporal stability vs. community matrix measures of stability and the role of weak interactions. *Ecology Letters* 23:1468–1478.
- Duffy, J. E., B. J. Cardinale, K. E. France, P. B. McIntyre, E. Thébault, and M. Loreau. 2007. The functional role of biodiversity in ecosystems: incorporating trophic complexity. *Ecology Letters* 10:522–538.
- Englund, G., and K. Leonardsson. 2008. Scaling up the functional response for spatially heterogeneous systems. *Ecology Letters* 11:440–449.
- Englund, G., G. Öhlund, C. L. Hein, and S. Diehl. 2011. Temperature dependence of the functional response. *Ecology Letters* 14:914–921.
- Essington, T. E., and S. Hansson. 2004. Predator-dependent functional responses and interaction strengths in a natural food web. *Canadian Journal of Fisheries and Aquatic Sciences* 61:2215–2226.
- Frank, K. T., B. Petrie, J. A. D. Fisher, and W. C. Leggett. 2011. Transient dynamics of an altered large marine ecosystem. *Nature* 477:86–89.
- Fukami, T. 2015. Historical Contingency in Community Assembly: Integrating Niches, Species Pools, and Priority Effects. *Annual Review of Ecology, Evolution, and Systematics* 46:1–23.
- Fulton, E. A., J. S. Link, I. C. Kaplan, M. Savina-Rolland, P. Johnson, C. Ainsworth, P. Horne, R. Gorton, R. J. Gamble, A. D. M. Smith, and D. C. Smith. 2011. Lessons in modelling and management of marine ecosystems: the Atlantis experience. *Fish and Fisheries* 12:171–188.
- Geary, W. L., M. Bode, T. S. Doherty, E. A. Fulton, D. G. Nimmo, A. I. T. Tulloch, V. J. D. Tulloch, and E. G. Ritchie. 2020. A guide to ecosystem models and their environmental applications. *Nature Ecology & Evolution*.
- Glazier, D. S. 2010. A unifying explanation for diverse metabolic scaling in animals and plants. *Biological Reviews* 85:111–138.
- Gravel, D., T. Poisot, C. Albouy, L. Velez, and D. Mouillot. 2013. Inferring food web structure from predator–prey body size relationships. *Methods in Ecology and Evolution* 4:1083–1090.
- Heather, F. J., J. L. Blanchard, G. J. Edgar, R. Trebilco, and R. D. Stuart-Smith. 2021. Globally consistent reef size spectra integrating fishes and invertebrates. *Ecology Letters* 24:572–579.
- Hein, A. M., C. Hou, and J. F. Gillooly. 2012. Energetic and biomechanical constraints on animal migration distance. *Ecology Letters* 15:104–110.

- Heymans, J. J., M. Coll, J. S. Link, S. Mackinson, J. Steenbeek, C. Walters, and V. Christensen. 2016. Best practice in Ecopath with Ecosim food-web models for ecosystem-based management. *Ecological Modelling* 331:173–184.
- Holling, C. S. 1959. Some Characteristics of Simple Types of Predation and Parasitism I. *The Canadian Entomologist* 91:385–398.
- Ingeman, K. E., J. F. Samhouri, and A. C. Stier. 2019. Ocean recoveries for tomorrow's Earth: Hitting a moving target. *Science* 363.
- Johnstone, J. F., C. D. Allen, J. F. Franklin, L. E. Frelich, B. J. Harvey, P. E. Higuera, M. C. Mack, R. K. Meentemeyer, M. R. Metz, G. L. Perry, T. Schoennagel, and M. G. Turner. 2016. Changing disturbance regimes, ecological memory, and forest resilience. *Frontiers in Ecology and the Environment* 14:369–378.
- Kitchel, Z. J., and M. L. Pinsky. 2023. Regional species gains outpace losses across North American continental shelf regions. *Global Ecology and Biogeography* 32:1205–1217.
- Kleiber, M. 1932. Body size and metabolism. *Hilgardia* 6:315–353.
- Lawton, J. H. 1999. Are There General Laws in Ecology? *Oikos* 84:177–192.
- Lindmark, M., J. Ohlberger, and A. Gårdmark. 2022. Optimum growth temperature declines with body size within fish species. *Global Change Biology* 28:2259–2271.
- Lindmark, M., J. Ohlberger, M. Huss, and A. Gårdmark. 2019. Size-based ecological interactions drive food web responses to climate warming. *Ecology Letters* 22:778–786.
- Lister, B. C., and A. Garcia. 2018. Climate-driven declines in arthropod abundance restructure a rainforest food web. *Proceedings of the National Academy of Sciences* 115:E10397–E10406.
- McCoy, M. W., and J. F. Gilgooly. 2008. Predicting natural mortality rates of plants and animals. *Ecology Letters* 11:710–716.
- Miller, T. E., C. P. terHorst, and J. H. Burns. 2009. The Ghost of Competition Present. *The American Naturalist* 173:347–353.
- Miller-ter Kuile, A., D. Orr, A. Bui, R. Dirzo, M. Klope, D. McCauley, C. Motta, and H. Young. 2021. Impacts of rodent eradication on seed predation and plant community biomass on a tropical atoll. *Biotropica* 53:232–242.
- Moustahfid, H., M. C. Tyrrell, J. S. Link, J. A. Nye, B. E. Smith, and R. J. Gamble. 2010. Functional feeding responses of piscivorous fishes from the northeast US continental shelf. *Oecologia* 163:1059–1067.

- Novak, M. 2010. Estimating interaction strengths in nature: experimental support for an observational approach. *Ecology* 91:2394–2405.
- Novak, M. 2013. Trophic omnivory across a productivity gradient: intraguild predation theory and the structure and strength of species interactions. *Proceedings of the Royal Society B: Biological Sciences* 280:20131415.
- Oksanen, L., S. D. Fretwell, J. Arruda, and P. Niemela. 1981. Exploitation Ecosystems in Gradients of Primary Productivity. *The American Naturalist* 118:240–261.
- Paine, R. T. 1992. Food-web analysis through field measurement of per capita interaction strength. *Nature* 355:73–75.
- Pawar, S., A. I. Dell, and Van M. Savage. 2012. Dimensionality of consumer search space drives trophic interaction strengths. *Nature* 486:485–489.
- Persson, L., K. Leonardsson, A. M. de Roos, M. Gyllenberg, and B. Christensen. 1998. Ontogenetic Scaling of Foraging Rates and the Dynamics of a Size-Structured Consumer-Resource Model. *Theoretical Population Biology* 54:270–293.
- Persson, L., A. Van Leeuwen, and A. M. De Roos. 2014. The ecological foundation for ecosystem-based management of fisheries: mechanistic linkages between the individual-, population-, and community-level dynamics. *ICES Journal of Marine Science* 71:2268–2280.
- Peters, R. H. 1983. *The Ecological Implications of Body Size*. Cambridge University Press, Cambridge.
- Poisot, T., D. B. Stouffer, and D. Gravel. 2015. Beyond species: why ecological interaction networks vary through space and time. *Oikos* 124:243–251.
- Pope, J. G., J. C. Rice, N. Daan, S. Jennings, and H. Gislason. 2006. Modelling an exploited marine fish community with 15 parameters – results from a simple size-based model. *ICES Journal of Marine Science* 63:1029–1044.
- Preston, D. L., L. P. Falke, J. S. Henderson, and M. Novak. 2019. Food-web interaction strength distributions are conserved by greater variation between than within predator–prey pairs. *Ecology* 100:e02816.
- Preston, D. L., J. S. Henderson, L. P. Falke, L. M. Segui, T. J. Layden, and M. Novak. 2018. What drives interaction strengths in complex food webs? A test with feeding rates of a generalist stream predator. *Ecology* 99:1591–1601.
- Rall, B. C., U. Brose, M. Hartvig, G. Kalinkat, F. Schwarzmüller, O. Vucic-Pestic, and O. L. Petchey. 2012. Universal temperature and body-mass scaling of feeding rates. *Philosophical Transactions of the Royal Society B: Biological Sciences* 367:2923–2934.

- Reum, J. C. P., J. L. Blanchard, K. K. Holsman, K. Aydin, and A. E. Punt. 2019. Species-specific ontogenetic diet shifts attenuate trophic cascades and lengthen food chains in exploited ecosystems. *Oikos* 128:1051–1064.
- Sandor, M. E., C. S. Elphick, and M. W. Tingley. 2022. Extinction of biotic interactions due to habitat loss could accelerate the current biodiversity crisis. *Ecological Applications* 32:e2608.
- Savage, V. M., J. F. Gillooly, J. H. Brown, G. B. West, and E. L. Charnov. 2004. Effects of Body Size and Temperature on Population Growth. *The American Naturalist* 163:429–441.
- Sheldon, R. W., A. Prakash, and W. H. Sutcliffe. 1972. The Size Distribution of Particles in the Ocean. *Limnology and Oceanography* 17:327–340.
- Smale, D. A., H. Teagle, S. J. Hawkins, H. L. Jenkins, N. Frontier, C. Wilding, N. King, M. Jackson-Bu e, and P. J. Moore. 2022. Climate-driven substitution of foundation species causes breakdown of a facilitation cascade with potential implications for higher trophic levels. *Journal of Ecology* 110:2132–2144.
- Soudijn, F. H., P. D. van Denderen, M. Heino, U. Dieckmann, and A. M. de Roos. 2021. Harvesting forage fish can prevent fishing-induced population collapses of large piscivorous fish. *Proceedings of the National Academy of Sciences* 118.
- Spence, M. A., R. B. Thorpe, P. G. Blackwell, F. Scott, R. Southwell, and J. L. Blanchard. 2021. Quantifying uncertainty and dynamical changes in multi-species fishing mortality rates, catches and biomass by combining state-space and size-based multi-species models. *Fish and Fisheries* 00.
- Stier, A. C., and J. W. White. 2014. Predator density and the functional responses of coral reef fish. *Coral Reefs* 33:235–240.
- Tilman, D. 1994. Competition and Biodiversity in Spatially Structured Habitats. *Ecology* 75:2–16.
- Uiterwaal, S. F., and J. P. DeLong. 2020. Functional responses are maximized at intermediate temperatures. *Ecology* 101.
- Urban, M. C., J. J. Tewksbury, and K. S. Sheldon. 2012. On a collision course: competition and dispersal differences create no-analogue communities and cause extinctions during climate change. *Proceedings of the Royal Society B: Biological Sciences* 279:2072–2080.
- West, G. B., J. H. Brown, and B. J. Enquist. 1997. A General Model for the Origin of Allometric Scaling Laws in Biology. *Science* 276:122–126.
- West, G., J. Brown, and B. Enquist. 2001. A general model for ontogenetic growth. *Nature* 413:628–31.

- White, C. R., P. Cassey, and T. M. Blackburn. 2007. Allometric Exponents Do Not Support a Universal Metabolic Allometry. *Ecology* 88:315–323.
- White, C. R., and R. S. Seymour. 2003. Mammalian basal metabolic rate is proportional to body mass^{2/3}. *Proceedings of the National Academy of Sciences* 100:4046–4049.
- Wootton, J. T., and M. Emmerson. 2005. Measurement of Interaction Strength in Nature. *Annual Review of Ecology, Evolution, and Systematics* 36:419–444.
- Yodzis, P., and S. Innes. 1992. Body Size and Consumer-Resource Dynamics. *The American Naturalist* 139:1151–1175.

2. CHAPTER I

Variation in body size drives spatial and temporal variation in lobster-urchin interaction strength

2.1. ABSTRACT

How strongly predators and prey interact is both notoriously context dependent and difficult to measure. Yet across taxa, interaction strength is strongly related to predator size, prey size, and prey density, suggesting that general cross-taxonomic relationships could be used to predict how strongly individual species interact. Here, we ask how accurately do general size-scaling relationships predict variation in interaction strength between specific species that vary in size and density across space and time? To address this question, we quantified the size and density-dependence of the functional response of the California spiny lobster (*Panulirus interruptus*), foraging on a key ecosystem engineer, the purple sea urchin (*Strongylocentrotus purpuratus*), in experimental mesocosms. Based on these results, we then estimated variation in lobster-urchin interaction strength across five sites and nine years of observational data. Finally, we compared our experimental estimates to predictions based on general size-scaling relationships from the literature. Our results reveal that predator and prey body size has the greatest effect on interaction strength when prey abundance is high. Due to consistently high urchin densities in the field, our simulations suggest that body size—relative to density—accounted for up to 87% of the spatiotemporal variation in interaction strength. However, general size-scaling relationships failed to predict the magnitude of interactions between lobster and urchin; even the best prediction from the literature was, on average, an order of magnitude (+18.7x) different than our experimental predictions. Harvest and climate change are driving reductions in the average body size of

many marine species. Anticipating how reductions in body size will alter species interactions is critical to managing marine systems in an ecosystem context. Our results highlight the extent to which differences in size-frequency distributions can drive dramatic variation in the strength of interactions across narrow spatial and temporal scales. Furthermore, our work suggests that species-specific estimates for the scaling of interaction strength with body size, rather than general size-scaling relationships, are necessary to quantitatively predict how reductions in body size will alter interaction strengths.

2.2. INTRODUCTION

The complexity and context dependency of species interactions has led numerous ecologists to argue that prediction in community ecology is impossible (Lawton, 1999). Yet, across species from widely different taxonomic groups there is considerable evidence for general patterns relating individual traits, like body size, to the strength of species interactions (Brown et al., 2004). For instance, recent syntheses of empirical work demonstrate that across taxa, how much predators consume at a given prey density—one measure of interaction strength (Berlow et al. 2004)—is strongly correlated with predator and prey size (Rall et al. 2012, Uiterwaal and DeLong 2020). Yet despite the strength of general size-scaling relationships, it is unclear how accurately these relationships predict interactions between specific species, and if these predictions might disentangle complexity in community ecology (e.g., Poisot et al. 2015). In this paper, we present a case study testing if general cross-taxonomic patterns relating interaction strength with predator and prey body size predict how strongly a focal predator-prey pair interact. Understanding if general size-scaling relationships can be used to predict interactions between focal species would be

powerful, particularly for species of management or conservation concern, whose large size, rarity, or highly migratory behavior make empirical estimates of interactions challenging (Geary et al., 2020).

Ontogenetic increases in body size can drive variation in the strength of interactions (Persson et al., 1998). As an individual predator grows, the amount, size, and species of prey it consumes changes (Barnes et al., 2010; De Roos et al., 2003; Werner & Gilliam, 1984). Likewise, as an individual prey grows, its risk of predation can decrease as it outgrows a predator's gape (Urban, 2007), improves predator evasion (Martin et al., 2021), or develops defenses such as spines (Laforsch & Tollrian, 2004). Such changes in feeding behavior or defensive capacity as individual predators and prey grow through ontogeny can drive variation in interaction strength (Brose 2010). This same phenomenon may extend to the scale of the community. Even if different communities have the same number of predator and prey individuals, differences in the distribution of biomass across size-classes may cause differences in how strongly predator and prey interact across space or time. For instance, communities with larger predators and smaller prey could have stronger interactions, while communities with smaller predators and larger prey may have weaker interactions (Fig. 1.1). A considerable body of prior work has quantified the effects of body size on consumption rates under controlled conditions (Uiterwaal and DeLong 2020, Brose et al. 2017 *for reviews*). A next step in this field is to pair similar controlled experiments with observational data in order to understand how differences in the size-structure of populations drives when and where predators interact strongly with their prey.

Across taxa, interaction strength tends to—*on average*—increase with predator size (Rall et al., 2012; Uiterwaal & DeLong, 2020), suggesting it may be possible to predict how

strongly specific species interact knowing only the size and density of individuals. Indeed, previous work has widely relied on theoretical scaling exponents based on metabolic arguments (e.g., Brown et al. 2004) as a null expectation to estimate interaction strength (Berlow et al., 2009; Petchey et al., 2008; Yodzis & Innes, 1992). Adopting a similar approach based on empirical size-scaling relationships could offer a simple means of making quantitative predictions of interaction strength without in-depth experimentation. However, there is considerable noise around the mean trend in general size scaling relationships due to differences in taxonomy (Rall et al., 2012), temperature (Englund et al., 2011), habitat dimensionality (Barrios-O'Neill et al., 2016; Pawar et al., 2012), and foraging mode (Barrios-O'Neill et al., 2019). Therefore, it is likely that for a given species pair, the relationship between body size and interaction strength differs from the mean trend across species. Yet understanding how far species pairs deviate from the mean trend will determine the utility of naively applying general-size scaling relationships.

Here, we explore the size-dependence of interaction strength for two economically and ecologically important species: the California spiny lobster (*Panulirus interruptus*, hereafter “lobster”) – a predator, and the purple sea urchin (*Strongylocentrotus purpuratus*, hereafter “urchin”) – a prey. Understanding when and where lobster impact urchin populations is critical because increases in urchin abundance can drive communities to switch from kelp to urchin dominated states (Ling et al., 2015). Previous studies have shown that a high abundance of urchin predators can increase the resistance of kelp communities to urchin-driven phase shifts (Hamilton & Caselle, 2015). Yet, empirical evidence for urchin regulation by lobsters remains equivocal, with some studies finding a strong top-down effect (Lafferty, 2004) and others finding only a weak effect of lobsters (Dunn & Hovel, 2019;

Guenther et al., 2012; Malakhoff & Miller, 2021). Previous work on California spiny lobster and other lobster species shows that larger lobsters consume more and larger urchins (Ling et al., 2009; Tegner & Levin, 1983), yet the relative role of lobster size, urchin size, and urchin density in driving interaction strength remains poorly understood.

In this manuscript, we test the hypothesis that general size-scaling relationships can be used to predict variation in lobster-urchin interactions. To test this hypothesis, we first quantified how the body size and density of lobster and urchins varied across space and through time. We then ask, how does urchin size, lobster size, and urchin density alter consumption rates of urchins in experimental mesocosms? By combining our empirical estimates of consumption rates with long-term observational data, we then disentangle the effects of lobster size, urchin size, and urchin density on spatiotemporal variation in interaction strength. Finally, we address the question: how well do general size-scaling relationships predict interaction strength between a specific predator-prey pair across natural variation in body size and density?

2.3. METHODS

How do lobsters and urchins vary in body size and density across space and through time?

We used 9-years of spatially explicit observational data collected by the Santa Barbara coastal long-term ecological research program (SBC LTER) to explore how lobster and urchin density (ind. m⁻²) and body size varied across space and time. The SBC LTER collects annual data on the abundance and size distribution of lobsters and urchins at five sites. Briefly, divers count the number of urchins greater than 20 mm in six quadrats uniformly spaced along 40 m transects at each site (3-8 transects per site) (Santa Barbara Coastal LTER et al., 2021b). Along a single transect, a diver estimates the test diameter of the

first ~50 urchins to the nearest 0.5 cm (Santa Barbara Coastal LTER et al., 2021c). Divers count and estimate the carapace length to the nearest mm of all lobsters in 1200 m² plots centered around each transect (Santa Barbara Coastal LTER et al., 2021a).

How does lobster predation on urchins vary with lobster size, urchin size, and urchin density?

While there are numerous definitions of interaction strength in the literature, here we define interaction strength as a predator's nonlinear functional response, which describes how consumption rates change as a function of prey density (Berlow et al. 2004 *for review*). Typically, consumption rates increase with prey density until predator satiation, at which point consumption becomes density-independent (Jeschke et al., 2002). The initial increase in consumption approximates the rate that a predator searches space and finds new prey items (i.e., the attack rate), while the predator's maximum consumption rate is limited by the time it takes to manipulate and digest prey (i.e., the handling time) (Holling, 1959). Together, these relationships describe a type II functional response, such that

$$C = \frac{\alpha N}{1 + \alpha h N} \quad \text{Eq. 1}$$

where C is consumption rate, N is the initial density of prey, α is attack rate, and h is handling time, or the inverse of a predator's maximum consumption rate ($1/C_{max}$).

Theory predicts that maximum consumption rates (i.e., $1/h$) scale with consumer body size at the same rate that metabolism scales with body size (Brown et al., 2004; Yodzis & Innes, 1992). Therefore, handling time ($1/C_{max}$) will decrease with consumer body size according to a negative power law function ($h \propto m_c^{-\beta}$). A predator's handling time may also be a function of prey size. Larger prey can be more challenging to manipulate or digest

resulting in longer handling times (Rall et al., 2012). Together, consumption rates at saturating prey densities are expected to vary according to:

$$\frac{1}{C_{max}} = h = h_0 m_c^{\beta_{h,c}} m_r^{\beta_{h,r}} \quad Eq. 2$$

where m_c and m_r are predator and prey mass, respectively, h_0 is a constant, and $\beta_{h,c}$ and $\beta_{h,r}$ are scaling coefficients (Uiterwaal and DeLong 2020).

Foraging theory and biomechanical arguments also provide expectations for how a predator's attack rate should vary with body size. Larger predators have higher mobility and larger prey are more easily detected (McGill & Mittelbach, 2006). Therefore, attack rates should increase according to power law functions of predator and prey size, such that

$$\alpha = \alpha_0 m_c^{\beta_{\alpha,c}} m_r^{\beta_{\alpha,r}} \quad Eq. 3$$

where α_0 is a constant, and $\beta_{\alpha,c}$ and $\beta_{\alpha,r}$ are scaling exponents (Rall et al. 2012, Uiterwaal and DeLong 2020). Previous work suggests that attack rates increase and then decrease as a function of predator size at a fixed prey size (Kalinkat et al., 2013; Uiterwaal et al., 2017). However, in preliminary analyses we found no evidence for a hump shaped relationship between attack rates and size (see *Appendix 6.1.1*). Therefore, we focus on the power-law scaling relationship (Eq. 3).

To determine the size-dependence of the lobster functional response, we conducted a factorial experiment where we manipulated urchin density, urchin size, and lobster size in mesocosms. The lobsters and urchins used in these experiments spanned the size range of local populations surveyed by the SBC LTER. We placed a single lobster in an experimental arena and fed each lobster one of three size classes of urchin at six different densities ($N = 2, 3, 5, 10, 16, 26$ ind. arena⁻¹). We selected urchin densities such that the highest density in experimental trials was representative of that in urchin-dominated areas (Rennick et al.,

2022). We conducted all foraging trials for 48 hours in 200 L arenas. Prior to a trial, we fed lobsters *ad libitum* for 48 hours and then starved the predators for 48 hours. For more detail on the specifics of mesocosm experiments refer to *Appendix 6.1.2*.

We then estimated the parameters of the size-dependent functional response using a Bayesian hierarchical model. Specifically, we estimated the number of urchins eaten as a function of the number of urchins offered, lobster size (g), and urchin size (g). We assumed that the number of urchins consumed in trial i by lobster j ($C_{i,j}$) followed a Poisson distribution such that

$$C_{i,j} \sim \text{Poisson}(\lambda_{i,j}) \quad \text{Eq. 4}$$

$$\lambda_{i,j} = \frac{\alpha_{i,j} N_i}{1 + \alpha_j h_j N_i}$$

$$\log(\alpha_j) = \log(\alpha_0) + \beta_{\alpha,c} \log(m_{c,j}) + \beta_{\alpha,r} \log(m_{r,j}) + \mu_{\alpha,j}$$

$$\log(h_j) = \log(h_0) + \beta_{h,c} \log(m_{c,j}) + \beta_{h,r} \log(m_{r,j}) + \mu_{h,j}$$

1)

where, α_j is the attack rate ($\text{d}^{-1} \text{m}^{-2}$) of lobster j , h_j is the handling time (d) of lobster j , and m_r was the average mass of the urchin size class that lobster j foraged on. We constructed informed priors on all β parameters, where the β 's were normally distributed with a mean based on theoretical predictions (Table S1). We assumed gamma distributions for the prior variances. We included a random effect of lobster individual on the estimation of α and h ($\mu_{\alpha,j}, \mu_{h,j}$), assuming that errors between individuals were normally distributed with mean 0.

We implemented the model in Stan (Stan Development Team, 2022) which uses a Hamiltonian Monte Carlo procedure to estimate parameters. We ran three chains for 25,000 iterations with a burnin of 12,500 iterations and thinned the chains to retain every 3rd

iteration. To diagnose model convergence, we visually assessed mixing of the model chains and confirmed using the Gelman-Rubin convergence diagnostic ($\hat{R} < 1.1$) (Brooks & Gelman, 1998). For more details on our modeling approach see *Appendix 6.1.1*.

How might lobster-urchin interaction strength have varied across space and through time?

To generate plausible estimates for how strongly lobsters and urchins interact under natural conditions, we combined the observational data with our experimentally parameterized functional response. We assumed that interactions were random at a site in a particular year, such that 1) any lobster could interact with any urchin and 2) lobster and urchin density was homogenous across a site. Specifically, we resampled with replacement 1000 individual body masses from the size distributions of lobsters and urchins at each site/year and estimated the interaction strength (IS) between predator i and prey j as

$$IS_{i,j} = \frac{\alpha_0 m_c^{\beta_{\alpha,c}} m_r^{\beta_{\alpha,r}} NP}{1 + \alpha_0 m_c^{\beta_{\alpha,c}} m_r^{\beta_{\alpha,r}} h_0 m_c^{\beta_{h,c}} m_r^{\beta_{h,r}} N} \quad Eq. 5$$

where N and P are the density of urchins and lobsters, respectively, averaged across transects at a site in a particular year, and m_x is the mass of lobster (c) and urchin (r) individuals in a particular draw from the size-distribution. For simplicity, we set all parameters (α_0 , h_0 , β_x) as the median posterior estimate from the Bayesian model. Based on this procedure, IS represents a distribution of plausible interactions between lobster and urchin individuals at each site and year.

Disentangling the effects of body size and density as drivers of variation in interaction strength

Many empirical studies of interaction strength focus on predator and prey density (Berlow et al. 1999, Novak et al. 2016 *for reviews*). However, estimating interaction strengths based on density alone may be inaccurate, particularly for species that experience nonlinear, indeterminate growth, like many marine species where a single large individual has the same mass as many smaller, younger individuals. Recent work highlights the importance of accounting for size-dependent consumption rates in estimating interaction strength (Atkins et al., 2015). But it is unclear how much of the variation in interaction strength would be missed by estimating interactions based solely on density.

To partition the amount of variation in interaction strength due to differences in body size versus density we used a simulation procedure. From eq. 5, it follows that there is an interaction between body size and density, such that at low urchin densities consumption rates will be determined by the size-dependence of lobster attack rates, while at high urchin densities consumption rates will be determined by the size-dependence of lobster handling times. To partition variance, we therefore compared the total variation in estimated interaction strengths accounting for variation in both density and body size to simulations where density varied at fixed values of lobster and urchin body size. We iterated this procedure across 625 different values of lobster size and urchin size such that sizes ranged from the maximum lobster mass and minimum urchin mass to the maximum urchin mass and minimum lobster mass. For each iteration, we estimated the proportion of variation due to differences in density as the correlation coefficient (R^2) of the simple linear regression between the estimated interaction strengths when both body size and density vary to the

estimated interaction strengths when density varied at a fixed combination of body sizes. Considering the only sources of uncertainty in our estimates were body size and density, we estimated the proportion of variation due to body size as $1 - R^2$ for each iteration and report the full range of values (see *Appendix 6.1.3* for further details).

How well can general size-scaling relationships predict species-specific interactions?

Resolving how accurately a given predator's consumption rate can be predicted from general size-scaling relationships and their covariates is at the crux of integrating our theoretical and experimental depth of knowledge about the size dependence of predator-prey interactions into ecosystem-based management practices. To determine how well general size-scaling relationships predict lobster-urchin interactions, we compared our experimental predictions with estimates from three published size-scaling relationships. Based on previous work demonstrating that both traits and taxonomy are important for predicting how strongly species interact (Rall et al., 2011), we hypothesized that size-scaling relationships from the literature would more precisely match our experimental predictions as they increased in taxonomic specificity. Therefore, we predicted how strongly lobsters and urchins interact based on a general cross-taxonomic estimate (Uiterwaal & DeLong, 2020), an estimate for marine invertebrates (Rall et al., 2012), and an estimate for active marine crustaceans foraging on static prey (Barrios-O'Neill et al., 2019) (Table S2). Each of these previous analyses included covariates such as temperature, arena size, or habitat dimensionality in their models of attack rates or handling times (Table S2). Therefore, we included these covariates when generating the predictions and fixed their values at the observed values in our mesocosm experiments (see *Appendix 6.1.4* for more details). We converted the units of

our observational variables (body size and density) into the units used in each previous study respectively, and then back converted all predicted values of interaction strength into urchins consumed per m² per day in order to compare with our experimental predictions. All analyses were implemented in R 4.0.4 (R Core Team, 2021).

2.4. RESULTS

Size-frequency distributions of lobsters relative to urchins varied widely in space and time

Lobster size ranged more than three orders of magnitude from 6.2 – 6184.0 g (393.6 [88.8 – 897.8] g, \bar{X} [95% CI] *unless otherwise specified*), while urchin mass was on average 39.2 [8.1 – 132.2] g (Fig. 1.1A). The relative difference in body mass between lobsters and urchins changed from site to site and year to year with some sites at a particular time having relatively large lobsters and small urchins, while others had relatively small lobsters and large urchins (Fig. S1.1). The average urchin density was 6.5 [0.8 – 27.8] ind. m⁻², while the average lobster density was 0.03 [0.004 – 0.097] ind. m⁻².

Interaction strength between lobsters and urchins increased with urchin density and lobster size but decreased with urchin size

In mesocosm experiments, the consumption rate of urchins by lobster increased with urchin density and lobster size, and decreased as urchin size increased (Fig. 1.2, Fig. S1.2). Only the largest lobsters regularly consumed the largest urchins. For example, lobsters smaller than the median body size only consumed two individual large urchins across all feeding trials. However, all size classes of lobster consumed small urchins, and maximum consumption rates were highest for the largest lobsters preying on the smallest urchins. We

found no evidence for variation in attack rates with lobster size or urchin size (Fig. 1.3a, $\beta_{\alpha,c} = 0.050[-0.12 - 0.41]$, $\beta_{\alpha,r} = 0.093[-0.15 - 0.45]$). However, handling time decreased with lobster size and increased with urchin size (Fig. 1.3b, $\beta_{h,c} = -1.61[-2.16 - -1.02]$, $\beta_{h,r} = 1.30[1.03 - 1.64]$). Despite the inclusion of informative priors, the posterior estimates for the scaling exponents differed from first principal expectations (Fig. S1.3, Table S1.1,S1.3). Handling time decreased at a faster rate than expected with lobster size (e.g., $\beta_{h,c}$) and at a higher rate than expected with urchin size (e.g., $\beta_{h,r}$).

How might lobster-urchin interaction strength have varied across space and through time?

By integrating our experimental model with long term data on lobster and urchin body sizes and densities, we generated plausible estimates for historic interaction strengths. We found that the inferred interaction strength between lobsters and urchins varied considerably across narrow spatial and temporal scales ($0.01 [0.0004 - 0.08]$ ind. $m^{-2} d^{-1}$, Fig. 1.4). The variation in interaction strength between sites ($\overline{CV}_{spatial} = 1.21 \pm 0.4$, $\bar{X} \pm 1$ SD) was similar to the variation between years ($\overline{CV}_{temporal} = 1.13 \pm 0.1$).

Variation in lobster-urchin interaction strength is caused by asymmetries in lobster and urchin body size rather than urchin density

Considering the extent of variation in inferred interaction strength across space and time, we tested how much of this variation could be attributed to differences in lobster-urchin body sizes versus densities. We found that body size accounted for the majority of the variation in inferred interaction strength (75-87%) compared to variation in density (Fig. 1.5a). To better understand the implication of body size accounting for the majority of

variation, we generated a hypothetical community of lobster and urchins. We then used our experimental estimate of the size-dependent functional response to simulate a 10-fold increase in mean urchin density with no change in lobster or urchin size distributions relative to a 10-fold increase in mean lobster size with no change in the density of urchins or lobsters (Fig. 1.5b). The increase in lobster body size resulted in a 230% increase in the median interaction strength, whereas the increase in urchin density resulted in only a 38% increase in interaction strength. In our estimates of interaction strength based on the field data, communities characterized by large lobsters relative to urchin size and high urchin density displayed the highest interaction strength, while interaction strength in communities with small lobsters relative to urchins and low urchin density approached zero (Fig. S1.4). Across all sites and years, lobster-urchin interactions were log-distributed with far more weak than strong interactions (Fig. 1.5a,c).

General size-scaling relationships failed to quantitatively predict lobster-urchin interactions

In general, size-scaling relationships from the literature provided similar rank order predictions for which sites or years displayed the strongest or the weakest interactions compared to our experimental estimates (Fig. S1.5, Spearman's rank order correlation test, $p < 0.001$). However, published size-scaling relationships failed to estimate the magnitude of inferred interactions between lobster and urchin. The closest prediction from the literature to the average of our experimental prediction was for active crustacean predators foraging on static prey (Barrios-O'Neill et al. 2019). However, the average of this prediction was still 18.7 times greater than the interaction strength estimated by our experimental model (Fig. 1.5c, Fig. S1.6). Furthermore, there was only a 15.6% overlap between the distribution of our

experimental prediction and the distribution of the closest prediction from the literature. The precision of the predictions increased as the taxonomic specificity increased. The average of the cross-taxa estimate (Uiterwaal and DeLong 2020) was five orders of magnitude lower than the experimental average, while the average estimate for marine invertebrates (Rall et al. 2012) was ~100 times less than the experimental average. The estimate for active marine crustacean predators performed the best.

3.5. DISCUSSION

Understanding when and where predators will interact strongly with prey is critical to disentangling context dependency in trophic ecology and can offer insight into the repercussions of disproportionate harvesting of species at the top of the food chain. Spatial and temporal heterogeneity in predator and prey size distributions driven by demographic variation (De Roos et al., 2003), spatially explicit size-structured harvest (Kay et al., 2012), and size-structured predation (Rudolf, 2008) may underlie much of the context dependency. Our findings demonstrate that body size is a strong determinant of lobster-urchin interactions in experimental trials and suggest that natural and human-induced variation in body size in the field may be a powerful driver of interaction strength between lobsters and urchins. Our results provide insight into when and where we expect lobsters to play a dominant predatory role and suggest that harvest-induced reductions in lobster size may have significant ecological consequences in kelp forest ecosystems.

Body size drives variation in the role of lobsters in the kelp forest

The hypothesis that lobsters control urchin populations is contested, with some research finding evidence for predator-induced declines in urchins (Ling et al., 2009) and other research finding no evidence at all (Malakhoff & Miller, 2021). Our results suggest two scenarios when lobsters could potentially impact urchin populations, thereby potentially buffering macroalgae resources. We found that interaction strength is greatest when urchin density is high, lobsters are large, and urchins are small. In marine protected areas where lobsters are protected from fishing, lobster size and density are greater than in fished areas (Kay et al., 2012; Peters et al., 2019). With a relatively high density of large lobsters our results suggest that there could be substantial predation pressure on urchins, which is consistent with recent modeling work that highlights the importance of size-selective predation on the recovery of kelp communities under different management strategies (Dunn et al., 2021). Alternatively, our foraging trials demonstrate that even small lobsters can be effective predators of small urchins. Purple urchins can recruit in large numbers to reefs if environmental and biological conditions allow (Okamoto et al., 2020). High densities of lobsters, even if small, may provide a bottleneck of mortality for small urchin recruits, effectively reducing the capacity of the urchin population to consume kelp (e.g., Rennick et al. 2022). However, strong interactions at one point in time could lead to weak interactions in the future as urchins grow large enough to experience reduced predation. Accounting for dynamic interactions between density and size-structure can lead to counterintuitive predictions, such as increases in total prey biomass even when predator induced mortality increases (Schröder et al., 2009). Therefore, to understand the long-term dynamics of lobster-urchin interactions a critical next step is to explicitly model the dynamics of size-structured communities.

Body size – not density – accounts for the majority of variation in interaction strength

Empirical research on predator-prey interactions has historically focused on estimating interaction strength based on species abundances (Novak et al., 2016). Typically, interaction strength is quantified by measuring the abundance of a focal species in the presence or absence of the interacting species (Wootton & Emmerson, 2005). This abundance-based approach implicitly assumes that intraspecific variation in traits has little impact on how strongly populations interact. Yet, there is evidence that intraspecific variation in traits can overshadow interspecific effects (Des Roches et al., 2018). For example, recent work showed that accounting for size-specific differences in consumption rates using theoretical size-scaling relationships (e.g., $m^{0.75}$) better predicts empirical interaction strength than density or biomass (Atkins et al., 2015).

Our study provides additional support for the critical role of accounting for intraspecific variation in body size in predicting interaction strength by demonstrating that lobster-urchin interactions are determined by their respective size distributions, more so than density. We attributed up to 89% of the variation in inferred interaction strength to variation in body size. One possible reason for this pattern is because lobster maximum consumption rates, not attack rates, were size-dependent. As consumption becomes more density independent (e.g., approaches C_{max}) it becomes more size dependent. Across our observational data set, urchin densities were high relative to the average maximum consumption rates of lobster at a site. Thus, it was unlikely that lobsters were limited by urchin availability, but rather by lobsters' ability to handle prey—a parameter that is strongly size-dependent. Therefore, we speculate that variation in predator and prey body size

accounted for the majority of variation in interaction strength because at the observed urchin densities lobsters foraged in a size-dependent, rather than density-dependent, manner.

Together, our results highlight the extent to which focusing on species densities or biomass alone could lead to inaccurate estimates of interactions. Accounting for traits like body size could resolve long-standing debates on the role of predators in regulating prey populations (Poisot et al., 2015) and move debates from the static question of *if* predators impact prey dynamics, to *when* and *where* predators play a strong role in a community.

Naïve predictions of interaction strength

Researchers are increasingly focused on implementing ecosystem-based approaches to management (EBM) that account for species interactions, physical forces, social drivers, and economic considerations (Long et al., 2015). One challenge to effective implementation of EBM is uncertainty in the strength of species interactions, particularly when system specific data are limited (Hunsicker et al., 2011). Previous work in food web ecology has utilized theoretical scaling relationships to determine the structure and resilience of ecological networks (Brose et al., 2006; Petchey et al., 2008). Recently, applied ecologists have adapted a similar approach to parameterize stage- or size structured models, where they assume theoretical size-scaling exponents to estimate interaction strength along with other life history parameters (Blanchard et al. 2017; *see* Reum et al. 2019, Spence et al. 2021 *for exceptions*). These models have led to conceptual advances in the consequences of harvest on populations (Andersen et al., 2009), communities (Andersen et al., 2015; Claessen et al., 2009), or whole ecosystems (Fulton et al., 2011; Heymans et al., 2016). Our results suggest that qualitative predictions for when predators display strong or weak interactions with their

prey may be resilient to inaccurate estimates of how consumption varies with body size for particular species. However, our case study on lobster-urchin interactions suggests that relying on general size-scaling relationships may fail to quantitatively predict the magnitude of trophic interactions between specific species. In other words, naïve estimates may accurately predict the direction and rank order of when and where predators interact strongly with prey but not the magnitude of these interactions. Failing to quantitatively estimate interactions is a critical deficiency in predicting harvest quotas in an EBM framework.

There are two likely reasons for the large discrepancy between our experimental estimates of interaction strength and estimates based on published size-scaling relationships. The first is that the relationship between body size and interaction strength is highly variable across different species and taxa (Rall et al. 2012, Uiterwaal and DeLong 2020), or even among different functional groups in the marine benthos (Barrios-O'Neill et al. 2019). Here, we focused on the mean trend in the relationship between size and interaction strength from these studies to determine how much information could be borrowed to estimate the interaction strength of particular predator-prey pairs. However, the considerable variation around the mean is certainly a source of imprecision in using cross-species size-scaling relationships to estimate interactions for specific species.

The other likely reason our experimental estimates differed from estimates based on published size-scaling relationships are discrepancies between consumption-size relationships within species pairs compared to across species pairs (Brose et al., 2017). Previous meta-analyses used the average body size of a predator species and the average body size of its prey species to estimate how the functional response varies with body size (Rall et al. 2012, Uitterwaal and DeLong 2020). However, body size varies among individuals, and

consumption is a nonlinear function of body size. Therefore, the consumption rate of the average sized individual will poorly approximate the average consumption rate across variation in body size (Bolnick et al., 2011). While size-scaling relationships generated across the average body size of species may uncover general ecological patterns (White et al., 2019), our results add to a growing body of evidence that general relationships may have little bearing on how a particular predator's consumption rate on a prey changes with ontogenetic growth (Aljetlawi et al., 2004; Uiterwaal et al., 2017). Exploring if there are any general patterns in the consumption-body size relationship within species pairs could improve the utility of using body size to estimate ontogenetic variation in interaction strength in the absence of species-specific data.

Conclusion

To sustainably harvest and conserve ecosystems, it is critical to predict how strongly predators interact with their prey—a challenging task considering the same species of predator can interact with its prey differently in different spatial or temporal contexts. Here, we used a simulation procedure to infer how strongly lobster and urchin may have interacted across narrow spatial and temporal scales. Our analysis suggests that variation in the body size of predator and prey, more so than variation in density, accounted for the majority of variation in lobster-urchin interaction strength. Our results highlight the importance of accounting for body size when determining fine-scale variation in interaction strength, as two sites may have the same density of species, but species may interact strongly at one site and not at all at the other depending on variation in individual body size. For lobsters and urchins, species-specific estimates for how consumption changes with body size, rather than general size-

scaling relationships, are necessary to sufficiently predict how changes in size drive changes in interaction strength.

Humans are driving reductions in the size of predators (Blanchard et al., 2005; Robinson et al., 2017) through the interactive effects of harvest and warming temperatures (Baudron et al., 2014; Lindmark et al., 2018; Pauly & Cheung, 2018). Such reductions in body size not only alter the economic and cultural value of the target population (Oke et al., 2020), but also lead to shifts in how strongly species interact in communities. Incorporating body size as a means of approximating how strongly species interact will improve ecologists' ability to predict when and where predators have strong effects on prey, a critical step in clarifying the context-dependence of trophic interactions and understanding the repercussions of the ongoing losses of large predators.

ACKNOWLEDGMENTS

We thank Drs. Jameal Samhouri, Dan Reed, Holly Moeller, Ana Miller-ter Kuile, and the Ocean Recoveries lab group for providing invaluable guidance on previous drafts of this manuscript. We would also like to thank Drs. Erik Ward, Stephen Proulx, and Dan Ovando for assistance in developing the Bayesian model. Joseph Curtis and many undergraduate researchers were integral to conducting the mesocosm experiment and maintaining the animals in captivity. Finally, the integration of experimental results with long-term data would not have been possible without the efforts of Clint Nelson, Li Kui, and many others involved with the SBC LTER. This work was funded by an NSF Graduate Research Fellowship, a University of California Chancellor's award, the California Sea Grant Prop 84

grant program (R/OPCOAH-2), and the Santa Barbara Coastal Long-Term Ecological Research program (NSF OCE 1831937).

AUTHOR CONTRIBUTIONS

Bartholomew DiFiore and Adrian Stier conceived the study. Bartholomew DiFiore collected and analyzed the data and wrote the first draft of the manuscript. Both authors contributed equally to revisions.

DATA AVAILABILITY STATEMENT

All data used in this manuscript are available through the Environmental Data Initiative (EDI) and linked to the Santa Barbara Coastal long-term ecological research (SBC LTER) data catalogue. Lobster size and density data used in this manuscript can be found at <https://doi.org/10.6073/PASTA/0BCDC7E8B22B8F2C1801085E8CA24D59> (Santa Barbara Coastal LTER et al., 2021a). For urchin size data see <https://doi.org/10.6073/PASTA/FD564DDDFE7B77FE9E4BD8417F166057> (Santa Barbara Coastal LTER et al., 2021b) and urchin density data see <https://doi.org/10.6073/pasta/f1cf070648d7654ada052835afb2cfe9> (Santa Barbara Coastal LTER et al., 2021c). Experimental results of the foraging trials can be found at <https://doi.org/10.6073/pasta/f3878aad622dfe9b05a7d0e75d39bddb> (Santa Barbara Coastal LTER et al., 2023). Code to source data files directly from EDI, analyze the data and generate figures is archived on Zenodo at <https://doi.org/10.5281/zenodo.7737746> (DiFiore & Stier, 2023).

3.6. REFERENCES

- Aljetlawi, A. A., Sparrevik, E., & Leonardsson, K. (2004). Prey–predator size-dependent functional response: Derivation and rescaling to the real world. *Journal of Animal Ecology*, *73*(2), 239–252. <https://doi.org/10.1111/j.0021-8790.2004.00800.x>
- Andersen, K. H., Farnsworth, K. D., Pedersen, M., Gislason, H., & Beyer, J. E. (2009). How community ecology links natural mortality, growth, and production of fish populations. *ICES Journal of Marine Science*, *66*(9), 1978–1984. <https://doi.org/10.1093/icesjms/fsp161>
- Andersen, K. H., Jacobsen, N. S., & Farnsworth, K. D. (2015). The theoretical foundations for size spectrum models of fish communities. *Canadian Journal of Fisheries and Aquatic Sciences*, *73*(4), 575–588. <https://doi.org/10.1139/cjfas-2015-0230>
- Atkins, R. L., Griffin, J. N., Angelini, C., O’Connor, M. I., & Silliman, B. R. (2015). Consumer–plant interaction strength: Importance of body size, density and metabolic biomass. *Oikos*, *124*(10), 1274–1281. <https://doi.org/10.1111/oik.01966>
- Barnes, C., Maxwell, D., Reuman, D. C., & Jennings, S. (2010). Global patterns in predator–prey size relationships reveal size dependency of trophic transfer efficiency. *Ecology*, *91*(1), 222–232. <https://doi.org/10.1890/08-2061.1>
- Barrios-O’Neill, D., Kelly, R., Dick, J. T. A., Ricciardi, A., MacIsaac, H. J., & Emmerson, M. C. (2016). On the context-dependent scaling of consumer feeding rates. *Ecology Letters*, *19*(6), 668–678. <https://doi.org/10.1111/ele.12605>
- Barrios-O’Neill, D., Kelly, R., & Emmerson, M. C. (2019). Biomass encounter rates limit the size scaling of feeding interactions. *Ecology Letters*, *22*(11), 1870–1878. <https://doi.org/10.1111/ele.13380>
- Baudron, A. R., Needle, C. L., Rijnsdorp, A. D., & Marshall, C. T. (2014). Warming temperatures and smaller body sizes: Synchronous changes in growth of North Sea fishes. *Global Change Biology*, *20*(4), 1023–1031. <https://doi.org/10.1111/gcb.12514>
- Berlow, E. L., Dunne, J. A., Martinez, N. D., Stark, P. B., Williams, R. J., & Brose, U. (2009). Simple prediction of interaction strengths in complex food webs. *Proceedings of the National Academy of Sciences*, *106*(1), 187–191. <https://doi.org/10.1073/pnas.0806823106>
- Berlow, E. L., Navarrete, S. A., Briggs, C. J., Power, M. E., & Menge, B. A. (1999). Quantifying Variation in the Strengths of Species Interactions. *Ecology*, *80*(7), 2206–2224. [https://doi.org/10.1890/0012-9658\(1999\)080\[2206:QVITSO\]2.0.CO;2](https://doi.org/10.1890/0012-9658(1999)080[2206:QVITSO]2.0.CO;2)
- Blanchard, J. L., Heneghan, R. F., Everett, J. D., Trebilco, R., & Richardson, A. J. (2017). From Bacteria to Whales: Using Functional Size Spectra to Model Marine Ecosystems. *Trends in Ecology & Evolution*, *32*(3), 174–186. <https://doi.org/10.1016/j.tree.2016.12.003>

- Blanchard, J. L., Mills, C., Jennings, S., Fox, C. J., Rackham, B. D., Eastwood, P. D., & O'Brien, C. M. (2005). Distribution-abundance relationships for North Sea Atlantic cod (*Gadus morhua*): Observation versus theory. *Canadian Journal of Fisheries and Aquatic Sciences*, *62*(9), 2001–2009. <https://doi.org/10.1139/f05-109>
- Bolnick, D. I., Amarasekare, P., Araújo, M. S., Bürger, R., Levine, J. M., Novak, M., Rudolf, V. H. W., Schreiber, S. J., Urban, M. C., & Vasseur, D. A. (2011). Why intraspecific trait variation matters in community ecology. *Trends in Ecology & Evolution*, *26*(4), 183–192. <https://doi.org/10.1016/j.tree.2011.01.009>
- Brooks, S. P., & Gelman, A. (1998). General Methods for Monitoring Convergence of Iterative Simulations. *Journal of Computational and Graphical Statistics*, *7*(4), 434–455. <https://doi.org/10.1080/10618600.1998.10474787>
- Brose, U., Blanchard, J. L., Eklöf, A., Galiana, N., Hartvig, M., Hirt, M. R., Kalinkat, G., Nordström, M. C., O’Gorman, E. J., Rall, B. C., Schneider, F. D., Thébault, E., & Jacob, U. (2017). Predicting the consequences of species loss using size-structured biodiversity approaches. *Biological Reviews*, *92*(2), 684–697. <https://doi.org/10.1111/brv.12250>
- Brose, U., Williams, R. J., & Martinez, N. D. (2006). Allometric scaling enhances stability in complex food webs. *Ecology Letters*, *9*(11), 1228–1236. <https://doi.org/10.1111/j.1461-0248.2006.00978.x>
- Brown, J. H., Gillooly, J. F., Allen, A. P., Savage, V. M., & West, G. B. (2004). Toward a metabolic theory of ecology. *Ecology*, *85*(7), 1771–1789. <https://doi.org/10.1890/03-9000>
- Claessen, D., de Vos, A. S., & de Roos, A. M. (2009). Bioenergetics, overcompensation, and the source–sink status of marine reserves. *Canadian Journal of Fisheries and Aquatic Sciences*, *66*(7), 1059–1071. <https://doi.org/10.1139/F09-061>
- De Roos, A. M., Persson, L., & McCauley, E. (2003). The influence of size-dependent life-history traits on the structure and dynamics of populations and communities. *Ecology Letters*, *6*(5), 473–487. <https://doi.org/10.1046/j.1461-0248.2003.00458.x>
- Des Roches, S., Post, D. M., Turley, N. E., Bailey, J. K., Hendry, A. P., Kinnison, M. T., Schweitzer, J. A., & Palkovacs, E. P. (2018). The ecological importance of intraspecific variation. *Nature Ecology & Evolution*, *2*(1), 57–64. <https://doi.org/10.1038/s41559-017-0402-5>
- Dunn, R. P., & Hovel, K. A. (2019). Experiments reveal limited top-down control of key herbivores in southern California kelp forests. *Ecology*, *100*(3), e02625. <https://doi.org/10.1002/ecy.2625>
- Dunn, R. P., Samhouri, J. F., & Baskett, M. L. (2021). Transient dynamics during kelp forest recovery from fishing across multiple trophic levels. *Ecological Applications*, *n/a*(n/a), e2367. <https://doi.org/10.1002/eap.2367>

- Englund, G., Öhlund, G., Hein, C. L., & Diehl, S. (2011). Temperature dependence of the functional response. *Ecology Letters*, *14*(9), 914–921. <https://doi.org/10.1111/j.1461-0248.2011.01661.x>
- Fulton, E. A., Link, J. S., Kaplan, I. C., Savina-Rolland, M., Johnson, P., Ainsworth, C., Horne, P., Gorton, R., Gamble, R. J., Smith, A. D. M., & Smith, D. C. (2011). Lessons in modelling and management of marine ecosystems: The Atlantis experience. *Fish and Fisheries*, *12*(2), 171–188. <https://doi.org/10.1111/j.1467-2979.2011.00412.x>
- Geary, W. L., Bode, M., Doherty, T. S., Fulton, E. A., Nimmo, D. G., Tulloch, A. I. T., Tulloch, V. J. D., & Ritchie, E. G. (2020). A guide to ecosystem models and their environmental applications. *Nature Ecology & Evolution*, 1–13. <https://doi.org/10.1038/s41559-020-01298-8>
- Guenther, C. M., Lenihan, H. S., Grant, L. E., Lopez-Carr, D., & Reed, D. C. (2012). Trophic Cascades Induced by Lobster Fishing Are Not Ubiquitous in Southern California Kelp Forests. *PLoS ONE*, *7*(11). <https://doi.org/10.1371/journal.pone.0049396>
- Hamilton, S. L., & Caselle, J. E. (2015). Exploitation and recovery of a sea urchin predator has implications for the resilience of southern California kelp forests. *Proceedings of the Royal Society B: Biological Sciences*, *282*(1799), 20141817. <https://doi.org/10.1098/rspb.2014.1817>
- Heymans, J. J., Coll, M., Link, J. S., Mackinson, S., Steenbeek, J., Walters, C., & Christensen, V. (2016). Best practice in Ecopath with Ecosim food-web models for ecosystem-based management. *Ecological Modelling*, *331*, 173–184. <https://doi.org/10.1016/j.ecolmodel.2015.12.007>
- Holling, C. S. (1959). Some Characteristics of Simple Types of Predation and Parasitism. *The Canadian Entomologist*, *91*(7), 385–398. <https://doi.org/10.4039/Ent91385-7>
- Hunsicker, M. E., Ciannelli, L., Bailey, K. M., Buckel, J. A., White, J. W., Link, J. S., Essington, T. E., Gaichas, S., Anderson, T. W., Brodeur, R. D., Chan, K.-S., Chen, K., Englund, G., Frank, K. T., Freitas, V., Hixon, M. A., Hurst, T., Johnson, D. W., Kitchell, J. F., ... Zador, S. (2011). Functional responses and scaling in predator–prey interactions of marine fishes: Contemporary issues and emerging concepts. *Ecology Letters*, *14*(12), 1288–1299. <https://doi.org/10.1111/j.1461-0248.2011.01696.x>
- Jeschke, J. M., Kopp, M., & Tollrian, R. (2002). Predator Functional Responses: Discriminating Between Handling and Digesting Prey. *Ecological Monographs*, *72*(1), 95–112. [https://doi.org/10.1890/0012-9615\(2002\)072\[0095:PFRDBH\]2.0.CO;2](https://doi.org/10.1890/0012-9615(2002)072[0095:PFRDBH]2.0.CO;2)
- Kalinkat, G., Schneider, F. D., Digel, C., Guill, C., Rall, B. C., & Brose, U. (2013). Body masses, functional responses and predator–prey stability. *Ecology Letters*, *16*(9), 1126–1134. <https://doi.org/10.1111/ele.12147>

- Kay, M. C., Lenihan, H. S., Guenther, C. M., Wilson, J. R., Miller, C. J., & Shroud, S. W. (2012). Collaborative assessment of California spiny lobster population and fishery responses to a marine reserve network. *Ecological Applications*, 22(1), 322–335. <https://doi.org/10.1890/11-0155.1>
- Lafferty, K. D. (2004). Fishing for Lobsters Indirectly Increases Epidemics in Sea Urchins. *Ecological Applications*, 14(5), 1566–1573. <https://doi.org/10.1890/03-5088>
- Laforsch, C., & Tollrian, R. (2004). Inducible Defenses in Multipredator Environments: Cyclomorphosis in *Daphnia Cucullata*. *Ecology*, 85(8), 2302–2311. <https://doi.org/10.1890/03-0286>
- Lawton, J. H. (1999). Are There General Laws in Ecology? *Oikos*, 84(2), 177–192. <https://doi.org/10.2307/3546712>
- Lindmark, M., Huss, M., Ohlberger, J., & Gårdmark, A. (2018). Temperature-dependent body size effects determine population responses to climate warming. *Ecology Letters*, 21(2), 181–189. <https://doi.org/10.1111/ele.12880>
- Ling, S. D., Johnson, C. R., Frusher, S. D., & Ridgway, K. R. (2009). Overfishing reduces resilience of kelp beds to climate-driven catastrophic phase shift. *Proceedings of the National Academy of Sciences*, 106(52), 22341–22345. <https://doi.org/10.1073/pnas.0907529106>
- Ling, S. D., Scheibling, R. E., Rassweiler, A., Johnson, C. R., Shears, N., Connell, S. D., Salomon, A. K., Norderhaug, K. M., Pérez-Matus, A., Hernández, J. C., Clemente, S., Blamey, L. K., Hereu, B., Ballesteros, E., Sala, E., Garrabou, J., Cebrian, E., Zabala, M., Fujita, D., & Johnson, L. E. (2015). Global regime shift dynamics of catastrophic sea urchin overgrazing. *Phil. Trans. R. Soc. B*, 370(1659), 20130269. <https://doi.org/10.1098/rstb.2013.0269>
- Long, R. D., Charles, A., & Stephenson, R. L. (2015). Key principles of marine ecosystem-based management. *Marine Policy*, 57, 53–60. <https://doi.org/10.1016/j.marpol.2015.01.013>
- Malakhoff, K. D., & Miller, R. J. (2021). After 15 years, no evidence for trophic cascades in marine protected areas. *Proceedings of the Royal Society B: Biological Sciences*, 288(1945), 20203061. <https://doi.org/10.1098/rspb.2020.3061>
- Martin, B., Gil, M., Fahimipour, A., & Hein, A. (2021). Informational constraints on predator–prey interactions. *Oikos*. <https://doi.org/10.1111/oik.08143>
- McGill, B. J., & Mittelbach, G. G. (2006). An allometric vision and motion model to predict prey encounter rates. *Evolutionary Ecology Research*, 8, 691–701.
- Novak, M., Yeakel, J. D., Noble, A. E., Doak, D. F., Emmerson, M., Estes, J. A., Jacob, U., Tinker, M. T., & Wootton, J. T. (2016). Characterizing Species Interactions to Understand Press Perturbations: What Is the Community Matrix? *Annual Review of*

- Ecology, Evolution, and Systematics*, 47(1), 409–432.
<https://doi.org/10.1146/annurev-ecolsys-032416-010215>
- Okamoto, D. K., Schroeter, S. C., & Reed, D. C. (2020). Effects of ocean climate on spatiotemporal variation in sea urchin settlement and recruitment. *Limnology and Oceanography*, 65(9), 2076–2091. <https://doi.org/10.1002/lno.11440>
- Oke, K. B., Cunningham, C. J., Westley, P. a. H., Baskett, M. L., Carlson, S. M., Clark, J., Hendry, A. P., Karatayev, V. A., Kendall, N. W., Kibele, J., Kindsvater, H. K., Kobayashi, K. M., Lewis, B., Munch, S., Reynolds, J. D., Vick, G. K., & Palkovacs, E. P. (2020). Recent declines in salmon body size impact ecosystems and fisheries. *Nature Communications*, 11(1), 4155. <https://doi.org/10.1038/s41467-020-17726-z>
- Pauly, D., & Cheung, W. W. L. (2018). Sound physiological knowledge and principles in modeling shrinking of fishes under climate change. *Global Change Biology*, 24(1), e15–e26. <https://doi.org/10.1111/gcb.13831>
- Pawar, S., Dell, A. I., & Van M. Savage. (2012). Dimensionality of consumer search space drives trophic interaction strengths. *Nature*, 486(7404), 485–489. <https://doi.org/10.1038/nature11131>
- Persson, L., Leonardsson, K., de Roos, A. M., Gyllenberg, M., & Christensen, B. (1998). Ontogenetic Scaling of Foraging Rates and the Dynamics of a Size-Structured Consumer-Resource Model. *Theoretical Population Biology*, 54(3), 270–293. <https://doi.org/10.1006/tpbi.1998.1380>
- Petchey, O. L., Beckerman, A. P., Riede, J. O., & Warren, P. H. (2008). Size, foraging, and food web structure. *Proceedings of the National Academy of Sciences*, 105(11), 4191–4196. <https://doi.org/10.1073/pnas.0710672105>
- Peters, J. R., Reed, D. C., & Burkepille, D. E. (2019). Climate and fishing drive regime shifts in consumer-mediated nutrient cycling in kelp forests. *Global Change Biology*, 25(9), 3179–3192. <https://doi.org/10.1111/gcb.14706>
- Poisot, T., Stouffer, D. B., & Gravel, D. (2015). Beyond species: Why ecological interaction networks vary through space and time. *Oikos*, 124(3), 243–251. <https://doi.org/10.1111/oik.01719>
- R Core Team. (2021). *R: A language and environment for statistical computing*. R Foundation for Statistical Computing. URL <https://www.R-project.org/>
- Rall, B. C., Brose, U., Hartvig, M., Kalinkat, G., Schwarzmüller, F., Vucic-Pestic, O., & Petchey, O. L. (2012). Universal temperature and body-mass scaling of feeding rates. *Philosophical Transactions of the Royal Society B: Biological Sciences*, 367(1605), 2923–2934. <https://doi.org/10.1098/rstb.2012.0242>

- Rall, B. C., Kalinkat, G., Ott, D., Vucic-Pestic, O., & Brose, U. (2011). Taxonomic versus allometric constraints on non-linear interaction strengths. *Oikos*, *120*(4), 483–492. <https://doi.org/10.1111/j.1600-0706.2010.18860.x>
- Rennick, M., DiFiore, B. P., Curtis, J., Reed, D. C., & Stier, A. C. (2022). Detrital supply suppresses deforestation to maintain healthy kelp forest ecosystems. *Ecology*, *n/a*(*n/a*), e3673. <https://doi.org/10.1002/ecy.3673>
- Reum, J. C. P., Blanchard, J. L., Holsman, K. K., Aydin, K., & Punt, A. E. (2019). Species-specific ontogenetic diet shifts attenuate trophic cascades and lengthen food chains in exploited ecosystems. *Oikos*, *128*(7), 1051–1064. <https://doi.org/10.1111/oik.05630>
- Robinson, J. P. W., Williams, I. D., Edwards, A. M., McPherson, J., Yeager, L., Vigliola, L., Brainard, R. E., & Baum, J. K. (2017). Fishing degrades size structure of coral reef fish communities. *Global Change Biology*, *23*(3), 1009–1022. <https://doi.org/10.1111/gcb.13482>
- Rudolf, V. H. W. (2008). Consequences of size structure in the prey for predator–prey dynamics: The composite functional response. *Journal of Animal Ecology*, *77*(3), 520–528. <https://doi.org/10.1111/j.1365-2656.2008.01368.x>
- Santa Barbara Coastal LTER, Bell, T. W., Cavanaugh, K. C., & Siegel, D. A. (2022). *SBC LTER: Time series of quarterly NetCDF files of kelp biomass in the canopy from Landsat 5, 7 and 8, since 1984 (ongoing)* [Data set]. Environmental Data Initiative. <https://doi.org/10.6073/PASTA/3FF5E56EA13C555B474EE2DB6DD6B3DF>
- Santa Barbara Coastal LTER, Reed, D. C., & Miller, R. J. (2021a). *SBC LTER: Reef: Abundance, size and fishing effort for California Spiny Lobster (Panulirus interruptus), ongoing since 2012* [Data set]. Environmental Data Initiative. <https://doi.org/10.6073/PASTA/0BCDC7E8B22B8F2C1801085E8CA24D59>
- Santa Barbara Coastal LTER, Reed, D. C., & Miller, R. J. (2021b). *SBC LTER: Reef: Annual time series of biomass for kelp forest species, ongoing since 2000* [Data set]. Environmental Data Initiative. <https://doi.org/10.6073/PASTA/F1CF070648D7654ADA052835AFB2CFE9>
- Santa Barbara Coastal LTER, Reed, D. C., & Miller, R. J. (2021c). *SBC LTER: Reef: Long-term experiment: Kelp removal: Urchin size frequency distribution* [Data set]. Environmental Data Initiative. <https://doi.org/10.6073/PASTA/FD564DDDFE7B77FE9E4BD8417F166057>
- Schröder, A., Persson, L., & Roos, A. M. de. (2009). Culling experiments demonstrate size-class specific biomass increases with mortality. *Proceedings of the National Academy of Sciences*, *106*(8), 2671–2676. <https://doi.org/10.1073/pnas.0808279106>
- Spence, M. A., Thorpe, R. B., Blackwell, P. G., Scott, F., Southwell, R., & Blanchard, J. L. (2021). Quantifying uncertainty and dynamical changes in multi-species fishing

- mortality rates, catches and biomass by combining state-space and size-based multi-species models. *Fish and Fisheries*, 00. <https://doi.org/10.1111/faf.12543>
- Stan Development Team. (2022). *Stan Modeling Language Users Guide and Reference Manual* (2.29). <https://mc-stan.org>
- Tegner, M. J., & Levin, L. A. (1983). Spiny lobsters and sea urchins: Analysis of a predator-prey interaction. *Journal of Experimental Marine Biology and Ecology*, 73(2), 125–150. [https://doi.org/10.1016/0022-0981\(83\)90079-5](https://doi.org/10.1016/0022-0981(83)90079-5)
- Uiterwaal, S. F., & DeLong, J. P. (2020). Functional responses are maximized at intermediate temperatures. *Ecology*, 101(4). <https://doi.org/10.1002/ecy.2975>
- Uiterwaal, S. F., Mares, C., & DeLong, J. P. (2017). Body size, body size ratio, and prey type influence the functional response of damselfly nymphs. *Oecologia*, 185(3), 339–346. <https://doi.org/10.1007/s00442-017-3963-8>
- Urban, M. C. (2007). The Growth–Predation Risk Trade-Off Under a Growing Gape-Limited Predation Threat. *Ecology*, 88(10), 2587–2597. <https://doi.org/10.1890/06-1946.1>
- Werner, E. E., & Gilliam, J. F. (1984). The Ontogenetic Niche and Species Interactions in Size-Structured Populations. *Annual Review of Ecology and Systematics*, 15(1), 393–425. <https://doi.org/10.1146/annurev.es.15.110184.002141>
- White, C. R., Marshall, D. J., Alton, L. A., Arnold, P. A., Beaman, J. E., Bywater, C. L., Condon, C., Crispin, T. S., Janetzki, A., Pirtle, E., Winwood-Smith, H. S., Angilletta, M. J., Chenoweth, S. F., Franklin, C. E., Halsey, L. G., Kearney, M. R., Portugal, S. J., & Ortiz-Barrientos, D. (2019). The origin and maintenance of metabolic allometry in animals. *Nature Ecology & Evolution*, 3(4), 598–603. <https://doi.org/10.1038/s41559-019-0839-9>
- Wootton, J. T., & Emmerson, M. (2005). Measurement of Interaction Strength in Nature. *Annual Review of Ecology, Evolution, and Systematics*, 36(1), 419–444. <https://doi.org/10.1146/annurev.ecolsys.36.091704.175535>
- Yodzis, P., & Innes, S. (1992). Body Size and Consumer-Resource Dynamics. *The American Naturalist*, 139(6), 1151–1175. <https://doi.org/10.1086/285380>

2.7. FIGURES AND FIGURE CAPTIONS

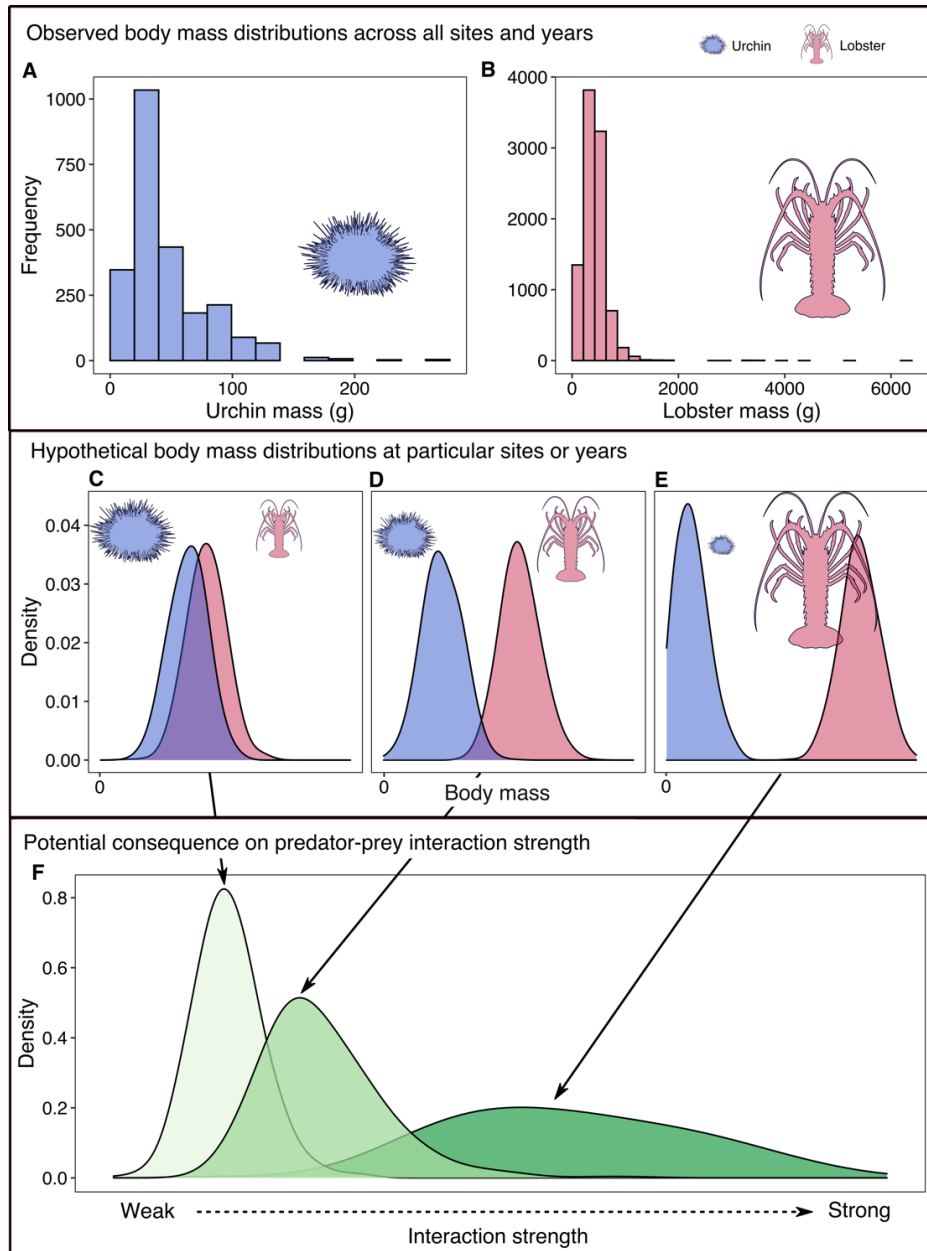


Figure 1.1. Observed body size distributions of a predator (*Panulirus interruptus* - lobster) (A) and their prey (*Strongylocentrotus purpuratus* - urchin) (B) across 5 sites monitored annually from 2012-2020. Different processes such as variation in recruitment, habitat suitability, or harvest can cause differences in the size of predators, like lobster, relative to their prey independent of density (C-E). Theory predicts that larger predators will consume more total prey biomass than smaller predators, and that predators tend to consume more small than large prey. Such size-dependent foraging at the scale of the individual could result in large variation in interaction strength at the population-scale at different sites or years (F).

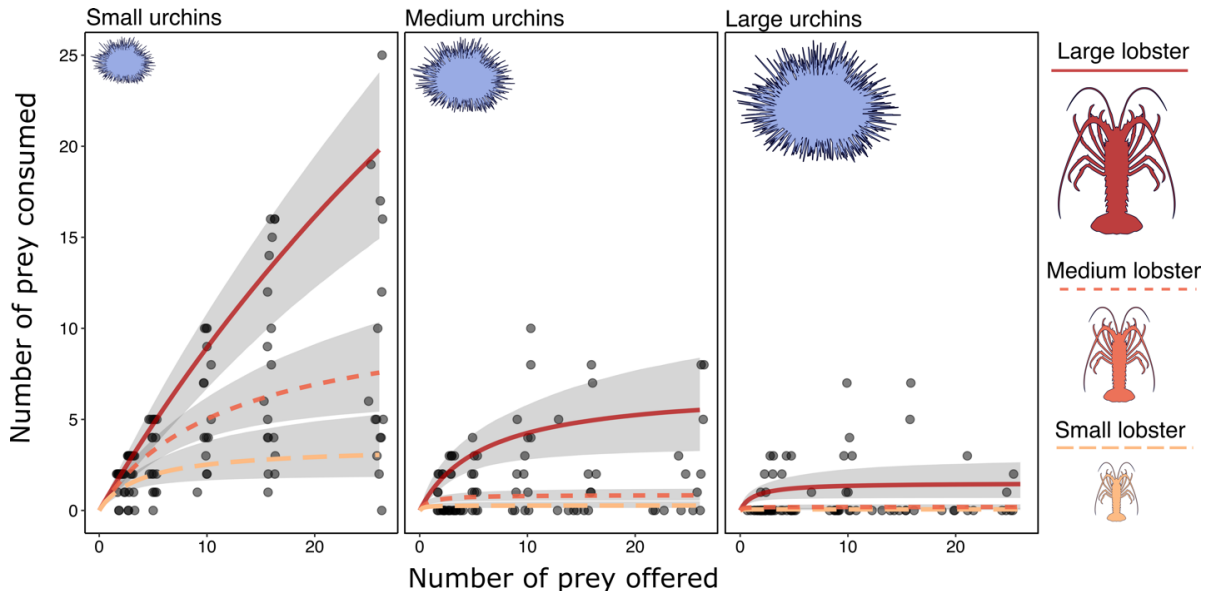


Figure 1.2. Purple sea urchin (*Strongylocentrotus purpuratus*) consumption rates by California spiny lobster (*Panulirus interruptus*) predators in mesocosm foraging trials. Individual lobsters ($n = 45$) foraged on a single urchin class at six different urchin abundances. Lines are posterior predictions (\tilde{X} [95% CI]) from a Bayesian model for the body size dependent functional response. Predictions are for hypothetical lobsters with body mass set to the 10th percentile, mean, and 90th percentile (e.g., small, medium, large) of the size distribution of lobster used in the experiment.

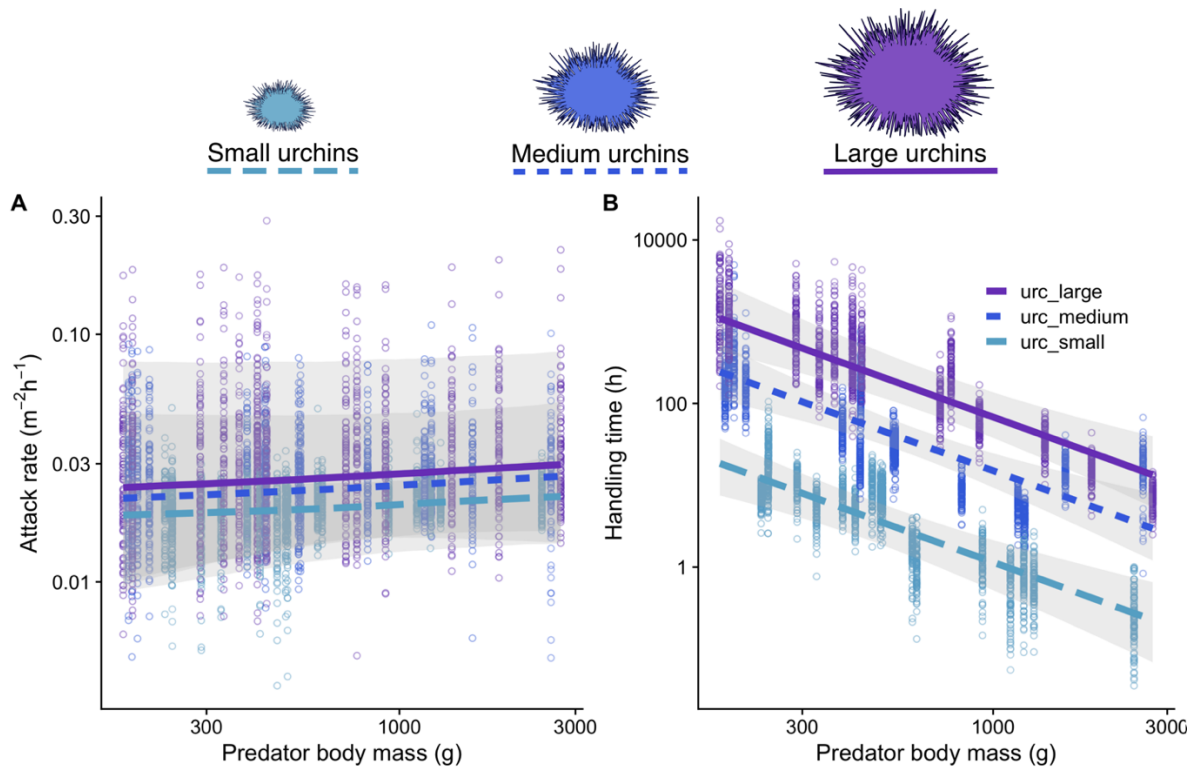


Figure 1.3. Body size scaling of the attack rate (A) and handling time (B) parameters of the functional response of California spiny lobster (*Panulirus interruptus*) foraging on purple urchins (*Strongylocentrotus purpuratus*). Lines are posterior predictions (\bar{X} [95% CI]) for the body size scaling of each parameter according to power law functions of predator and prey mass (see *Methods* for details). Data points are 100 sampled draws from the posterior distributions of α and h for each individual predator foraging on a particular prey size class using a Bayesian hierarchical model. Note the \log_{10} transformations of both axes.

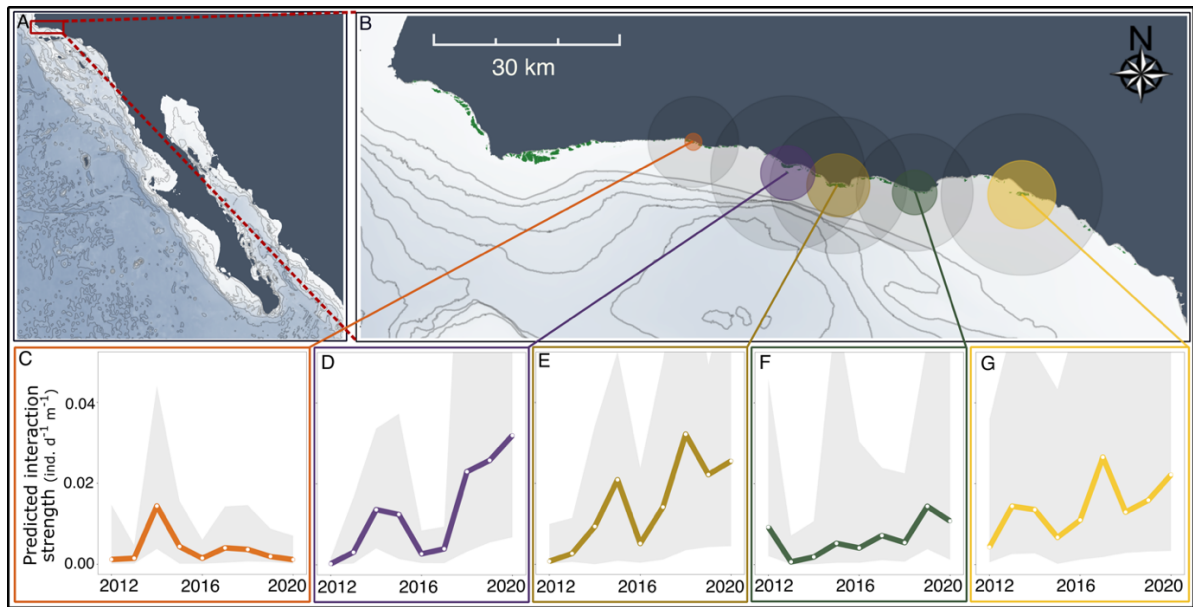


Figure 1.4. Predicted interaction strength between California spiny lobster (*Panulirus interruptus*) predators and purple sea urchin (*Strongylocentrotus purpuratus*) prey at five sites in the Santa Barbara Channel, USA from 2012-2020 (A-B). Points and surrounding grayscale circles represent the median and upper 95% CI of interaction strength simulated for historic observations of lobster and urchin size-distributions and densities using a body size-dependent functional response parameterized from mesocosm foraging experiments. Inset plots (C-G) are the median interaction strength through time at each site. Green polygons along coastline are the historic extent of giant kelp forests estimated via satellite imagery (Santa Barbara Coastal LTER et al., 2022).

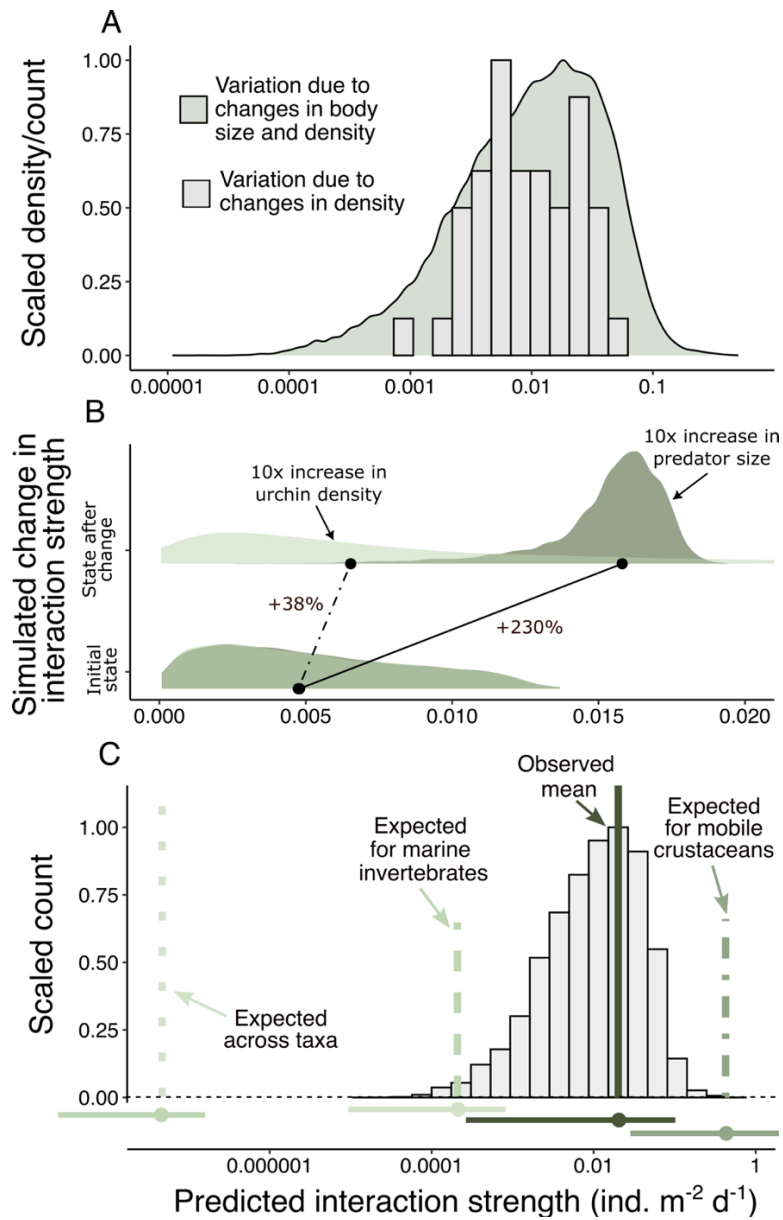


Figure 1.5. (A) Predicted interaction strengths between individual lobster predators (*Panulirus interruptus*) and their urchin prey (*Strongylocentrotus purpuratus*) across five sites and nine years of observational data. Variation in urchin and lobster body size accounted for 82-89% of the total variation in interactions, while variation in density accounted for the remainder. (B) A hypothetical simulation demonstrating the change in interaction strength for a 10-fold increase in urchin density with no change in lobster size compared to a 10-fold increase in lobster body mass with no change in urchin density. In this simulation, interaction strength was estimated using the parameters from the experimental size-scaling relationship for lobster-urchin interactions. (C) Comparison of three estimates of the size-scaling of interaction strength from the literature with experimental predictions. Points and intervals at the bottom are mean and 95% CIs of each distribution. Note the \log_{10} transformation on the x-axes in panels A and C.

3. CHAPTER II:

Resource acquisition increases with body size faster than metabolic requirements in a marine invertebrate predator: evidence for hyperallometric scaling of consumption

3.1. ABSTRACT

Across taxa, organisms' body size is tightly linked to their metabolism, leading to the widely held assumption that animals' foraging rates can be predicted by their size. However, few empirical studies have explicitly linked the physiological and consumption rates across ontogenetic variation in body size. Here, we tested between multiple competing hypotheses for the scaling of metabolism and consumption with body size using California spiny lobster (*Panulirus interruptus*) as a model predator. Specifically, we estimated the size-dependent functional response of lobster foraging on mussels (*Mytilus galloprovincialis*). We then connected the parameters of the functional response (attack rate and maximum consumption rate), with different metrics of lobster physiology, including standard and maximum metabolic rate. We found that contrary to prevailing theoretical expectations, larger lobsters consumed disproportionately more than smaller conspecifics (e.g., *hyperallometric* scaling of consumption), despite declining metabolic requirements. Anthropogenic impacts, including harvest and global climate change, have driven declines in the body size of terrestrial and marine consumers. Our results suggest that changes in community structure or function associated with the loss of large consumers may not be compensated for by increases in the abundance of smaller size classes.

3.2. INTRODUCTION

Body size is perhaps the most conspicuous of animal characteristics and is a critical driver of animal physiology and ecology. For instance, body size is correlated with how fast an animal grows (West et al. 2001), how far an animal migrates (Hein et al. 2012), how biomass is distributed across size classes in ecosystems (Sheldon et al. 1972, Heather et al. 2021), and the growth (Savage et al. 2004) or mortality (McCoy and Gillooly 2008) rates of populations. Understanding what underlies this powerful connection between animal body size and animal biology is a fundamental component of considering how ecosystems are likely to change as the average body size of species continues to decline due to human impacts (Robinson et al. 2017, Santini and Isaac 2021).

The most widely accepted mechanism underlying the connection between animal body size and animal ecology is the strong positive relationship between body size and metabolism. While the exact exponent is widely debated (White et al. 2007), metabolic rate (b) typically increases as a power-law function of body mass (m)

$$b \propto m^{\beta} \quad (1)$$

where the scaling exponent or slope (β) is remarkably consistent across taxa ($\beta \cong 0.6-0.8$; (Kleiber 1932, West et al. 1997, White and Seymour 2003, Glazier 2010). This means that larger species (White et al. 2007), or larger individuals within a species (Killen et al. 2010), have higher absolute metabolic rates, but lower mass-specific metabolic rates. Theory posits that because animals must consume enough energy to meet their basic metabolic requirements (termed standard metabolic rate), the total amount an animal eats should increase with body size, while the amount of energy an animal consumes per unit mass should decrease with body size (Rall et al. 2012). This assumption that consumption rates can

be predicted based on body size has led to seminal advances in the field of food web ecology, from body size being used as the bioenergetic basis of consumer-resource dynamics (Yodzis and Innes 1992, Weitz and Levin 2006, Kalinkat et al. 2013) to predicting the structure and stability of complex food webs (Emmerson and Raffaelli 2004, Berlow et al. 2009). Yet, despite the prevalence of this assumption, the relationship between the scaling of metabolism and consumption with body size is still debated (Marshall and White 2019), and how well an individual's metabolism predicts its consumption rate remains an open question.

There are two common hypotheses for how metabolism and consumption scale with body size. The metabolic theory of ecology suggests that per unit mass an organism's maximum consumption rate (C_{\max}) will decrease with body size at the same rate (e.g., the same exponent, β) that standard metabolic rate decreases with body size (Peters 1983, Brown et al. 2004) (Fig. 2.1A - H_0). Alternatively, mechanistic theories of ontogenetic growth generally assume that standard metabolism decreases with body size at a slower rate (i.e., higher β) than consumption increases with body size (Kooijman 2000, West et al. 2001, Hou et al. 2008), which has been proposed as an explanation for asymptotic size (Essington et al. 2001, West et al. 2001, Hou et al. 2008) (Fig. 2.1 - H_1). However, there are surprisingly few studies that have simultaneously linked the physiology and ecology of individual animals to empirically test how consumption and metabolism increase with body size (Marshall and White 2019). Instead, syntheses have focused on understanding how metabolism and consumption independently change with body size across species (e.g., interspecific scaling, (Rall et al. 2012, Uiterwaal and DeLong 2020)), which may have little bearing on how energy acquisition and metabolic requirements scale with body size within a species (e.g., intraspecific scaling, (Lindmark et al. 2022)). Better linking between the physiology and

ecology of animal feeding could offer a mechanistic understanding of how shifts in body size are likely to change population and ecosystem dynamics.

While most research assumes that consumption increases with body size at the same or slower rate than standard metabolism increases with body size (Marshall and White 2019), there is empirical evidence that consumption may increase with body size at a faster rate than metabolism (Fig. 2.1, *H2*). Previous studies have demonstrated that consumption scales with body size at a rate greater than one (e.g., *hyperallometric* scaling, $1 > \beta_{C_{max}}$) for crustacean predators (Barrios-O'Neill et al. 2019) or consumers foraging in a 3-D environment (Pawar et al. 2012), despite metabolism scaling with body size at a slower rate (e.g., $1 > \beta_{SMR} \cong 0.6-0.8$) across taxa (Brown et al. 2004). If consumption rates increase and SMR decreases with body size per unit mass, then the ratio of energy intake to energy requirements, which we call *factorial energy acquired*, can increase with body size, resulting in larger animals having disproportionately more available energy (Fig. 2.1B).

One potential explanation for why energy acquisition (e.g., consumption) may increase at a faster rate than standard metabolic requirements with body size is that how much an animal consumes may be driven by more complex physiological needs than only its standard metabolic rate (SMR). Aerobic performance is limited by an animal's maximum metabolic rate (MMR, Fig. 2.1D), and the ratio of an animal's maximum to standard metabolic rate, referred to as factorial aerobic scope (FAS = MMR/SMR), describes the factor by which an animal can increase metabolism above maintenance levels to support all fitness-enhancing physiological processes, including growth, feeding, digestion, reproduction, and predator evasion (Careau et al. 2014). Similarly, the difference between an animal's maximum and standard metabolic rates, called absolute aerobic scope (AAS =

MMR-SMR), describes the animal's absolute aerobic capacity to expend energy beyond standard metabolic needs. Empirical evidence suggests that across taxa, standard metabolic rates scale with body size slower (e.g., lower β) than maximum metabolic rates (Darveau et al. 2002), although it is possible that MMR and SMR scale at the same rate with body size (Killen et al. 2016), or that SMR scales with body size at a faster rate than MMR (Fig. 2.1D). If SMR per unit mass decreases with body size at a faster rate than MMR (i.e., $\beta_{SMR} < \beta_{MMR}$; Fig. 2.1D - H_5), then larger animals would have lower energetic constraints (i.e., greater FAS, Fig. 2.1E - H_5). Therefore, larger animals may utilize this larger aerobic scope to consume disproportionately more than smaller conspecifics, if, for example, the cost of reproduction increases with ontogenetic growth (Marshall and White 2019, Jutfelt et al. 2021). Alternatively, consumption is energetically costly, due to the costs of foraging and digestion. Recent work shows that animals may regulate consumption in order to preserve aerobic scope and that how much aerobic scope is preserved changes with body size (Jutfelt et al. 2021). If organisms systematically decrease their need to preserve aerobic scope during digestion with ontogeny, for instance due to declining predation risk with body size (Preisser and Orrock 2012), then larger organisms may consume more than predicted by their standard metabolic rate relative to smaller organisms. Therefore, either changing energetic costs or shifting behaviors as individuals grow could lead to larger organisms consuming disproportionately more than smaller organisms (Fig. 2.1, H_2).

Here, we test between multiple alternative hypotheses for how consumption and metabolism scale with body size in California spiny lobster (*Panulirus interruptus*, hereafter lobster), a commercially and ecologically important marine invertebrate predator. We first estimate how consumption varies across gradients of prey density, prey size, and predator

size in laboratory mesocosms. We then quantified four metrics of metabolic rate (SMR, MMR, FAS, AAS) for each individual predator. Finally, we examined the scaling relationships between body size, metabolism, and consumption rate to determine how energy acquisition and energetic requirements vary with consumer body size.

3.3. METHODS

To determine the relationship between how much an animal eats, its metabolic requirements, and body size, we examined the bioenergetics of lobsters preying on the naturalized Mediterranean mussel (*Mytilus galloprovincialis*, hereafter mussel) (Robles 1987). Lobster are important predators on rocky subtidal reefs stretching from the central Baja peninsula, Mexico to Point Conception, CA, USA and are a commercially important species harvested throughout their range. Lobster are an ideal predator to examine the relationship between a consumer's foraging and metabolic requirements because they are ectothermic predators that forage in a size structured manner (DiFiore and Stier 2023) and there are established methodologies to estimate their physiological rates (Csik et al. 2023).

How does consumption vary with lobster size, mussel size, and mussel density?

How much a consumer eats (e.g., consumption rate) is determined by both intrinsic factors (e.g., metabolic rate, satiation, etc.) and extrinsic factors, including resource availability (Holling 1959), resource size (McCoy et al. 2011), temperature (Englund et al. 2011), or predation risk (Schmitz et al. 1997, DiFiore et al. 2019). Here we focus on the role of lobster size, mussel size, and mussel density in driving lobster consumption rates.

Typically, consumption rates increase asymptotically with resource density according to a type II functional response, which is dependent on two parameters: attack rate and

handling time (Real 1977). The attack rate, or space clearance rate (Uiterwall and DeLong 2020), describes the area that a consumer searches per unit time, while the handling time describes the time required for a consumer to manipulate and digest an individual prey (Jeschke et al. 2002). The inverse of handling time provides an estimate of a consumer's maximum consumption rate

$$C_{max} = 1/h \quad (2)$$

Together, a type II functional response can be described by

$$C = \frac{\alpha N}{1 + \alpha h N} \quad (3)$$

where N is initial resource density, α is the attack rate describing the initial slope at low resource densities, and h is the handling time.

A consumer's functional response can be modified to account for body size by assuming size-scaling relationships for h and α . Theory predicts that when resources are not limiting, a consumer's consumption rate (e.g., C_{max}) should increase with consumer size according to a power-law function of body mass similar to the scaling of metabolism with body mass (Yodzis and Innes 1992, Rall et al. 2012). Maximum consumption rates, however, likely decline as a power-law function of prey mass (Uiterwaal and DeLong 2020).

Therefore, handling times should follow vary with body size according to:

$$h = h_0 m_c^{\beta_{h,c}} m_r^{\beta_{h,r}} \quad (4)$$

where h_0 is a normalization constant, m_c and m_r are the mass of consumer (here lobster) and resource (here mussel) respectively, and $\beta_{c,c}$ and $\beta_{c,r}$ are scaling exponents on consumer and resource mass respectively. Similarly, first principles predict that attack rates increase as a power-law function of consumer size due to increases in the motility and visual acuity of

larger consumers (McGill and Mittelbach 2006). Increases in prey size may cause increases in a consumer's attack rate (Rall et al. 2012) or could cause increases followed by declines in attack rate (Brose 2010, Kalinkat et al. 2013). Preliminary analysis of the data, however, showed no evidence for a hump shaped relationship between attack rates and body size. Therefore, we focused on power-law functions of body mass such that:

$$\alpha = \alpha_0 m_c^{\beta_{\alpha,c}} m_r^{\beta_{\alpha,r}} \quad (5)$$

where α_0 is a normalization constant, and $\beta_{\alpha,c}$ and $\beta_{\alpha,r}$ are scaling exponents on consumer and resource mass respectively.

To estimate the size-dependence of the lobster functional response, we conducted a factorial experiment where we manipulated lobster size, mussel size, and mussel density. We collected lobsters and mussels from the Santa Barbara Channel (CA, USA). Lobster ($n = 11$) ranged in size from 176-1199 g. We allowed each lobster to forage on three size classes of mussel (20-35, 35-50, and 50-65 mm) at five different densities (2, 5, 10, 20, 50 ind. arena⁻¹). We conducted all foraging trials in 171-liter tanks divided in half by a permeable barrier with one lobster per side under a natural photoperiod (12 light: 12 dark). All lobsters were maintained under ambient sea water temperature. To ensure lobsters entered feeding trials at a similar level of satiation, we fed lobsters mussels *ad libitum*, and then starved lobsters for 48 hrs. To initiate a trial, each lobster was given a random density of mussel of a particular size class. We measured each mussel prior to the start of a trial. After 24 hours, we removed, counted, and re-measured all un-eaten mussels.

To estimate the functional response of each lobster foraging on each size class of mussel, we used a Bayesian hierarchical model. A Bayesian hierarchical approach allowed us to account for the structure in the data (i.e., non-independent observations of foraging in any

trial i), while informing the scaling exponents based on first principle expectations.

Specifically, we assumed that the number of mussels consumed in trial i (C_i) followed a Poisson distribution such that:

$$C_i \sim \text{Poisson}(\lambda_{i,j,k})$$

$$\lambda_{i,j,k} = \frac{\alpha_{j,k} N_i}{1 + \alpha_{j,k} h_{j,k} N_i} \quad (6)$$

$$\log(\alpha_{j,k}) = \log(\alpha_0) + \beta_{\alpha,c} \log(m_{c,j}) + \beta_{\alpha,r} \log(m_{r,k}) + \mu_{\alpha,j}$$

$$\log(h_{j,k}) = \log(h_0) + \beta_{h,c} \log(m_{c,j}) + \beta_{h,r} \log(m_{r,k}) + \mu_{h,j}$$

where, $\alpha_{j,k}$ is the attack rate ($\text{d}^{-1} \text{m}^{-2}$) of lobster j foraging on mussel size class k , and $h_{j,k}$ is the handling time (d) of lobster j foraging on mussel size class k . We constructed informed priors on all β parameters, where the β s were normally distributed with a mean based on theoretical predictions (Table S1). We assumed gamma distributions with mean 0 for the prior variances. We included a random effect of lobster individual on the estimation of α and h ($\mu_{\alpha,j}$, $\mu_{h,j}$), assuming that errors between individuals were normally distributed with mean 0. See Table S2.1 for further details.

We implemented the model in Stan (Stan Development Team 2022) which uses a Hamiltonian Monte Carlo procedure to estimate parameters. We ran three chains for 25,000 iterations with a burnin of 12,500 iterations and thinned the chains to retain every 3rd iteration. To diagnose model convergence, we visually assessed mixing of the model chains and confirmed using the Gelman-Rubin convergence diagnostic ($\hat{R} < 1.1$) (Brooks and Gelman 1998).

How does metabolism vary with lobster size?

To estimate how lobster metabolism scales with lobster body size, we measured oxygen consumption rates using intermittent flow respirometry. We estimated the metabolism for each lobster used in the foraging trials in addition to thirteen lobster not used in the foraging trials (176 - 1381 g, n = 24 total). Prior to trials, we starved lobsters for 24 h. We then elicited MMR, by chasing lobsters and repeatedly exposing them to air (30 s chase, 30 s air exposure). We performed this sequence 3 times, for a total of 3 minutes, then the lobster was air exposed for 1 min to ensure exhaustion. Immediately following, we placed the lobster in custom-build respirometry chambers (17.89 L; $14.79 \pm 0.09^\circ\text{C}$, $\bar{X} \pm \text{SE}$) and measured oxygen consumption rate to estimate MMR. Lobsters remained in the respirometers overnight (~ 24 hours) while their oxygen consumption was measured on automated cycles (8 min measurement: 15 min flush) to assess SMR. We measured background respiration rates in empty chambers after each respirometry trial and determined that background respiration was negligible.

We estimated each lobster's metabolic rate according to

$$M_{\text{O}_2} = (V - m) \frac{\Delta O_2}{\Delta t} \quad (7)$$

where M_{O_2} is in $\text{mgO}_2 \text{ min}^{-1}$, ΔO_2 is the change in oxygen concentration in water (mgO_2/L), V is the volume of respirometry chamber (L), m is the weight of the lobster (kg), Δt is the measurement length (min). We calculated MMR by estimating the steepest 60-120 s regression slope within the first O_2 measurement cycle. We estimated standard metabolic rate, the metabolism in resting, non-digesting, thermally acclimated individual, by calculating the lowest 15th quantile of all MO_2 values (min = 47, max = 63, average = 56) recorded over

~24 h (Chabot et al. 2016). We calculated AAS by subtracting MMR and SMR (mgO_2/min) and FAS by dividing MMR by SMR.

To determine how standard and maximum metabolic rates vary with body size, we fit power law functions using a Bayesian regression model via the *rstanarm* package (Goodrich et al. 2023). Specifically, we estimated the slope of the relationship between body size, standard metabolic rate, maximum metabolic rate, and their interaction using a log-log regression with weakly informative priors (Table S2). Using a similar procedure, we also estimated the slope of the relationship between body size and absolute aerobic scope and body size and factorial aerobic scope.

Converting to units of energy acquisition and energy required

Our primary goal was to understand how the processes of energy acquisition, or the energetic value of mussels consumed by lobster, and energy requirements, or the energy required to meet an individual's metabolic rate, increase with body size. Therefore, we converted our metric of metabolism ($\text{mg O}_2 \text{ min}^{-1}$) and consumption ($\text{ind. d}^{-1} \text{ m}^{-2}$) to energetic rates (kJ d^{-1}). To convert indices of metabolism we assumed that 1 g oxygen is associated with the release of 13.6 kJ of energy (Cho et al. 1982, Eliason et al. 2008, Steell et al. 2019). To estimate the energetic content of mussels, we first converted all mussel shell lengths to shell-free dry mass (Ceccherelli and Rossi 1984) and then converted to shell-free wet mass using a conversion factor generated for local populations of *M. galloprovincialis* (LTER et al. 2016). Finally, we estimated the energetic content of mussels assuming 0.99 kJ g^{-1} shell-free wet mass (Prado et al. 2020).

3.4. RESULTS

The number of mussels lobster consumed increased with mussel density and lobster size and decreased with mussel size (Fig. 2.2). Changes in the functional response with body size were largely due to the size-dependence of maximum consumption rates (C_{max}). We found no evidence for variation in attack rates with lobster ($\beta_{\alpha,c} = -0.031 [-0.23, 0.07]$, median \pm 95% CI's *unless otherwise noted*) or mussel ($\beta_{\alpha,r} = 0.139 [-0.01, 0.31]$) body size (Fig. S2.1), while maximum consumption rates (the inverse of handling time, h) increased with lobster size ($\beta_{C_{max,c}} = 1.50 [1.12, 1.85]$) and decreased with prey size ($\beta_{C_{max,r}} = -1.33 [-1.05, -1.62]$; Fig. S2.1). However, in units of energy (kJ d⁻¹), the data suggest that lobster consume the same caloric content of mussels regardless of mussel size (Fig. S2.2). For example, an average sized lobster (~540 g) tends to consume 77.2 kJ of mussel whether those calories come from many small or a few large mussels.

As expected, larger lobsters had higher whole animal standard and maximum metabolic rates than smaller lobsters (Fig. 2.3a, Fig. S2.3), but lower mass-specific metabolic rates. Standard and maximum metabolic rates increased with body size at similar rates ($\beta_{SMR}: 0.86 [0.64, 1.06]$, $\beta_{MMR}: 0.77 [0.56, 0.98]$, Table S2.3), with no evidence for differences in the slopes of MMR and SMR ($-0.09 [-0.38, 0.21]$). Accordingly, mass-specific absolute aerobic scope decreased with lobster size ($\beta_{AAS}: -0.23 [-0.48, 0.02]$), while there was no relationship between factorial aerobic scope and body size (Fig. 2.3c; $\beta_{FAS}: -0.09 [-0.38, 0.22]$; Table S2.3).

Despite larger lobsters requiring less energy per unit mass to meet their standard metabolic rate ($\beta_{SMR} < 1$), we found strong evidence that larger lobsters consumed disproportionately more than smaller lobsters. Maximum consumption rate (kJ d⁻¹) increased

with body size to an exponent greater than 1 ($\beta_{C_{max,c}} = 1.50 [1.12, 1.85]$), Fig. 2.3b), such that mass-specific consumption increased with lobster size (e.g., Fig. 1 - H_2). Together our results show that per unit mass, larger lobsters had lower metabolic requirements and higher energy intake rates (Fig. 2.4). Therefore, factorial energy acquired, or the ratio of energy acquisition to energy expenditure on standard metabolic processes, increased with body size (Fig. 2.3d, Fig. 2.4).

3.5. DISCUSSION

Ecologists have traditionally assumed that consumption rates increase with body size at the same or a slower rate than metabolism increases with body size (Peters 1983, Brown et al. 2004, Marshall and White 2019). However, surprisingly few empirical studies have examined the relationships between consumption, metabolism, and body size for individual consumers. Here, we present strong evidence that consumption increased with body size at a faster rate than whole-animal metabolism in California spiny lobster, suggesting that consumer energy intake rates are not necessarily constrained by standard metabolic requirements as previously assumed. Furthermore, our results show that it is possible for larger consumers to consume disproportionately more than smaller conspecifics despite larger consumers having lower mass-specific metabolic requirements (e.g., Fig. 2.1 - H_2). While prevailing theory has assumed that consumption should scale with body size at the same or a slower rate than SMR, acknowledging the possibility for hyperallometric scaling of consumption could dramatically alter the predictions of size-structured trophic models (e.g., (Yodzis and Innes 1992, Berlow et al. 2009)). Moving forward, resolving the relationship between an individual's physiology and their ecological role in a community will

be an important component of advancing mechanistic understanding of how ecosystems function and predicting the consequences of the loss of large consumers.

Across ecosystem types, humans are disproportionately impacting the largest consumers or the largest individuals in consumer populations (Blanchard et al. 2005, Robinson et al. 2017) through harvest and warming temperatures (Baudron et al. 2014, Lindmark et al. 2018, Pauly and Cheung 2018). Despite increases in the abundance of smaller consumers, smaller consumers are often unable to fill the ecological role of their larger counterparts (Shackell et al. 2010, Rudolf and Rasmussen 2013), but the reasons why remain opaque. Basic metabolic arguments would predict that if consumers ate in proportion to their standard metabolic rate, then two smaller individuals should consume more than one large individual of the same biomass (Reiss et al. 2011). For example, empirical work on sunfish predators shows that two small individuals consume a greater amount than one large individual of equivalent biomass (Chalcraft and Resetarits 2004). Our results, however, demonstrate that larger lobster consume disproportionately more than smaller lobster, suggesting that in some instances changes in community structure or function associated with the loss of large consumers may not be compensated for by increases in the abundance of smaller size classes.

There are several potential reasons why larger individuals may consume disproportionately more than smaller individuals. First, larger individuals may have greater energetic requirements than smaller individuals causing larger individuals to consume more per unit mass. Lobster species, like many other marine species (Barneche et al. 2018), display hyperallometric increases in reproductive capacity (DeMartini et al. 2003, MacCormack and DeMont 2003). Increases in mass-specific consumption with size may therefore be a strategy

to cope with the increased costs of reproduction. However, we found that factorial aerobic scope did not change with lobster body size because both SMR and MMR had similar scaling relationships. Because larger lobsters did not have lower metabolic constraints (i.e., higher FAS), it is unlikely that increased energetic costs of reproduction were the driver of larger lobster consuming disproportionately more energy. An alternative explanation is that smaller individuals may reduce their foraging relative to larger conspecifics as a behavioral response. Capturing, processing, and digesting a meal is an energetically costly, and potentially dangerous, process. Therefore, smaller individuals may reduce consumption relative to their larger conspecifics, in order to reserve energy for defense or escape (Jutfelt et al. 2021). Critically, this is a behavioral response and is independent of the scaling of FAS with body size. Smaller lobster are prey to many fish species, while larger lobster are less vulnerable to predation (Loflen and Hovel 2010). Thus, our results suggest that smaller lobsters may be altering their foraging behavior by reducing the amount they eat relative to the amount expected based on their metabolic demand in order to preserve aerobic scope. By not consuming as much food as they could, these smaller individuals may be choosing to avoid allocating energy towards food acquisition and digestion to be able to escape predators.

We acknowledge that it is possible that the observed increases in mass-specific consumption were an experimental artifact. Foraging in natural conditions is far more complex than in simplified mesocosms. Smaller lobster may prefer different prey types than larger lobster, causing depressed foraging in single prey experiments. However, lobster of all sizes are known to forage on mussels (Robles 1987, McCormick 2016), and recent work has demonstrated similar hyperallometric scaling of sea urchin (DiFiore and Stier 2023) and mussel (Csik et al. 2023) consumption by lobster in separate experimental trials.

The extent to which hyperallometric scaling of consumption is common across taxa is largely unclear. Synthetic work on the interspecific scaling of consumption rate with body size found that consumption rates can scale hyperallometrically for consumers foraging in 3-D environments (Pawar et al. 2012). However, the finding was criticized because it did not account for ontogenetic (e.g., intraspecific) variation in body size and because hyperallometry would violate prevailing theory on asymptotic body size (Giacomini et al. 2013). We would argue that hyperallometric scaling of consumption is biologically feasible if a) larger conspecifics have disproportionately higher energetic costs (e.g., for reproduction), b) assimilated energy scales at a lower rate than consumed energy due to the scaling of other physiological processes (excretion, Maino and Kearney 2015; specific dynamic action, Steell et al. 2019) or c) smaller conspecifics are reducing foraging as a behavioral response. A recent meta-analysis of fish species found little evidence for hyperallometric scaling of consumption (Lindmark et al. 2022). However, hyperallometry has been found in the consumption rates of marine invertebrates (Barrios-O'Neill et al. 2019), land snails (Astor et al. 2015), some insects (Maino and Kearney 2015), and in the energy intake rates of large carnivores (Rizzuto et al. 2018). While it remains unclear how common hyperallometry is across different consumers foraging on different prey, accounting for the possibility of hyperallometry could heavily influence current understanding of community and ecosystem dynamics. The recent focus on ecosystem-based approaches to management has increased the use of multispecies to whole-ecosystem models that seek to simulate different harvest scenarios using canonical scaling exponents to estimate consumption rates ($\beta_{C_{max}} = 0.67, 0.75$; Andersen 2019, Blanchard et al. 2014, Soudijn et al. 2022). Exploring how the hyperallometric scaling of consumption rates might alter the predictions of simulation

models, could therefore lead to different advice to decision makers responsible for either consumer or resource populations.

Understanding the physiological mechanisms by which reductions in body size will impact the ecological role of consumers may improve the ability to forecast species interactions in a changing future. Here, we showed lobster metabolic rates were strongly linked to their foraging capacity, but consumption rates did not scale with metabolic rates as predicted by prevailing theory. Rather we found that lobster maximum consumption rates increased with body size per unit mass, despite declining standard metabolic requirements, contrary to commonly assumed bioenergetic scaling relationships. How common the observed patterns are across different consumers or if the pattern holds under natural foraging conditions remains to be seen. However, the possibility that consumption is not constrained by the scaling of standard metabolic rate with body size could be powerful in further developing the bioenergetic factors that drive foraging. Integrating individual organisms' physiology with their ecological role in communities will serve to uncover how and why reductions in consumer body size will alter ecosystems in the future.

ACKNOWLEDGMENTS

I thank Drs. Jameal Samhouri, Dan Reed, Holly Moeller, and the Ocean Recoveries lab group for providing invaluable guidance on previous drafts of this manuscript. This work was funded by an NSF Graduate Research Fellowship, a University of California Chancellor's award, the California Sea Grant Prop 84 grant program (R/OPCOAH-2), and the Santa Barbara Coastal Long-Term Ecological Research program (NSF OCE 1831937).

While this work represents my individual efforts, it would not have been possible without the efforts of many valuable collaborators. Erika Eliason and her lab group including,

Krista Kraskura, Terra Dressler, and Alex Little, conducted the respirometry portions of the experiment. Krista, many thanks for the numerous zoom calls to discuss body size and talk through physiology. Joseph Curtis and Samantha Csik assisted in conducting the foraging experiments. Emily Hardison assisted in revising physiological sections of this manuscript and guided me through estimating the energy content of prey. Michael McCoy constructed previous Bayesian analyses that formed the basis of my own modeling efforts. Adrian Stier and Erika Eliason originally conceived of the project and have been involved in all aspects of its development.

3.6. REFERENCES

- Andersen, K. H. 2019. Preface. Pages ix–x *Fish Ecology, Evolution, and Exploitation*. Princeton University Press.
- Astor, T., L. Lenoir, and M. P. Berg. 2015. Measuring feeding traits of a range of litter-consuming terrestrial snails: leaf litter consumption, feces production and scaling with body size. *Oecologia* 178:833–845.
- Barneche, D. R., D. R. Robertson, C. R. White, and D. J. Marshall. 2018. Fish reproductive-energy output increases disproportionately with body size. *Science* 360:642–645.
- Barrios-O’Neill, D., R. Kelly, and M. C. Emmerson. 2019. Biomass encounter rates limit the size scaling of feeding interactions. *Ecology Letters* 22:1870–1878.
- Baudron, A. R., C. L. Needle, A. D. Rijnsdorp, and C. T. Marshall. 2014. Warming temperatures and smaller body sizes: synchronous changes in growth of North Sea fishes. *Global Change Biology* 20:1023–1031.
- Berlow, E. L., J. A. Dunne, N. D. Martinez, P. B. Stark, R. J. Williams, and U. Brose. 2009. Simple prediction of interaction strengths in complex food webs. *Proceedings of the National Academy of Sciences* 106:187–191.
- Blanchard, J. L., C. Mills, S. Jennings, C. J. Fox, B. D. Rackham, P. D. Eastwood, and C. M. O’Brien. 2005. Distribution-abundance relationships for North Sea Atlantic cod (*Gadus morhua*): observation versus theory. *Canadian Journal of Fisheries and Aquatic Sciences* 62:2001–2009.
- Blanchard, J. L., K. H. Andersen, F. Scott, N. T. Hintzen, G. Piet, and S. Jennings. 2014. Evaluating targets and trade-offs among fisheries and conservation objectives using a multispecies size spectrum model. *Journal of Applied Ecology* 51:612–622.
- Brooks, S. P., and A. Gelman. 1998. General Methods for Monitoring Convergence of Iterative Simulations. *Journal of Computational and Graphical Statistics* 7:434–455.
- Brose, U. 2010. Body-mass constraints on foraging behavior determine population and food-web dynamics. *Functional Ecology* 24:28–34.
- Brown, J. H., J. F. Gillooly, A. P. Allen, V. M. Savage, and G. B. West. 2004. Toward a metabolic theory of ecology. *Ecology* 85:1771–1789.
- Careau, V., S. S. Killen, and N. B. Metcalfe. 2014. Adding fuel to the “fire of life”: energy budgets across levels of variation in ectotherms and endotherms. Pages 219–233 *Integrative Organismal Biology*.
- Ceccherelli, V., and R. Rossi. 1984. Settlement, growth and production of the mussel *Mytilus galloprovincialis*. *Marine Ecology Progress Series* 16:173–184.

- Chalcraft, D. R., and W. J. Reserits. 2004. Metabolic Rate Models and the Substitutability of Predator Populations. *Journal of Animal Ecology* 73:323–332.
- Cho, C. Y., S. J. Slinger, and H. S. Bayley. 1982. Bioenergetics of salmonid fishes: Energy intake, expenditure and productivity. *Comparative Biochemistry and Physiology Part B: Comparative Biochemistry* 73:25–41.
- Csik, S. R., B. P. DiFiore, K. Kraskura, E. A. Hardison, J. S. Curtis, E. J. Eliason, and A. C. Stier. 2023. The metabolic underpinnings of temperature-dependent predation in a key marine predator. *Frontiers in Marine Science* 10.
- Darveau, C.-A., R. K. Suarez, R. D. Andrews, and P. W. Hochachka. 2002. Allometric cascade as a unifying principle of body mass effects on metabolism. *Nature* 417:166–170.
- DeMartini, E., G. T. DiNardo, and H. A. Williams. 2003. Temporal changes in population density, fecundity, and egg size of the Hawaiian spiny lobster (*Panulirus marginatus*) at Necker Bank, Northwestern Hawaiian Islands. *Fishery Bulletin* 101:22–31.
- DiFiore, B. P., and A. C. Stier. 2023. Variation in body size drives spatial and temporal variation in lobster–urchin interaction strength. *Journal of Animal Ecology* 92:1075–1088.
- DiFiore, B., S. Queenborough, E. Madin, V. Paul, M. Decker, and A. Stier. 2019. Grazing halos on coral reefs: predation risk, herbivore density, and habitat size influence grazing patterns visible from space. *Marine Ecology Progress Series*.
- Eliason, E. J., D. A. Higgs, and A. P. Farrell. 2008. Postprandial gastrointestinal blood flow, oxygen consumption and heart rate in rainbow trout (*Oncorhynchus mykiss*). *Comparative Biochemistry and Physiology Part A: Molecular & Integrative Physiology* 149:380–388.
- Emmerson, M. C., and D. Raffaelli. 2004. Predator–prey body size, interaction strength and the stability of a real food web. *Journal of Animal Ecology* 73:399–409.
- Englund, G., G. Öhlund, C. L. Hein, and S. Diehl. 2011. Temperature dependence of the functional response. *Ecology Letters* 14:914–921.
- Essington, T. E., J. F. Kitchell, and C. J. Walters. 2001. The von Bertalanffy growth function, bioenergetics, and the consumption rates of fish. *Canadian Journal of Fisheries and Aquatic Sciences* 58:2129–2138.
- Giacomini, H. C., B. J. Shuter, D. T. de Kerckhove, and P. A. Abrams. 2013. Does consumption rate scale superlinearly? *Nature* 493:E1–E2.
- Glazier, D. S. 2010. A unifying explanation for diverse metabolic scaling in animals and plants. *Biological Reviews* 85:111–138.

- Heather, F. J., J. L. Blanchard, G. J. Edgar, R. Trebilco, and R. D. Stuart-Smith. 2021. Globally consistent reef size spectra integrating fishes and invertebrates. *Ecology Letters* 24:572–579.
- Hein, A. M., C. Hou, and J. F. Gillooly. 2012. Energetic and biomechanical constraints on animal migration distance. *Ecology Letters* 15:104–110.
- Holling, C. S. 1959. Some Characteristics of Simple Types of Predation and Parasitism. *The Canadian Entomologist* 91:385–398.
- Hou, C., W. Zuo, M. E. Moses, W. H. Woodruff, J. H. Brown, and G. B. West. 2008. Energy Uptake and Allocation during Ontogeny. *Science (New York, N.Y.)* 322:736–739.
- Jeschke, J. M., M. Kopp, and R. Tollrian. 2002. Predator Functional Responses: Discriminating Between Handling and Digesting Prey. *Ecological Monographs* 72:95–112.
- Jutfelt, F., T. Norin, E. R. Åsheim, L. E. Rowsey, A. H. Andreassen, R. Morgan, T. D. Clark, and B. Speers-Roesch. 2021. ‘Aerobic scope protection’ reduces ectotherm growth under warming. *Functional Ecology* 35:1397–1407.
- Kalinkat, G., F. D. Schneider, C. Digel, C. Guill, B. C. Rall, and U. Brose. 2013. Body masses, functional responses and predator–prey stability. *Ecology Letters* 16:1126–1134.
- Killen, S. S., D. Atkinson, and D. S. Glazier. 2010. The intraspecific scaling of metabolic rate with body mass in fishes depends on lifestyle and temperature. *Ecology Letters* 13:184–193.
- Killen, S. S., D. S. Glazier, E. L. Rezende, T. D. Clark, D. Atkinson, A. S. T. Willener, and L. G. Halsey. 2016. Ecological Influences and Morphological Correlates of Resting and Maximal Metabolic Rates across Teleost Fish Species. *The American Naturalist* 187:592–606.
- Kleiber, M. 1932. Body size and metabolism. *Hilgardia* 6:315–353.
- Kooijman, S. A. L. M. 2000. *Dynamic Energy and Mass Budgets in Biological Systems*. Cambridge University Press.
- Lindmark, M., M. Huss, J. Ohlberger, and A. Gårdmark. 2018. Temperature-dependent body size effects determine population responses to climate warming. *Ecology Letters* 21:181–189.
- Lindmark, M., J. Ohlberger, and A. Gårdmark. 2022. Optimum growth temperature declines with body size within fish species. *Global Change Biology* 28:2259–2271.

- Loflen, C., and K. Hovel. 2010. Behavioral responses to variable predation risk in the California spiny lobster *Panulirus interruptus*. *Marine Ecology Progress Series* 420:135–144.
- LTER, S. B. C., J. C. Nelson, D. C. Reed, S. Harrer, and R. J. Miller. 2016. SBC LTER: Reef: Kelp Forest Community Dynamics: Kelp Forest Data to support “Estimating biomass of benthic kelp forest invertebrates from body size and percent cover.” Environmental Data Initiative.
- MacCormack, T. J., and M. E. DeMont. 2003. Regional Differences in Allometric Growth in Atlantic Canadian Lobster (*Homarus Americanus*). *Journal of Crustacean Biology* 23:258–264.
- Maino, J. L., and M. R. Kearney. 2015. Ontogenetic and interspecific scaling of consumption in insects. *Oikos* 124:1564–1570.
- Marshall, D. J., and C. R. White. 2019. Have We Outgrown the Existing Models of Growth? *Trends in Ecology & Evolution* 34:102–111.
- McCormick, M. 2016. Variable Spiny Lobster Foraging Across a Variable Intertidal Landscape. SNS Masters Theses 6.
- McCoy, M. W., B. M. Bolker, K. M. Warkentin, and J. R. Vonesh. 2011. Predicting Predation through Prey Ontogeny Using Size-Dependent Functional Response Models. *The American Naturalist* 177:752–766.
- McCoy, M. W., and J. F. Gillooly. 2008. Predicting natural mortality rates of plants and animals. *Ecology Letters* 11:710–716.
- McGill, B. J., and G. G. Mittelbach. 2006. An allometric vision and motion model to predict prey encounter rates. *Evolutionary Ecology Research* 8:691–701.
- Pauly, D., and W. W. L. Cheung. 2018. Sound physiological knowledge and principles in modeling shrinking of fishes under climate change. *Global Change Biology* 24:e15–e26.
- Pawar, S., A. I. Dell, and Van M. Savage. 2012. Dimensionality of consumer search space drives trophic interaction strengths. *Nature* 486:485–489.
- Peters, R. H. 1983. *The Ecological Implications of Body Size*. Cambridge University Press, Cambridge.
- Prado, P., A. Peñas, C. Ibáñez, P. Cabanes, L. Jornet, N. Álvarez, and N. Caiola. 2020. Prey size and species preferences in the invasive blue crab, *Callinectes sapidus*: Potential effects in marine and freshwater ecosystems. *Estuarine, Coastal and Shelf Science* 245:106997.

- Preisser, E. L., and J. L. Orrock. 2012. The allometry of fear: interspecific relationships between body size and response to predation risk. *Ecosphere* 3:art77.
- Rall, B. C., U. Brose, M. Hartvig, G. Kalinkat, F. Schwarzmüller, O. Vucic-Pestic, and O. L. Petchey. 2012. Universal temperature and body-mass scaling of feeding rates. *Philosophical Transactions of the Royal Society B: Biological Sciences* 367:2923–2934.
- Real, L. A. 1977. The Kinetics of Functional Response. *The American Naturalist* 111:289–300.
- Reiss, J., R. A. Bailey, D. M. Perkins, A. Pluchinotta, and G. Woodward. 2011. Testing effects of consumer richness, evenness and body size on ecosystem functioning. *Journal of Animal Ecology* 80:1145–1154.
- Rizzuto, M., C. Carbone, and S. Pawar. 2018. Foraging constraints reverse the scaling of activity time in carnivores. *Nature Ecology & Evolution* 2:247–253.
- Robinson, J. P. W., I. D. Williams, A. M. Edwards, J. McPherson, L. Yeager, L. Vigliola, R. E. Brainard, and J. K. Baum. 2017. Fishing degrades size structure of coral reef fish communities. *Global Change Biology* 23:1009–1022.
- Robles, C. 1987. Predator Foraging Characteristics and Prey Population Structure on a Sheltered Shore. *Ecology* 68:1502–1514.
- Rudolf, V. H. W., and N. L. Rasmussen. 2013. Ontogenetic functional diversity: Size structure of a keystone predator drives functioning of a complex ecosystem. *Ecology* 94:1046–1056.
- Santini, L., and N. J. B. Isaac. 2021. Rapid Anthropocene realignment of allometric scaling rules. *Ecology Letters* 24:1318–1327.
- Savage, V. M., J. F. Gillooly, J. H. Brown, G. B. West, and E. L. Charnov. 2004. Effects of Body Size and Temperature on Population Growth. *The American Naturalist* 163:429–441.
- Schmitz, O. J., A. P. Beckerman, and K. M. O'Brien. 1997. Behaviorally Mediated Trophic Cascades: Effects of Predation Risk on Food Web Interactions. *Ecology* 78:1388–1399.
- Shackell, N. L., K. T. Frank, J. A. D. Fisher, B. Petrie, and W. C. Leggett. 2010. Decline in top predator body size and changing climate alter trophic structure in an oceanic ecosystem. *Proceedings of the Royal Society B: Biological Sciences* 277:1353–1360.
- Sheldon, R. W., A. Prakash, and W. H. Sutcliffe. 1972. The Size Distribution of Particles in the Ocean. *Limnology and Oceanography* 17:327–340.

- Soudijn, F. H., P. D. van Denderen, M. Heino, U. Dieckmann, and A. M. de Roos. 2021. Harvesting forage fish can prevent fishing-induced population collapses of large piscivorous fish. *Proceedings of the National Academy of Sciences* 118.
- Stan Development Team. 2022. *Stan Modeling Language Users Guide and Reference Manual*. 2.29.
- Steell, S. C., T. E. Van Leeuwen, J. W. Brownscombe, S. J. Cooke, and E. J. Eliason. 2019. An appetite for invasion: digestive physiology, thermal performance and food intake in lionfish (*Pterois* spp.). *Journal of Experimental Biology* 222:jeb209437.
- Uiterwaal, S. F., and J. P. DeLong. 2020. Functional responses are maximized at intermediate temperatures. *Ecology* 101:e02975.
- Weitz, J. S., and S. A. Levin. 2006. Size and scaling of predator–prey dynamics. *Ecology Letters* 9:548–557.
- West, G. B., J. H. Brown, and B. J. Enquist. 1997. A General Model for the Origin of Allometric Scaling Laws in Biology. *Science* 276:122–126.
- West, G., J. Brown, and B. Enquist. 2001. A general model for ontogenic growth. *Nature* 413:628–31.
- White, C. R., P. Cassey, and T. M. Blackburn. 2007. Allometric Exponents Do Not Support a Universal Metabolic Allometry. *Ecology* 88:315–323.
- White, C. R., and R. S. Seymour. 2003. Mammalian basal metabolic rate is proportional to body mass^{2/3}. *Proceedings of the National Academy of Sciences* 100:4046–4049.
- Yodzis, P., and S. Innes. 1992. Body Size and Consumer-Resource Dynamics. *The American Naturalist* 139:1151–1175.

3.7. FIGURES AND FIGURE CAPTIONS

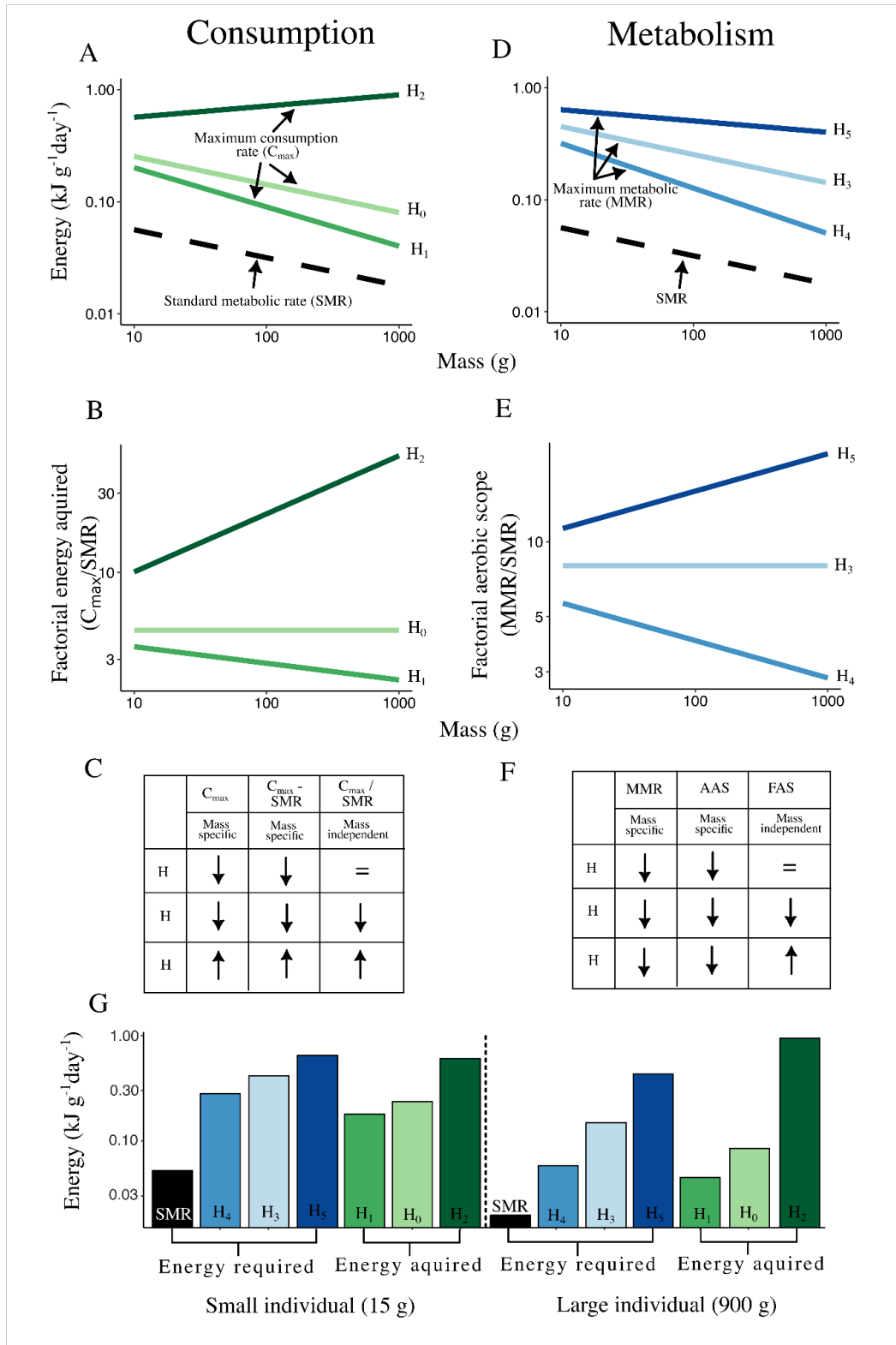


Figure 2.1. There are three hypothetical relationships between maximum consumption rate (C_{max} , energy intake), SMR (energy required), and body size (A). Energy intake per unit mass

may decrease with body size at a slower rate than metabolism (H_1), decrease with body size at the same rate as metabolism (H_0), or increase with body size at a faster rate than metabolism (H_3). Factorial energy acquired, or ratio of energy acquired and energy required to meet SMR, varies depending on how energy intake scales with body size (B, C). Across taxa and across individuals within a species, SMR and MMR tend to decrease with body size per unit mass (D). However, the relationship between the scaling of SMR and MMR with body size is largely unknown. MMR may scale with body size at the same rate as SMR (H_3), decrease with body size at a faster rate than SMR (H_4), or decrease with body size at a slower rate than SMR (H_5). Differences in the scaling of MMR relative to SMR can lead to differences in factorial aerobic scope ($FAS = MMR/SMR$) or absolute aerobic scope ($AAS = MMR - SMR$) (C, E). Absolute aerobic scope represents the amount of energy an organism has to conduct physiological processes after meeting its standard metabolic requirements and is considered to represent the energetic *capacity* of the organism. Factorial aerobic scope is a unitless, mass-independent estimate and represents the energetic *constraints* on an organism. Panel G summarizes the bioenergetics of two hypothetical consumers at both ends of the size range (15 and 900 g). For scaling coefficients see *Appendix 6.2.1*.

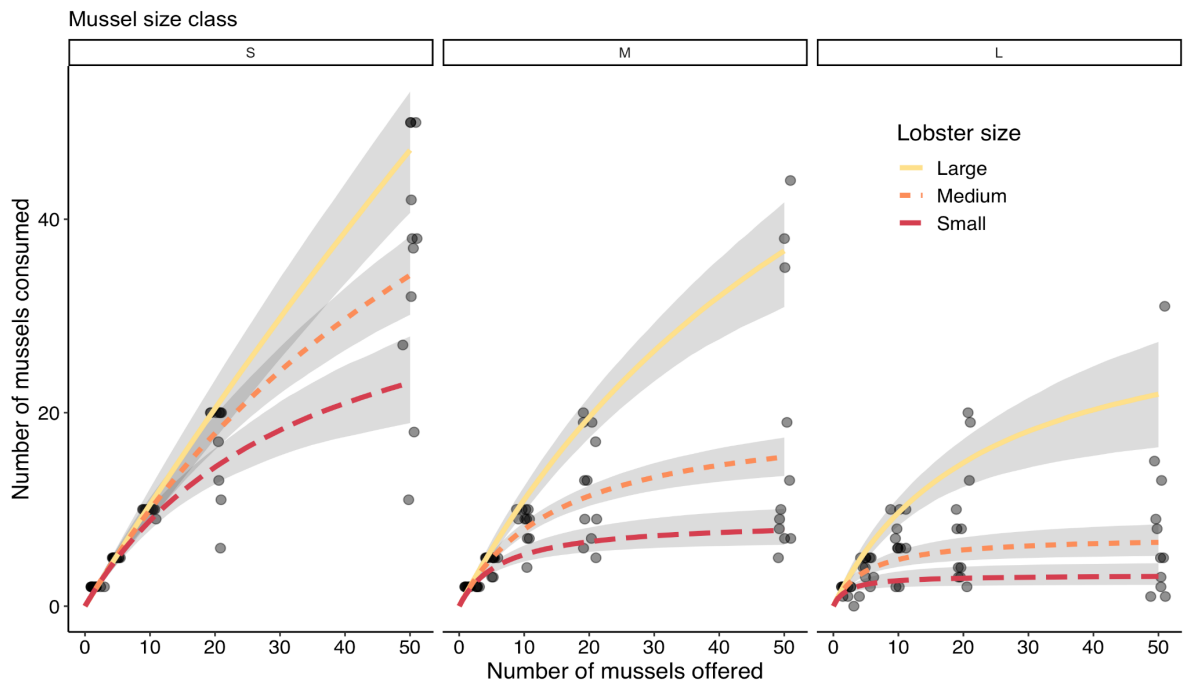


Figure 2.2. Functional response of lobster consuming mussel prey. Data points are observed consumption from mesocosm foraging experiments where individual lobsters preyed on different densities of three size classes of mussels. Colored lines and surrounding gray shading are the median \pm 95% CIs predicted consumption rates from a Bayesian hierarchical model for lobster at the 10th, mean, and 90th percentiles (small, medium, and large respectively) of the size distribution of lobsters used in the experiment.

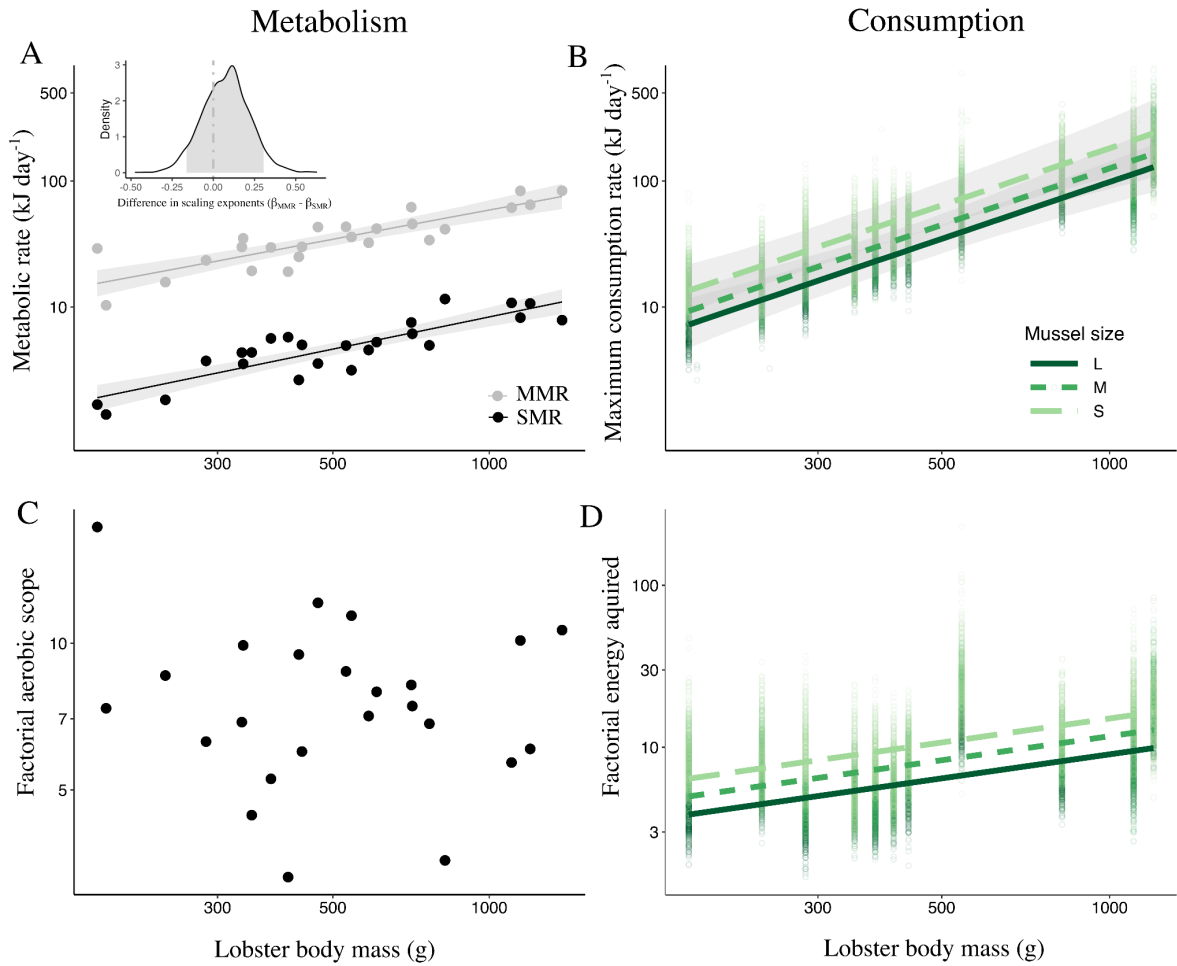


Figure 2.3. (A) Scaling of maximum (MMR, $\beta_{MMR} = 0.77$ [0.5-1.0]) and standard (SMR, $\beta_{SMR} = 0.85$ [0.7-1.1]) metabolic rates with lobster body size. Lines and surrounding gray shading are the median \pm 95% CI from a Bayesian regression model. Inlaid panel in A is the posterior estimate for the difference in scaling coefficients for MMR and SMR. (B) Estimated maximum consumption rates (C_{max} , $\beta_{C_{max}} = 1.50$ [1.1 - 1.9]) for each lobster preying on different sized mussels. Data are 100 draws from the posterior distribution of each lobster's C_{max} , while lines and surrounding shading at median \pm 95% CIs for the scaling of energy intake with body size for each mussel size class. (C) Factorial aerobic scope did not vary with lobster body size because MMR and SMR scaled at similar rates ($\beta_{FAS} = -0.082$ [-0.37, 0.20]). However, (D) factorial energy acquired (FEA = C_{max} / SMR) increased with lobster body size ($\beta_{FEA} = 0.49$). Lines in D are median posterior predictions from a Bayesian regression model. Confidence intervals are not plotted in D because they would be dependent on the number of draws from the posterior for the C_{max} of each lobster.

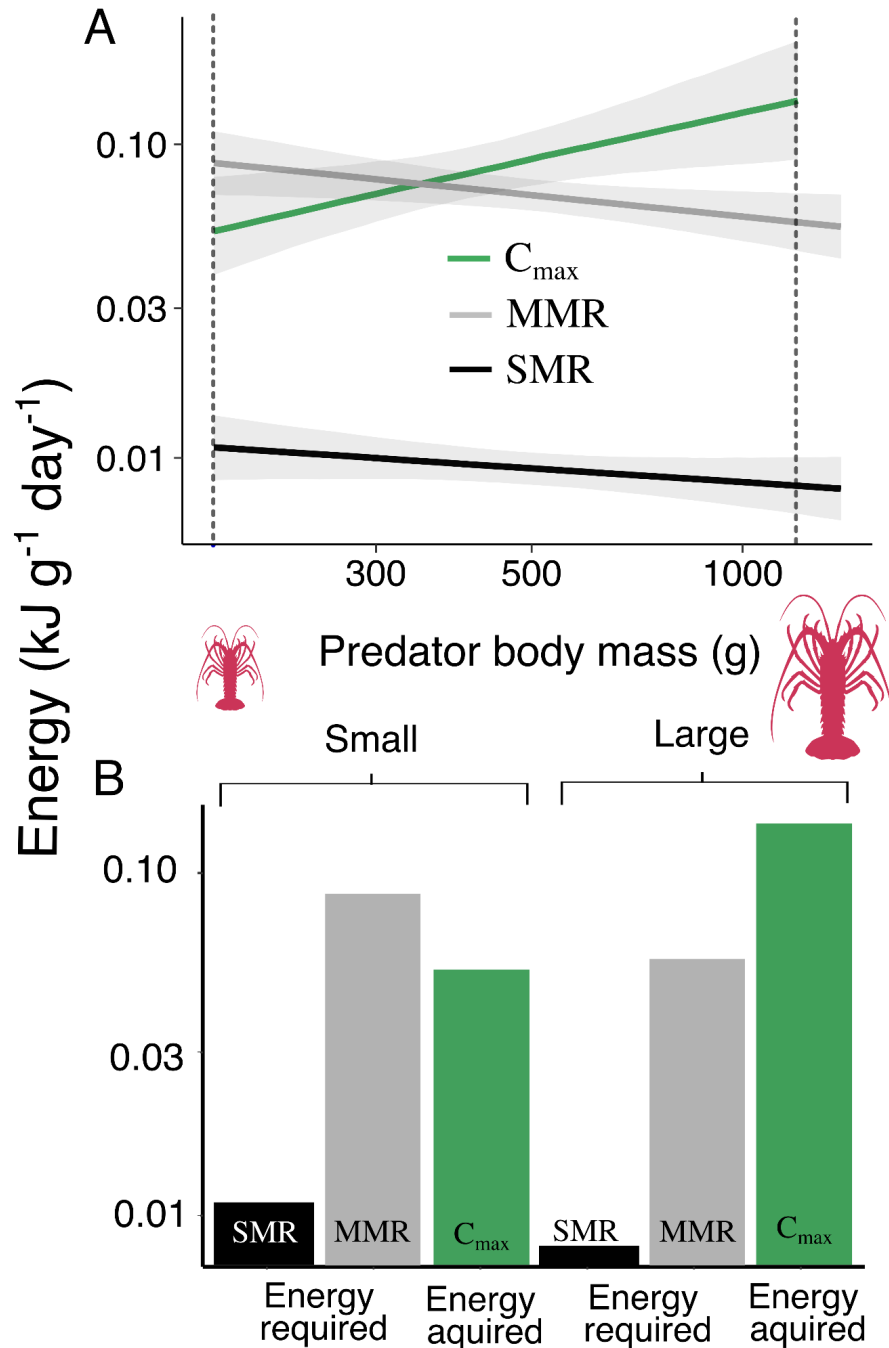


Figure 2.4. (A) Mass specific rates of energy intake and energy requirements for lobster foraging on mussel prey. Model predictions are the same as Fig. 2.3 except displayed per unit mass. Energy intake increases with lobster body size per unit mass at a rate > 1 , while the energy required to meet standard and maximum metabolic rate decreases per unit mass. Vertical dashed lines represent the size of lobster in B. (B) Estimated rates of energy required and acquired for small (176 g) and large (1199 g) lobster.

4. CHAPTER III

Historical variability in a marine foundation species mediates benthic competition to determine current community structure.

4.1. ABSTRACT

Healthy populations of foundation species mediate the structure, function, and services of the communities they inhabit. However, anthropogenic effects, including species introductions and global climate change, are causing the decline of foundation species in a diverse array of systems on land and in the ocean. Such declines have spurred numerous efforts to restore foundation species, under the assumption that restoring the foundation will restore the ecosystem and the services it provides. Yet, effective restoration will depend on understanding how long after a foundation species is lost will its role in the community dissipate, and how long after it recovers will the community regain its structure and function. Here, we address these general questions by testing the role that historic population fluctuations play in mediating non-trophic interactions in communities structured by giant kelp (*Macrocystis pyrifera*), a marine, canopy-forming foundation species. First, we used a theoretical model of kelp forest community dynamics to generate hypotheses for how historic disturbance regimes (frequency, severity, and timing) to giant kelp impact the benthic cover of two major functional groups, epilithic sessile invertebrates and understory algae, that compete for space on the seafloor. We then tested the directional hypotheses generated by our model using a data set that combined multi-decadal time series of kelp canopy cover with observational data of benthic community structure collected at 68 locations. Our results showed that the cover of understory algae and sessile invertebrate cover was best explained by current kelp canopy biomass. However, the time since the last kelp canopy absence and

disturbance frequency were important components of predicting spatial variation in benthic community structure. Together, our results highlight how historic fluctuation in a foundation species can cause variation in ecological communities across space, and may aid restoration of kelp forests, and other ecosystems organized around foundation species.

4.2. INTRODUCTION

Foundation species are habitat forming organisms such as trees, corals, and seagrasses that form the major structural elements of an ecosystem and have disproportionately strong impacts on the surrounding community (Dayton 1972, Ellison et al. 2005). By generating favorable physical environments and providing resources or habitat to other species (Jones et al. 1994, Jenkins et al. 1999, Thomsen et al. 2018), thriving populations of foundation species can bolster biodiversity, facilitate biogeochemical cycling, and mediate ecosystem processes through non-trophic interactions (Baiser et al. 2013, Borst et al. 2018, *see* Ellison 2019 *for review*). Despite their indispensable role in ecosystems, many populations of foundation species have experienced considerable declines (Vergés et al. 2016, Case et al. 2017, Sorte et al. 2017, Fields and Silbiger 2022). However, to fully understand the consequences of declining foundation species and the utility of their restoration ecologists need to answer two critical questions: 1) Following the loss of a foundation species, how much time elapses before its effects fade away? 2) Over what duration must a foundation species persist for its impacts to be present? Answering these questions will help to uncover the drivers of spatial and temporal variation in community structure and generate key insights into management and restoration that focuses on foundation species as indicators of ecosystem health and services.

Ecological theory can offer insight into how historic dynamics, such as the time since a foundation species is lost or reestablished, alter the role a foundation species plays in the surrounding community. For example, in a paper titled “The ghost of competition present” Miller et al (2009) showed that even when a species is outcompeted from a system, its temporary presence alters species interactions into the future. The literature on historical contingencies and ecological memory shows that the timing of species arrivals in the past (e.g., priority effects, Fukami 2015), legacy effects associated with prior disturbances (Fukami 2001, Chase 2007, Cuddington 2011, Johnstone et al. 2016, Hughes et al. 2019) or biotic legacies stemming from the remnant skeletons or nutrients of dead organisms (Miller et al. 2021, Kopecky et al. 2023) can profoundly reshape the pathways of community assembly. Therefore, the loss of a foundation species may not cause immediate community collapse because of the services or structures they leave behind. Likewise, it may take time for a community to recover following the reestablishment of a foundation species because of past contingencies whose effects may still dissipate into the present.

Kelp forests are productive, biodiverse ecosystems centered around canopy-forming algae that function as foundation species by providing habitat, modulating environmental conditions, and mediating trophic and non-trophic interactions in the associated community (Schiel and Foster 2015, Teagle et al. 2017, Miller et al. 2018). Recent analyses suggest that there is substantial geographic variation in the long-term trends of kelp populations (Krumhansl et al. 2016, Cavanaugh et al. 2019a). However, well-publicized evidence for regional declines in kelp abundance (Beas-Luna et al. 2020, McPherson et al. 2021, Starko et al. 2022), have spurred numerous calls to restore kelp habitat (California Protection Council 2021), in hopes of mitigating the associated loss of ecosystem services (e.g., Smale et al.

2019). Kelp populations display highly variable temporal dynamics across a range of spatial scales (Castorani et al. 2015) due to wave disturbance (Reed et al. 2011), urchin herbivory (Bell et al. 2015, Rennick et al. 2022), and natural senescence (Rodriguez et al. 2013, Bell and Siegel 2022), making the goal of kelp restoration a seeming “moving target” (*sensu* Ingeman et al. 2019). Therefore, the historic dynamics of a foundation species, like kelp, could have long-lasting implications on the structure and function of a community, which would be critical to understand in order to inform restoration efforts.

Here, we ask, how does spatial variation in the historic population dynamics of a foundation species mediate spatial variability in community structure? To address this question, we focused on rocky subtidal reef communities dominated by the canopy-forming alga *Macrocystis pyrifera* (*hereafter*, kelp). Kelp grows exceptionally fast (3.5% d⁻¹ average; Rassweiler et al. 2018) and has a short lifespan (<5 years; Dayton et al. 1999) relative to other foundation species, making kelp communities an excellent system to examine the effects of historic variability on community structure. We specifically focus on non-trophic interactions between the canopy-forming kelp and two functional groups that compete for space on the seafloor: epilithic sessile invertebrates (e.g., sponges, bryozoans, bivalves, anthozoans, ascidians, *hereafter* “sessile invertebrates”) and understory macroalgae (e.g., small low-lying foliose, filamentous, subcanopy algae, *hereafter* “understory algae”). Unlike sessile invertebrates, understory algae require light to grow. Previous work has shown that increases in kelp canopy result in decreases in the cover of understory algae, allowing for an indirect positive effect on the cover of sessile invertebrates (Fig. 3.1a, Arkema et al. 2009). Based on the evidence that kelp mediates competition between guilds on the benthos, we hypothesized that historic fluctuations in kelp canopy cover could impact the relative balance

of sessile invertebrates and understory algae into the future, and underlying spatial variation in benthic community structure (Fig. 3.1b,c).

To test our hypothesis that historical fluctuations in kelp impact current benthic structure we used a combination of theoretical modeling and empirical data. Because of the inherent variability in kelp population dynamics, we first used a theoretical model to determine: 1) how historic disturbance intensity, frequency, and timing alters the current structure of kelp communities, and 2) how long we might expect shifts in benthic structure to persist. We then tested the directional hypotheses that emerged from our theoretical simulations using a data set that combined multi-decadal time series of satellite-derived kelp canopy biomass with observations of kelp communities at 68 different locations.

Understanding how historic fluctuations in a foundation species impact the structure of the associated community uncovers the mechanisms driving variation in ecological communities across space and helps to inform the restoration of not only kelp forests, but other critical habitats organized around foundation species.

4.3. Methods

Theoretical model and simulations

Kelp populations are highly dynamic and their associated communities can be notoriously variable across space and time (Dayton 1985, Bell and Siegel 2022). To understand when and to what extent historic kelp dynamics might impact benthic community structure, we modified an existing ordinary differential equation model of kelp community dynamics (*see* Detmer et al. 2021). Our goal in simulating community dynamics from the model was to generate directional hypotheses that we could test using observational data.

Specifically, we sought to understand a) the levels of historic disturbance (frequency, timing, and intensity) that lead to changes in the relative percent cover of understory algae and sessile invertebrates and b) how long these changes might persist in the benthic community.

Here, we briefly review the model but please refer to Appendix 6.3.1 and Detmer et al. (2021) for a more detailed description and equations. We modeled kelp population dynamics by tracking three stages in kelp life-history: the recruitment of haploid gametophytes, small juvenile sporophytes, and large canopy-forming adult sporophytes. In this model, the gametophytic stage experiences constant external recruitment (Reed et al. 1997), and maturation from gametophyte to juvenile sporophyte and juvenile to adult sporophyte is governed by light availability to the seafloor. Growth of adult kelp is light-dependent, and adults senesce according to a phenomenological function (Rodriguez et al. 2013) that allows for synchronous and asynchronous senescence depending on the time since the last disturbance event.

We assumed that sessile invertebrates and understory algae competed for physical space on the seafloor according to classic Lotka-Volterra competition equations. Unlike sessile invertebrates, understory macroalgae are photosynthetic. Therefore, understory algae growth was dependent on the amount of light reaching the seafloor, which, in turn, was mediated by the abundance of canopy-forming kelp. We explicitly model light using an exponential decay function that depended on adult kelp abundance, such that when adult kelp was at its carrying capacity, only 10% of light reached the seafloor (Reed and Foster 1984). In the model, when kelp is absent and benthic light levels are high, understory algae grow rapidly and outcompete invertebrates. By contrast, when kelp is abundant, its dense canopy shades the benthos and reduces the growth rate of understory algae, thereby indirectly

facilitating sessile invertebrate populations (Fig. 3.1a). Sessile invertebrates and understory algae experience a constant external recruitment and senescence. Detmer et al. (2021) showed that the model was able to replicate the benthic dynamics in observational data collected at one site by emulating a similar historical disturbance regime.

We used this model structure to simulate different historic dynamics in the kelp population, and tracked how these historic effects impacted the sessile invertebrate and understory algae populations (Fig. 3.1b,c). We first calculated the equilibrium abundances of kelp, invertebrates, and algae in the absence of any disturbance. We then ran simulations in which we varied the intensity, frequency, and the time since the last historic disturbance. Large wave events, a major cause of disturbance to kelp (Reed et al. 2011), might only affect the kelp population. However, if the wave event is large enough, it may also remove sessile invertebrates, understory algae, and juvenile kelp sporophytes, a process we term benthic scouring. We assumed that disturbances occur annually, that 100% of kelp was removed at each disturbance, and we manipulated the scouring (e.g., percent removal) of sessile inverts and understory algae.

Despite the extensive work on California kelp forest ecosystems, little is currently known on the strength of competition, growth rates, or recruitment dynamics of sessile invertebrates and understory algae. To explore the sensitivity of our results to these parameters, we therefore also ran simulations in which we varied competition coefficients, growth rates, and external recruitment (Table S1).

Through these simulations we were interested in understanding what metrics of historic disturbance (frequency, intensity, or time since the last disturbance) had the strongest impact on benthic structure and how long the community took to recover. To estimate

community recover time, we calculated the length of time for sessile invertebrates and understory algae percent cover to return to within 5% of pre-disturbance conditions.

Satellite-derived estimates of historic kelp variability

To estimate historic variability in kelp dynamics we utilized quarterly kelp canopy biomass estimates derived from Landsat satellite images (SBC LTER et al. 2023). This data set was developed by estimating the fraction of each 30x30 m Landsat pixel occupied by kelp and converting that fraction into an estimate of kelp canopy biomass (Bell et al. 2020).

Our theoretical analysis of community recovery times suggested that benthic communities likely recover from historic disturbances within at least 10 years (Fig. 3.2). Therefore, we focused on a 10-year period (2008-2018), to assess metrics of kelp disturbance in the satellite data set. We defined a disturbance not by a specific mechanism (e.g., large wave event, sand inundation, urchin herbivory, etc.), but as an 80% decline in kelp canopy biomass that persisted for at least 6-months (two quarters). To avoid pinpointing disturbances when kelp biomass was already low, kelp canopy biomass had to be $\geq 10\%$ of its 10-year maximum. Thus, we estimated disturbance frequency (E) as

$$E = \sum_{t=1}^{t=n} \begin{cases} 1, & k_{t-1} \geq 0.1 * k_{max} \\ & k_t < 0.2 * k_{t-1} \\ & k_{t+1} < 0.2 * k_{t-1} \\ 0 \end{cases} \quad (1)$$

where t is time in quarters of a year, k is kelp canopy biomass, and k_{max} is the maximum canopy biomass over the 10-year period.

We also estimated the amount of time since the last 6-month period when kelp canopy was absent and the proportion of time over the 10-year period when kelp canopy biomass was estimated from the satellite imagery to be zero. The Landsat sensor may fail to

accurately estimate kelp canopy cover when kelp cover is low ($\leq 16\%$ occupancy in a pixel), and all estimated values below this threshold are assigned 0% cover in the data set. Thus, while we discuss instances where kelp was absent, it is possible that kelp was present but at low density. For a summary of all metrics of historic variability see Table S2.

Observational data on kelp community structure

Using the historic kelp canopy data set, and identified 69 locations (*hereafter*, transects) spread across 17 distinct kelp patches (e.g., Castorani et al. 2015, Cavanaugh et al. 2019, *hereafter* sites) that differed along a gradient from highly disturbed to highly persistent kelp dynamics. At each transect, we assessed benthic community structure along 40 x 2 m transects using a combination of swath, quadrat, and uniform point count (UPC) survey techniques. We estimated the current biomass of kelp by counting the number of fronds > 1 m along the 40 x 2 m swath and converting to biomass using an established regression relationship (Rassweiler et al. 2018). We estimated the abundance of two species of sea urchin (*Strongylocentrotus purpuratus*, *Mesocentrotus franciscanus*) using 1 m² quadrats at 6 locations evenly spaced along the transect and converted urchin abundance to urchin biomass using relationships developed for the study region (Reed et al. 2016). Finally, we measured the percent cover of the seafloor occupied by understory algae, sessile invertebrates, and sand using UPC method at 80 points evenly spaced 0.5 m away from either side of the center transect line. The UPC technique quantified the presence of each species under a single point due to the layered nature of the benthos. Thus, percent cover estimates can exceed 100%.

We located the starting coordinates of each transect using the onboard GPS (~3 m accuracy), and recorded the transect bearing from a dive compass, such that we could

estimate the end location of the transect. We assumed that kelp canopy adjacent to the transect would impact benthic community structure through shading effects. Therefore, we created a 30 m buffer around the transect line and extracted historic kelp-canopy data for a 120x60 m region centered on each transect.

Data analysis

To analyze the observational data on algal and invertebrate cover, we used a generalized linear mixed effects modeling (GLMM) approach. Specifically, we modeled how the percent cover of sessile invertebrates and understory algae responded to three metrics of historic variability in kelp disturbance (number of disturbances, time since last disturbance, and proportion of time kelp canopy was absent). Previous work shows that kelp forest community structure is strongly impacted by sea urchin abundance, sand cover, and current kelp biomass (Miller et al. 2018, Castorani et al. 2021, Rennick et al. 2022). Therefore, we included current kelp biomass, urchin biomass, and the percent cover of sand estimated from the observational surveys as covariates in our models. We treated percent cover as the response variable and included a categorical predictor indicating if the percent cover was sessile invertebrate or understory algae. We then modeled the interactions between benthic guild and each continuous predictor. To compare the magnitude of each continuous predictor, we scaled all variables such that $\bar{X} = 0$ and $\sigma = 1$. To account for the fact that transects were nested within sites and that kelp biomass dynamics at transects within sites were not independent, we included a random intercept effect of site.

We implemented the generalized linear mixed effects models in a Bayesian framework using the *rstanarm* package (Goodrich et al. 2023). Percent cover data must be

positive and our UPC surveys allowed for estimates of percent cover greater than 100%. Therefore, we assumed the data followed a gamma distribution. We used weakly informative priors on all parameters, and we assessed model fit using the \hat{r} statistic and visual inspection of posterior chains.

While we were interested in exploring how historic variability in kelp dynamics impacted the aggregate cover of sessile invertebrates and understory algae, species within these groups may respond differently to kelp variability based on their specific ecology and life histories. To assess the multivariate response of the benthic community to the three metrics of historic kelp variability, we conducted a canonical correlation analysis (CCA) of the Bray-Curtis dissimilarity matrix using the *vegan* package (Oksanen et al. 2022). We also identified the 10 most common species within each benthic guild and estimated the Spearman's rank order correlation coefficient between the percent cover of each species and each metric of historic kelp variability in order to identify whether different species within the broad taxonomic groups responded differently to historic variation in kelp canopy biomass.

4.4. Results

Simulations of theoretical model

Our model simulations showed that immediately following a disturbance, understory algae cover increased due to increased light availability. However, kelp canopy rapidly recovers, reducing light levels and allowing sessile invertebrates to outcompete understory algae and reclaim space on the seafloor (Fig. 3.2a). Typically, this process was rapid: sessile invertebrates and understory algae returned to equilibrium levels within 4-5 years of the

event (Fig. 3.2b). Increasing the number of historic disturbances from 1 to 2, doubled the return time of the community, but there was little effect of disturbance frequency on recovery time after three consecutive disturbances (Fig. 3.2b). The slowest recoveries were associated with disturbances that eliminated 100% of kelp and 100% of the benthic community, while lower levels of benthic scouring increased the speed that the community recovered (Fig. 3.2c).

Altering the life-history parameters of sessile invertebrates relative to their competitors changed the equilibrium cover of both guilds. Decreasing the growth rate or the rate of external recruitment of sessile invertebrates relative to understory algae, slowed the recovery of the community, allowing understory algae to persist at higher cover for longer (Fig. S3.1a,b). Similarly, making sessile invertebrates the stronger competitor, while simultaneously lowering their growth rates and external recruitment (e.g., more k-selected) lengthened the time it took for the community to recover relative to default parameters (Fig. S3.1c).

We used the results of our theoretical simulations to guide our analyses and generate directional hypotheses that could be tested with observational data. Because the model suggested that the benthic community would recover within 3-5 years, we selected a 10-year historical window to examine the effects of kelp variability on benthic structure. Within this 10-year period, we then tested the prediction, stemming from the model simulations, that the time since the last disturbance will have a greater impact on benthic structure than other characteristics of historic kelp dynamics, like disturbance frequency.

Impact of historic variability in kelp canopy biomass on observed benthic community structure

Satellite-derived estimates of kelp canopy biomass revealed stark variation in historic kelp dynamics among transects (Fig. 3.3a,b). At some sites kelp canopy biomass fluctuated dramatically (Fig. 3.3c), while at others kelp was disturbed and failed to recover to previous levels (Fig. 3.3d) or recovered after a prolonged absence (Fig. 3.3e).

These different patterns in kelp dynamics were associated with differences in the structure of the benthic community. Results of the GLMMs showed the strongest predictor of current benthic structure (e.g., the percent cover of sessile invertebrates and understory algae), on average, was current kelp biomass (Fig. 3.4a). Higher current kelp biomass was correlated with a higher percent cover of sessile invertebrates and a lower percent cover of understory algae, which is consistent with prevailing evidence that kelp indirectly facilitates the cover of sessile invertebrates by limiting the growth and percent cover of understory algae (e.g., Fig. 3.1a). However, metrics of historic kelp variability had impacts on current benthic structure that were almost as strong as current kelp biomass (Fig. 3.4a). For example, time since the last kelp absence had 56% as strong of a negative effect on understory algae cover and 44% as strong of a positive effect on sessile invertebrate cover as current kelp biomass.

Our theoretical simulations suggested that time since the last kelp absence should have a stronger impact on community structure than disturbance frequency. However, we found that the effect size of disturbance frequency and time since the last kelp absence were of similar magnitude (Fig. 3.4b,c). As the frequency of historic disturbances increased from 0-7, we observed a 41.2% increase in understory algae and a 20.0% decrease in sessile

invertebrate cover (Fig. 3.4c). Similarly, as the time since the last kelp canopy absence increased from 0 to 10 years, understory algae declined by 28.2%, and sessile invertebrates cover increased 32.9% (Fig. 3.4b). There was little evidence that the proportion of time kelp was absent had any impact on sessile invertebrate or understory algae cover. Urchin biomass was negatively correlated with understory algae and positively correlated with sessile invertebrate cover. The proportion of the transect that was sand was negatively associated with sessile invertebrate and positively associated with understory algae (Fig. 3.4a).

Species-level responses to historic kelp variability

Understory algae and sessile invertebrate guilds are composed of many species, each with specific life history and ecological characteristics that may result in different responses to historic disturbance. In multivariate space, species in the benthic community differentiated along axes associated with metrics of historic kelp variability. Sessile invertebrate species tended to be associated with increases in current kelp biomass and the time since the last kelp extinction, while understory algae species were associated with increases in the number of disturbances (Fig. 3.5a). However, there was considerable interspecific variation in how species responded to these metrics of historic kelp dynamics. For example, *most* algae displayed positive correlations and *most* invertebrates displayed negative correlations with disturbance frequency (Fig. 3.5c), consistent with the results of our guild-level models (e.g., Fig. 3.4). However, one alga and four invertebrates displayed the opposite or no correlation with disturbance frequency (Fig. 3.5c). We found a similar pattern for the effects of time since last kelp absence, with many species responding as expected by their guild-level responses, but a few responding differently (Fig. 3.5d). Thus, our functional group

classifications are not monoliths. Rather, there is considerable species-level complexity in the responses to historic variability in the foundation, which interacts with their relative percent cover to determine the guild-level responses.

4.5. DISCUSSION

Many of the world's foundation species have seen significant declines in recent decades due to global climate change and other anthropogenic impacts (Vergés et al. 2016, Case et al. 2017, Sorte et al. 2017, Ramus et al. 2017, Fields and Silbiger 2022). However, climate change is expected to not only drive directional declines in populations but increase stochasticity in population dynamics (Boyce et al. 2006, Pearson et al. 2014). While the effects of foundation species loss are well documented (Ellison 2019), it is unclear how increased variability in the population dynamics of the foundation species will impact the associated community. Understanding how population fluctuations in the foundation species alters the web of interactions in a community is essential to effective restoration efforts. Here, we use a fast-growing foundation species with a short generation time to demonstrate that the historic dynamics of the foundation species are a strong determinant of the current structure of the community. Our results suggest that accounting for historic dynamics will be critical to restoration efforts that aim to revitalize the structure, function, and services of communities following the loss, or recovery, of foundation species.

Predictions of community structure using novel technologies

Considering the extent by which climate change and other anthropogenic drivers are impacting foundation species, there is a pressing need to develop technologies that monitor

not only the foundation species but their associated community. Satellite remote sensing has expanded ecologists' ability to monitor patterns and processes at landscape to global scales (Lui et al. 2002, Westberry et al. 2023, Pettoirelli et al. 2018), yet most work has focused on species visible in satellite imagery. Only recently have researchers begun to explore the use of satellite remote sensing to monitor the structure of ecological communities not delineated in the imagery (Skidmore et al. 2021). For example, remote sensing has been used to monitor species interactions on coral reefs (Madin et al. 2019, DiFiore et al. 2019), to predict changes in the structure of temperate open-ocean communities (Decker et al. 2023), or to inform species distribution models in marine (Kavanaugh et al. 2021) or terrestrial environments (Pinto-Ledezma and Cavender-Bares 2021). Here, we demonstrate the utility of using satellite remote sensing of kelp canopy biomass to estimate changes in benthic community structure. Our results show that both current kelp canopy and the history of kelp canopy dynamics are necessary to predict the relative abundance of sessile invertebrates and understory algae. By combining *in situ* data from long-term ecological monitoring programs with satellite-derived estimates of foundation species abundance, it may be possible to integrate historic population fluctuations into predictions of community structure, which could aid monitoring and restoration efforts across different ecosystem types.

The role of historic contingencies in kelp forest community dynamics

Kelp forest communities can display considerable variation from site to site and year to year, and an abundance of work has sought to understand the factors that underlie this variability (Harrold and Reed 1985, Miller et al. 2018, Rennick et al. 2022, Liu and Gaines 2022). Yet, to date, only a few studies have explored the extent to which historic

contingencies account for variation in the structure of kelp forest communities. For example, Brynes et al. (2011) demonstrated that sessile invertebrate diversity was affected by the previous year's kelp abundance almost as strongly as the current kelp abundance. More recently, researchers conducted a decade-long experiment where they annually removed kelp, and demonstrated that disturbance frequency, more than disturbance severity, impacted kelp community structure (Castorani et al. 2018). Increasing biomass of understory algae increased net primary productivity from understory algae (NPP), but such increases in NPP were not able to compensate for the loss of kelp associated NPP (Castorani et al. 2021). Our research contributes to this growing body of work by suggesting that interactions between benthic guilds is, at least in part, controlled by historical context. Knowing only the current abundance of kelp cover is not enough to predict the relative abundance of algae and invertebrates on the seafloor. Rather, it is critical to also account for the historic dynamics of kelp—as the timing and frequency of disturbances to kelp is linked to the relative cover of algae and sessile invertebrates.

The matches and mismatches between the theoretical model simulations and analysis of the observational data provides insight into the potential mechanisms through which history impacts community structure. Our initial simulation analysis assumed that light attenuation on the benthos by kelp was mediated by the time since the last kelp disturbance—not disturbance frequency—and that those factors drove benthic structure and recovery time. We did not include explicit mechanisms by which stochastic processes, such as random variability in benthic recruitment, birth/death rates, or resulting priority effects (e.g., Song et al. 2020, Dudgeon and Petraitis 2022), may have impacted the community's response to historic kelp dynamics. As a result, recovery in the model was determined by the relative

cover of the benthic community following the last disturbance and the growth rates and competitive abilities of both functional guilds. However, from the analysis of the observational data, we found compelling evidence that the frequency of historic disturbances was a strong driver of benthic structure. We suspect that the importance of disturbance frequency on observed benthic structure may hint at the prevalence of stochastic community assembly processes, such as priority effects, operating in kelp forest systems (e.g., Chase 2003, Fukami et al. 2010). Increases in the number of historic disturbances could interact with recruitment events to allow the proliferation of particular algae species limiting resource availability (e.g., space) for sessile invertebrates. Adding this important complexity to the theoretical model introduced here is a ripe area for future research.

The suspicion that stochastic community assembly processes is a potential means through which historic fluctuations in the foundation species impact community structure is supported by our species level analysis. Sessile invertebrates and understory algae did not display monolithic responses to metrics of historic variability, suggesting that there is considerable interspecific complexity in how species respond to previous kelp fluctuations. While it is generally assumed that understory algae are faster growing than sessile invertebrates (Lamy et al. 2020), there is likely overlap in the growth rates and generation times of specific understory algae and sessile invertebrate species. For example, crustose coralline algae (EC) are long-lived perennials and appear to respond to historic kelp variability in a similar manner to most sessile invertebrate species (e.g., decreasing with the number of disturbances and increasing with the time since the last disturbance). However, more ephemeral algae species, such as *Desmarestia ligulata* (DE), were negatively correlated with the time since the last kelp absence and showed only weak positive correlations with

disturbance frequency. Thus, our results reinforce the pattern documented in many systems that more ephemeral species grow rapidly following a kelp disturbance, before being outcompeted by slower growing more persistent species.

Implications of historical contingencies for restoration

Global initiatives such as the United Nation's Decade of Restoration (2021-2030) highlight the need to develop better strategies for ecosystem restoration (Cooke et al. 2019, Smith et al. 2023). Foundation species are often targeted for restoration under the assumption that reviving the foundation will revive the ecosystem and associated services (Saunders et al. 2020). However, not all restoration efforts are successful (van der Heide et al. 2007), or restoration efforts succeed in recovering the foundation, but the associated ecosystem services either fail to recover or display lagged responses (Suding 2011). Our results add to the body of evidence that historical contingencies, such as the historic population fluctuations in a foundation species studied here, can have lasting implications on community structure (Chase 2003, Fukami et al. 2015) and alter the outcomes of restoration efforts (Catano et al. 2023). Thus, incorporating the historical dynamics of a foundation species could help to explain variation in restoration outcomes (Brudvig et al. 2017), identify restoration targets (Ingeman et al. 2019), and improve predictions of when and where restoration will be successful (Brudvig and Catano 2021). By understanding the historic context of the foundation species, practitioners may be able to accelerate the restoration of ecosystems, reviving the structure, function, and essential services they provide to humans and nature.

ACKNOWLEDGMENTS

I thank the Ocean Recoveries lab group for providing invaluable guidance on previous drafts of this manuscript. This research would not have been possible without the efforts of all personnel at the SBC LTER. In particular, I would like to thank Joe Curtis, Sarah Sampson, and Clint Nelson for their field sampling efforts. This work was funded by an NSF Graduate Research Fellowship, a University of California Chancellor's award, the California Sea Grant Prop 84 grant program (R/OPCOAH-2), and the Santa Barbara Coastal Long-Term Ecological Research program (NSF OCE 1831937).

While this work represents my individual efforts, it would not have been possible without many valuable collaborators. Raine Detmer developed the theoretical model that we modified to run simulations in this paper. An Bui, Kai Kopecky, and Billie Beckley helped develop models, revised previous drafts, and ran supplemental analyses. Dan Reed, Bob Miller, Max Castorani, Tom Bell, Li Kui, Jameal Samhour, and Holly Moeller provided data guidance, field sampling support, and revised previous versions of the manuscript. Adrian Stier, along with myself and others, conceived the study and advised on all aspects of its completion. Adrian, many thanks for your patience seeing this project through to the end.

4.6. REFERENCES

- Arkema, K. K., D. C. Reed, and S. C. Schroeter. 2009. Direct and indirect effects of giant kelp determine benthic community structure and dynamics. *Ecology* 90:3126–3137.
- Baiser, B., N. Whitaker, and A. M. Ellison. 2013. Modeling foundation species in food webs. *Ecosphere* 4:art146.
- Beas-Luna, R., F. Micheli, C. B. Woodson, M. Carr, D. Malone, J. Torre, C. Boch, J. E. Caselle, M. Edwards, J. Freiwald, S. L. Hamilton, A. Hernandez, B. Konar, K. J. Kroeker, J. Lorda, G. Montaña-Moctezuma, and G. Torres-Moye. 2020. Geographic variation in responses of kelp forest communities of the California Current to recent climatic changes. *Global Change Biology* 26:6457–6473.
- Bell, T. W., J. G. Allen, K. C. Cavanaugh, and D. A. Siegel. 2020. Three decades of variability in California’s giant kelp forests from the Landsat satellites. *Remote Sensing of Environment* 238:110811.
- Bell, T. W., K. C. Cavanaugh, D. C. Reed, and D. A. Siegel. 2015. Geographical variability in the controls of giant kelp biomass dynamics. *Journal of Biogeography* 42:2010–2021.
- Bell, T. W., and D. A. Siegel. 2022. Nutrient availability and senescence spatially structure the dynamics of a foundation species. *Proceedings of the National Academy of Sciences* 119.
- Borst, A. C. W., W. C. E. P. Verberk, C. Angelini, J. Schotanus, J.-W. Wolters, M. J. A. Christianen, E. M. van der Zee, M. Derksen-Hooijberg, and T. van der Heide. 2018. Foundation species enhance food web complexity through non-trophic facilitation. *PLOS ONE* 13:e0199152.
- Boyce, M. S., C. V. Haridas, C. T. Lee, and the N. S. D. W. Group. 2006. Demography in an increasingly variable world. *Trends in Ecology & Evolution* 21:141–148.
- Brudvig, L. A., R. S. Barak, J. T. Bauer, T. T. Caughlin, D. C. Laughlin, L. Larios, J. W. Matthews, K. L. Stuble, N. E. Turley, and C. R. Zirbel. 2017. Interpreting variation to advance predictive restoration science. *Journal of Applied Ecology* 54:1018–1027.
- Brudvig, L. A., and C. P. Catano. 2021. Prediction and uncertainty in restoration science. *Restoration Ecology* n/a:e13380.
- Byrnes, J. E., D. C. Reed, B. J. Cardinale, K. C. Cavanaugh, S. J. Holbrook, and R. J. Schmitt. 2011. Climate-driven increases in storm frequency simplify kelp forest food webs. *Global Change Biology* 17:2513–2524.
- California Protection Council. 2021. Interim action plan for Protecting and Restoring California’s Kelp Forests.

- Case, B. S., H. L. Buckley, A. A. Barker-Plotkin, D. A. Orwig, and A. M. Ellison. 2017. When a foundation crumbles: forecasting forest dynamics following the decline of the foundation species *Tsuga canadensis*. *Ecosphere* 8:e01893.
- Castorani, M. C. N., S. L. Harrer, R. J. Miller, and D. C. Reed. 2021. Disturbance structures canopy and understory productivity along an environmental gradient. *Ecology Letters* 24:2192–2206.
- Castorani, M. C. N., D. C. Reed, and R. J. Miller. 2018. Loss of foundation species: disturbance frequency outweighs severity in structuring kelp forest communities. *Ecology* 99:2442–2454.
- Castorani, M. C., D. C. Reed, F. Alberto, T. W. Bell, R. D. Simons, K. C. Cavanaugh, D. A. Siegel, and P. T. Raimondi. 2015. Connectivity structures local population dynamics: a long-term empirical test in a large metapopulation system. *Ecology* 96:3141–3152.
- Catano, C. P., A. M. Groves, and L. A. Brudvig. 2023. Community assembly history alters relationships between biodiversity and ecosystem functions during restoration. *Ecology* 104:e3910.
- Cavanaugh, K. C., D. C. Reed, T. W. Bell, M. C. N. Castorani, and R. Beas-Luna. 2019a. Spatial Variability in the Resistance and Resilience of Giant Kelp in Southern and Baja California to a Multiyear Heatwave. *Frontiers in Marine Science* 6.
- Cavanaugh, K. C., D. A. Siegel, P. T. Raimondi, and F. Alberto. 2019b. SBC LTER: Spatial definitions of giant kelp (*Macrocystis pyrifera*) patches in southern and central California. Environmental Data Initiative.
- Chase, J. M. 2003. Community assembly: when should history matter? *Oecologia* 136:489–498.
- Chase, J. M. 2007. Drought mediates the importance of stochastic community assembly. *Proceedings of the National Academy of Sciences* 104:17430–17434.
- Cooke, S. J., J. R. Bennett, and H. P. Jones. 2019. We have a long way to go if we want to realize the promise of the “Decade on Ecosystem Restoration.” *Conservation Science and Practice* 1:e129.
- Cuddington, K. 2011. Legacy Effects: The Persistent Impact of Ecological Interactions. *Biological Theory* 6:203–210.
- Dayton, P. K. 1972. Toward an understanding of community resilience and the potential effects of enrichments to the benthos at McMurdo Sound, Antarctica. Pages 81–96 *Proceedings of the Colloquium on Conservation Problems in Antarctica*. Allen Press.
- Dayton, P. K. 1985. Ecology of Kelp Communities. *Annual Review of Ecology and Systematics* 16:215–245.

- Dayton, P. K., M. J. Tegner, P. B. Edwards, and K. L. Riser. 1999. Temporal and spatial scales of kelp demography: The role of oceanographic climate. *Ecological Monographs* 69.
- Decker, M. B., R. D. Brodeur, L. Ciannelli, L. L. Britt, N. A. Bond, B. P. DiFiore, and G. L. Hunt. 2023. Cyclic variability of eastern Bering Sea jellyfish relates to regional physical conditions. *Progress in Oceanography* 210:102923.
- Detmer, A. R., R. J. Miller, D. C. Reed, T. W. Bell, A. C. Stier, and H. V. Moeller. 2021. Variation in disturbance to a foundation species structures the dynamics of a benthic reef community. *Ecology* 102:e03304.
- DiFiore, B. P., S. A. Queenborough, E. M. P. Madin, V. J. Paul, M. B. Decker, and A. C. Stier. 2019. Grazing halos on coral reefs: predation risk, herbivore density, and habitat size influence grazing patterns that are visible from space. *Marine Ecology Progress Series* 627:71–81.
- Dudgeon, S. R., and P. S. Petraitis. 2022. Experimental evidence for resilience of rockweeds on rocky shores in the Gulf of Maine, USA. *Limnology and Oceanography* 67:S211–S223.
- Ellison, A. M. 2019. Foundation Species, Non-trophic Interactions, and the Value of Being Common. *iScience* 13:254–268.
- Ellison, A. M., M. S. Bank, B. D. Clinton, E. A. Colburn, K. Elliott, C. R. Ford, D. R. Foster, B. D. Kloeppel, J. D. Knoepp, G. M. Lovett, J. Mohan, D. A. Orwig, N. L. Rodenhouse, W. V. Sobczak, K. A. Stinson, J. K. Stone, C. M. Swan, J. Thompson, B. V. Holle, and J. R. Webster. 2005. Loss of Foundation Species: Consequences for the Structure and Dynamics of Forested Ecosystems. *Frontiers in Ecology and the Environment* 3:479.
- Fields, J., and N. Silbiger. 2022. Foundation species loss alters multiple ecosystem functions within temperate tidepool communities. *Marine Ecology Progress Series* 683:1–19.
- Fukami, T. 2001. Sequence effects of disturbance on community structure. *Oikos* 92:215–224.
- Fukami, T. 2015. Historical Contingency in Community Assembly: Integrating Niches, Species Pools, and Priority Effects. *Annual Review of Ecology, Evolution, and Systematics* 46:1–23.
- Fukami, T., I. A. Dickie, J. Paula Wilkie, B. C. Paulus, D. Park, A. Roberts, P. K. Buchanan, and R. B. Allen. 2010. Assembly history dictates ecosystem functioning: evidence from wood decomposer communities: Carbon dynamics and fungal community assembly. *Ecology Letters* 13:675–684.
- Goodrich, B., J. Gabry, I. Ali, and S. Brilleman. 2023. *rstanarm*: Bayesian applied regression modeling via Stan.

- Harrold, C., and D. C. Reed. 1985. Food Availability, Sea Urchin Grazing, and Kelp Forest Community Structure. *Ecology* 66:1160–1169.
- van der Heide, T., E. H. van Nes, G. W. Geerling, A. J. P. Smolders, T. J. Bouma, and M. M. van Katwijk. 2007. Positive Feedbacks in Seagrass Ecosystems: Implications for Success in Conservation and Restoration. *Ecosystems* 10:1311–1322.
- Hughes, T. P., J. T. Kerry, S. R. Connolly, A. H. Baird, C. M. Eakin, S. F. Heron, A. S. Hoey, M. O. Hoogenboom, M. Jacobson, G. Liu, M. S. Pratchett, W. Skirving, and G. Torda. 2019. Ecological memory modifies the cumulative impact of recurrent climate extremes. *Nature Climate Change* 9:40–43.
- Ingeman, K. E., J. F. Samhour, and A. C. Stier. 2019. Ocean recoveries for tomorrow's Earth: Hitting a moving target. *Science* 363.
- Jenkins, J. C., J. D. Aber, and C. D. Canham. 1999. Hemlock woolly adelgid impacts on community structure and N cycling rates in eastern hemlock forests. *Canadian Journal of Forest Research* 29:630–645.
- Johnstone, J. F., C. D. Allen, J. F. Franklin, L. E. Frelich, B. J. Harvey, P. E. Higuera, M. C. Mack, R. K. Meentemeyer, M. R. Metz, G. L. Perry, T. Schoennagel, and M. G. Turner. 2016. Changing disturbance regimes, ecological memory, and forest resilience. *Frontiers in Ecology and the Environment* 14:369–378.
- Jones, C. G., J. H. Lawton, and M. Shachak. 1994. Organisms as Ecosystem Engineers. *Oikos* 69:373–386.
- Kavanaugh, M. T., T. Bell, D. Catlett, M. A. Cimino, S. C. Doney, W. Klajbor, M. Messié, E. Montes, F. E. Muller-Karger, D. Otis, J. A. Santora, I. D. Schroeder, J. Triñanes, and D. A. Siegel. 2021. Satellite Remote Sensing and the Marine Biodiversity Observation Network: Current Science and Future Steps. *Oceanography* 34:62–79.
- Kopecky, K. L., A. C. Stier, R. J. Schmitt, S. J. Holbrook, and H. V. Moeller. 2023. Material legacies can degrade resilience: Structure-retaining disturbances promote regime shifts on coral reefs. *Ecology* 104:e4006.
- Krumhansl, K. A., D. K. Okamoto, A. Rassweiler, M. Novak, J. J. Bolton, K. C. Cavanaugh, S. D. Connell, C. R. Johnson, B. Konar, S. D. Ling, F. Micheli, K. M. Norderhaug, A. Pérez-Matus, I. Sousa-Pinto, D. C. Reed, A. K. Salomon, N. T. Shears, T. Wernberg, R. J. Anderson, N. S. Barrett, A. H. Buschmann, M. H. Carr, J. E. Caselle, S. Derrien-Courtel, G. J. Edgar, M. Edwards, J. A. Estes, C. Goodwin, M. C. Kenner, D. J. Kushner, F. E. Moy, J. Nunn, R. S. Steneck, J. Vásquez, J. Watson, J. D. Witman, and J. E. K. Byrnes. 2016. Global patterns of kelp forest change over the past half-century. *Proceedings of the National Academy of Sciences* 113:13785–13790.
- Lamy, T., C. Koenigs, S. J. Holbrook, R. J. Miller, A. C. Stier, and D. C. Reed. 2020. Foundation species promote community stability by increasing diversity in a giant kelp forest. *Ecology* 101:e02987.

- Liu, J., J. M. Chen, J. Cihlar, and W. Chen. 2002. Net primary productivity mapped for Canada at 1-km resolution. *Global Ecology and Biogeography* 11:115–129.
- Liu, O. R., and S. D. Gaines. 2022. Environmental context dependency in species interactions. *Proceedings of the National Academy of Sciences* 119:e2118539119.
- Madin Elizabeth M. P., Harborne Alastair R., Harmer Aaron M. T., Luiz Osmar J., Atwood Trisha B., Sullivan Brian J., and Madin Joshua S. 2019. Marine reserves shape seascapes on scales visible from space. *Proceedings of the Royal Society B: Biological Sciences* 286:20190053.
- McPherson, M. L., D. J. I. Finger, H. F. Houskeeper, T. W. Bell, M. H. Carr, L. Rogers-Bennett, and R. M. Kudela. 2021. Large-scale shift in the structure of a kelp forest ecosystem co-occurs with an epizootic and marine heatwave. *Communications Biology* 4:1–9.
- Miller, A. D., H. Inamine, A. Buckling, S. H. Roxburgh, and K. Shea. 2021. How disturbance history alters invasion success: biotic legacies and regime change. *Ecology Letters* 24:687–697.
- Miller, R. J., K. D. Lafferty, T. Lamy, L. Kui, A. Rassweiler, and D. C. Reed. 2018. Giant kelp, *Macrocystis pyrifera*, increases faunal diversity through physical engineering. *Proceedings of the Royal Society B: Biological Sciences* 285:20172571.
- Miller, T. E., C. P. terHorst, and J. H. Burns. 2009. The Ghost of Competition Present. *The American Naturalist* 173:347–353.
- Oksanen, J., G. L. Simpson, F. G. Blanchet, R. Kindt, P. Legendre, P. R. Minchin, R. B. O’Hara, P. Solymos, M. H. H. Stevens, E. Szoecs, H. Wagner, M. Barbour, M. Bedward, B. Bolker, D. Borcard, G. Carvalho, M. Chirico, M. D. Caceres, S. Durand, H. B. A. Evangelista, R. FitzJohn, M. Friendly, B. Furneaux, G. Hannigan, M. O. Hill, L. Lahti, D. McGlenn, M.-H. Ouellette, E. R. Cunha, T. Smith, A. Stier, C. J. F. T. Braak, and J. Weedon. 2022. *vegan: Community Ecology Package*.
- Pearson, R. G., J. C. Stanton, K. T. Shoemaker, M. E. Aiello-Lammens, P. J. Ersts, N. Horning, D. A. Fordham, C. J. Raxworthy, H. Y. Ryu, J. McNees, and H. R. Akçakaya. 2014. Life history and spatial traits predict extinction risk due to climate change. *Nature Climate Change* 4:217–221.
- Pettorelli, N., H. Schulte to Bühne, A. Tulloch, G. Dubois, C. Macinnis-Ng, A. M. Queirós, D. A. Keith, M. Wegmann, F. Schrodtt, M. Stellmes, R. Sonnenschein, G. N. Geller, S. Roy, B. Somers, N. Murray, L. Bland, I. Geijzendorffer, J. T. Kerr, S. Broszeit, P. J. Leitão, C. Duncan, G. El Serafy, K. S. He, J. L. Blanchard, R. Lucas, P. Mairota, T. J. Webb, and E. Nicholson. 2018. Satellite remote sensing of ecosystem functions: opportunities, challenges and way forward. *Remote Sensing in Ecology and Conservation* 4:71–93.

- Pinto-Ledezma, J. N., and J. Cavender-Bares. 2021. Predicting species distributions and community composition using satellite remote sensing predictors. *Scientific Reports* 11:16448.
- Ramus, A. P., B. R. Silliman, M. S. Thomsen, and Z. T. Long. 2017. An invasive foundation species enhances multifunctionality in a coastal ecosystem. *Proceedings of the National Academy of Sciences* 114:8580–8585.
- Rassweiler, A., D. C. Reed, S. L. Harrer, and J. C. Nelson. 2018. Improved estimates of net primary production, growth, and standing crop of *Macrocystis pyrifera* in Southern California. *Ecology* 99:2132–2132.
- Reed, D. C., J. C. Nelson, S. L. Harrer, and R. J. Miller. 2016. Estimating biomass of benthic kelp forest invertebrates from body size and percent cover data. *Marine Biology* 163:101.
- Reed, D. C., A. Rassweiler, M. H. Carr, K. C. Cavanaugh, D. P. Malone, and D. A. Siegel. 2011. Wave disturbance overwhelms top-down and bottom-up control of primary production in California kelp forests. *Ecology* 92:2108–2116.
- Rennick, M., B. P. DiFiore, J. Curtis, D. C. Reed, and A. C. Stier. 2022. Detrital supply suppresses deforestation to maintain healthy kelp forest ecosystems. *Ecology* 103:e3673.
- Rodriguez, G. E., A. Rassweiler, D. C. Reed, and S. J. Holbrook. 2013. The importance of progressive senescence in the biomass dynamics of giant kelp (*Macrocystis pyrifera*). *Ecology* 94:1848–1858.
- Saunders, M. I., C. Doropoulos, E. Bayraktarov, R. C. Babcock, D. Gorman, A. M. Eger, M. L. Vozzo, C. L. Gillies, M. A. Vanderklift, A. D. L. Steven, R. H. Bustamante, and B. R. Silliman. 2020. Bright Spots in Coastal Marine Ecosystem Restoration. *Current Biology* 30:R1500–R1510.
- SBC LTER, S. B. C., T. W. Bell, K. C. Cavanaugh, and D. A. Siegel. 2023. SBC LTER: Time series of quarterly NetCDF files of kelp biomass in the canopy from Landsat 5, 7 and 8, since 1984 (ongoing). Environmental Data Initiative.
- Schiel, D. R., and M. S. Foster. 2015. *The Biology and Ecology of Giant Kelp Forests*.
- Skidmore, A. K., N. C. Coops, E. Neinavaz, A. Ali, M. E. Schaepman, M. Paganini, W. D. Kissling, P. Vihervaara, R. Darvishzadeh, H. Feilhauer, M. Fernandez, N. Fernández, N. Gorelick, I. Geijzendorffer, U. Heiden, M. Heurich, D. Hobern, S. Holzwarth, F. E. Muller-Karger, R. Van De Kerchove, A. Lausch, P. J. Leitão, M. C. Lock, C. A. Mücher, B. O’Connor, D. Rocchini, C. Roeoesli, W. Turner, J. K. Vis, T. Wang, M. Wegmann, and V. Wingate. 2021. Priority list of biodiversity metrics to observe from space. *Nature Ecology & Evolution* 5:896–906.

- Smale, D. A., T. Wernberg, E. C. J. Oliver, M. Thomsen, B. P. Harvey, S. C. Straub, M. T. Burrows, L. V. Alexander, J. A. Benthuyssen, M. G. Donat, M. Feng, A. J. Hobday, N. J. Holbrook, S. E. Perkins-Kirkpatrick, H. A. Scannell, A. Sen Gupta, B. L. Payne, and P. J. Moore. 2019. Marine heatwaves threaten global biodiversity and the provision of ecosystem services. *Nature Climate Change* 9:306–312.
- Smith, R. S., S. L. Cheng, and M. C. N. Castorani. 2023. Meta-analysis of ecosystem services associated with oyster restoration. *Conservation Biology* 37:e13966.
- Song, C., S. V. Ahn, R. P. Rohr, and S. Saavedra. 2020. Towards a Probabilistic Understanding About the Context-Dependency of Species Interactions. *Trends in Ecology & Evolution* 35:384–396.
- Sorte, C. J. B., V. E. Davidson, M. C. Franklin, K. M. Benes, M. M. Doellman, R. J. Etter, R. E. Hannigan, J. Lubchenco, and B. A. Menge. 2017. Long-term declines in an intertidal foundation species parallel shifts in community composition. *Global Change Biology* 23:341–352.
- Starko, S., C. J. Neufeld, L. Gendall, B. Timmer, L. Campbell, J. Yakimishyn, L. Druehl, and J. K. Baum. 2022. Microclimate predicts kelp forest extinction in the face of direct and indirect marine heatwave effects. *Ecological Applications* 32:e2673.
- Suding, K. N. 2011. Toward an Era of Restoration in Ecology: Successes, Failures, and Opportunities Ahead. *Annual Review of Ecology, Evolution, and Systematics* 42:465–487.
- Teagle, H., S. J. Hawkins, P. J. Moore, and D. A. Smale. 2017. The role of kelp species as biogenic habitat formers in coastal marine ecosystems. *Journal of Experimental Marine Biology and Ecology* 492:81–98.
- Thomsen, M. S., A. H. Altieri, C. Angelini, M. J. Bishop, P. E. Gribben, G. Lear, Q. He, D. R. Schiel, B. R. Silliman, P. M. South, D. M. Watson, T. Wernberg, and G. Zotz. 2018. Secondary foundation species enhance biodiversity. *Nature Ecology & Evolution* 2:634–639.
- Vergés, A., C. Doropoulos, H. A. Malcolm, M. Skye, M. Garcia-Pizá, E. M. Marzinelli, A. H. Campbell, E. Ballesteros, A. S. Hoey, A. Vila-Concejo, Y.-M. Bozec, and P. D. Steinberg. 2016. Long-term empirical evidence of ocean warming leading to tropicalization of fish communities, increased herbivory, and loss of kelp. *Proceedings of the National Academy of Sciences* 113:13791–13796.
- Westberry, T. K., G. M. Silsbe, and M. J. Behrenfeld. 2023. Gross and net primary production in the global ocean: An ocean color remote sensing perspective. *Earth-Science Reviews* 237:104322.

4.7. FIGURES AND FIGURE CAPTIONS

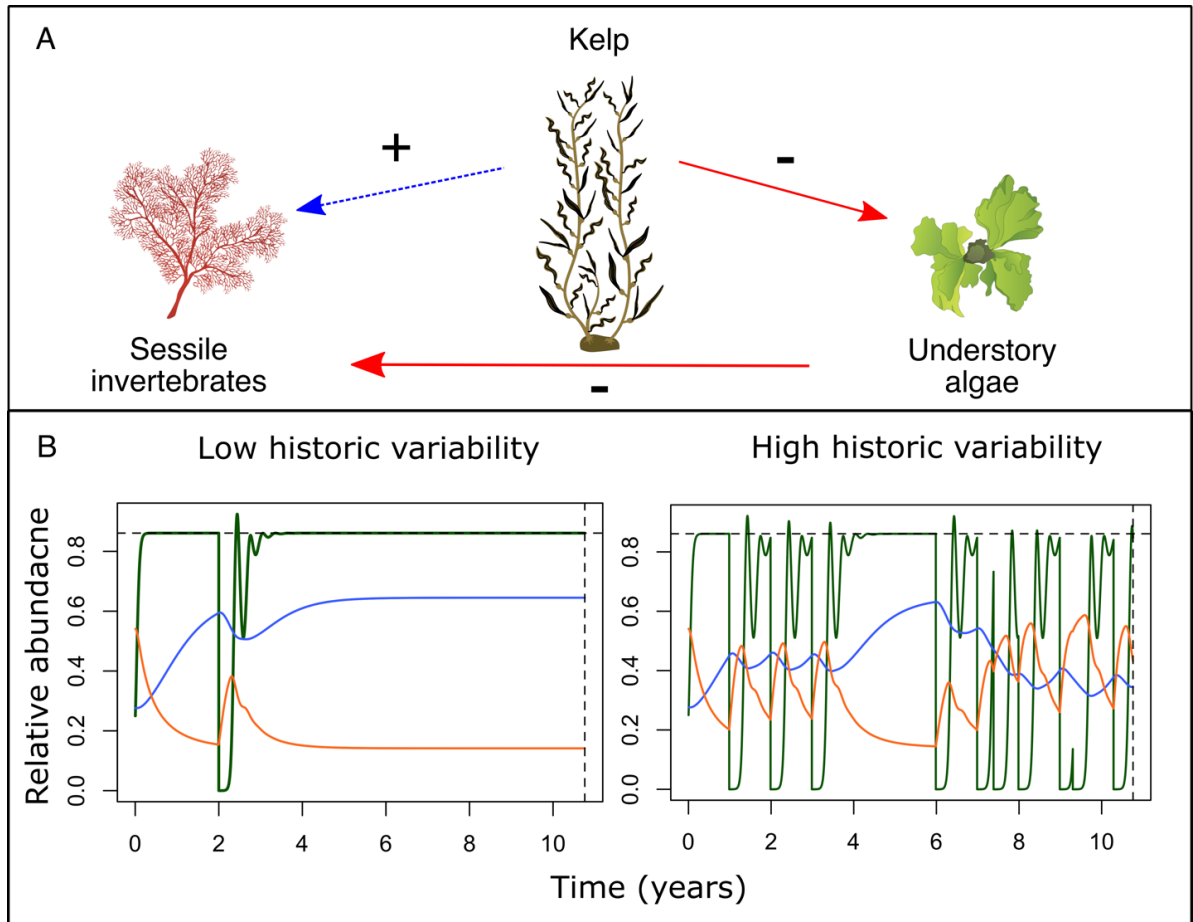


Figure 3.1. Conceptual diagram of non-trophic interactions between three benthic functional groups in California kelp forests (A). Kelp (*Macrocystis pyrifera*) forms a dense canopy, reducing light levels to the seafloor, leading to declines in understory algae abundance. Understory algae and epilithic sessile invertebrates compete for space. Therefore, kelp indirectly facilitates sessile invertebrate cover. In this paper, we hypothesize that it is not just the current kelp abundance that mediates benthic competition, but historic kelp population dynamics. For instance, at a site with low historic kelp variability, understory algae cover may be at low relative to sessile invertebrate cover when kelp is at its carrying capacity (B, Kelp = green, understory algae = orange, sessile invertebrates = blue). However, at a site with highly variable kelp dynamics, kelp can be at the same abundance, but understory algae may dominate the benthos. Time series were generated by simulating a theoretical model of kelp community dynamics (see *Methods* for details).

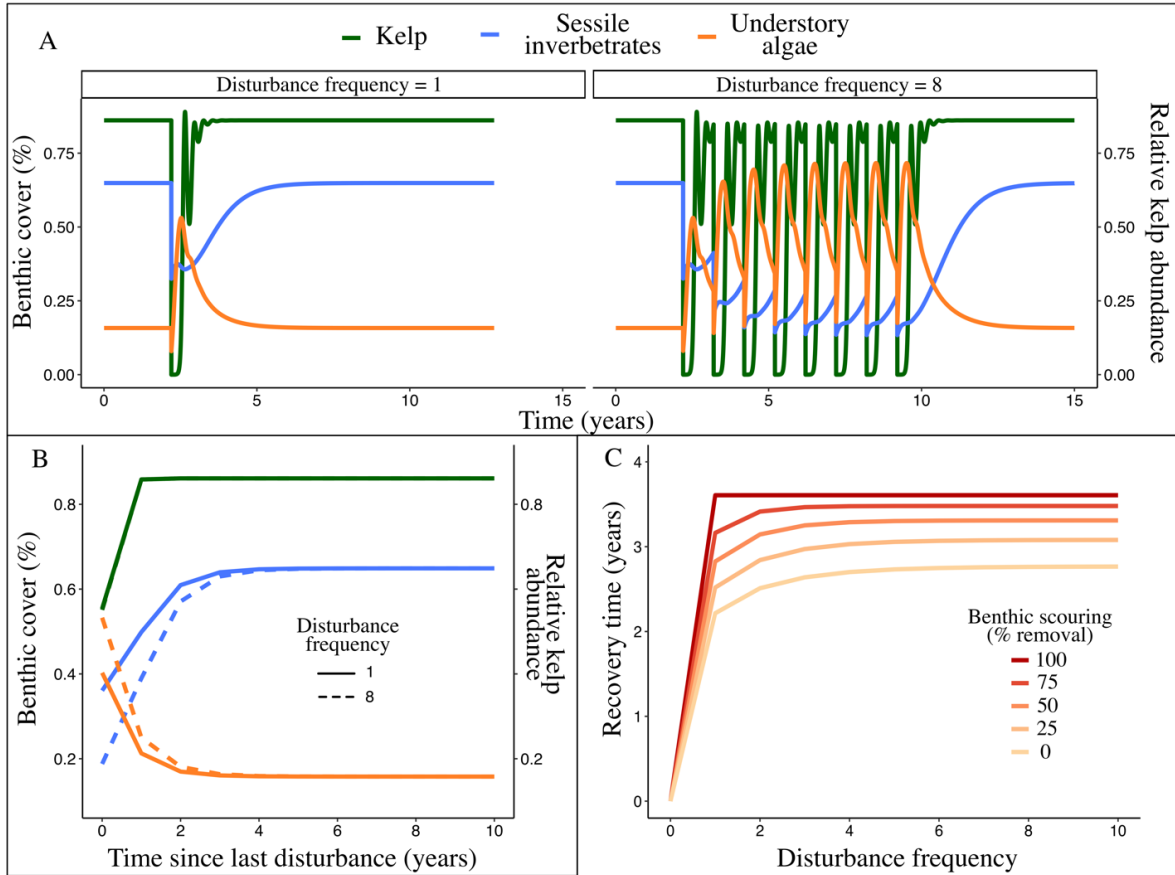


Figure 3.2. Example simulations from a theoretical model of non-trophic interactions between three benthic functional groups in California kelp forests (A). Disturbances were assumed to occur annually, and always removed 100% of adult kelp. However, disturbances could also affect juvenile kelp, sessile invertebrates, and understory algae on the seafloor, via benthic scouring (e.g., the percent-removal of benthic functional groups). We simulated 1-25 consecutive annual disturbances and tracked how the community responded for 25 years following the last disturbance (B). Community recovery time, or the time it took for sessile invertebrate and understory algae to recover to within 5% of pre-disturbance levels, was dependent on disturbance frequency and the level of benthic scouring (C). Simulations in A and B assumed 50% benthic scouring. All other parameters were held constant across the simulations. For visualization purposes, only 10 years following the last disturbance and disturbance frequencies ≤ 10 are displayed.

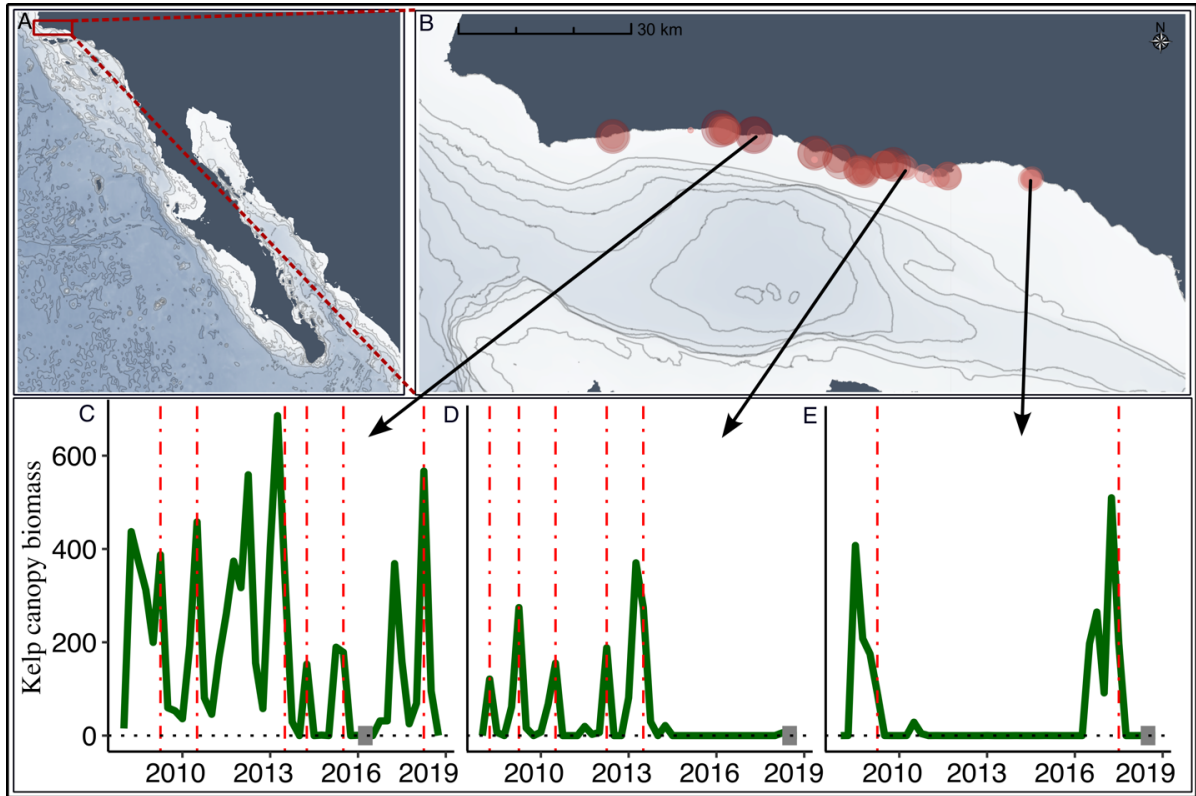


Figure 3.3. Observational data on benthic community structure was collected at 68 locations in the Santa Barbara Channel, USA from July-October 2018 (A, B). At each location, the historic kelp canopy dynamics were extracted from a satellite-derived dataset of kelp canopy biomass dynamics estimated at 30 m spatial resolution, every 3-months since 1984. (C-E) Three example time series of kelp canopy dynamics for the 10 years prior to the collection of benthic community data. Red vertical dashed lines represent time points identified as disturbances to kelp canopy, while gray blocks represent the last time when kelp canopy was absent for a 6-month period.

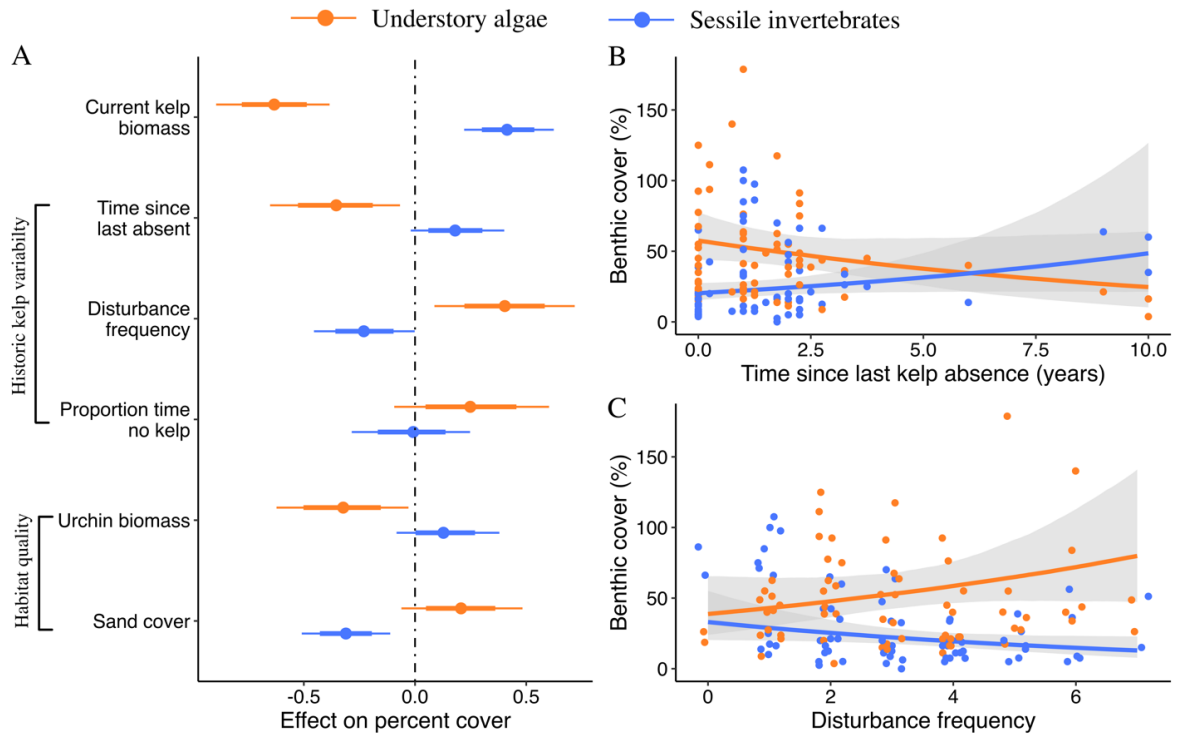


Figure 3.4. (A) Effect size of current kelp biomass, metrics of historic kelp variability, and habitat quality on observed benthic community structure. Each point represents the effect of each predictor on the difference in the percent cover of sessile invertebrates and understory algae. Points and surrounding intervals are the median \pm 75% and 95% credible intervals of the posterior prediction from a Bayesian generalized linear mixed effects model. Continuous relationships between time since the last kelp absence (B) or disturbance frequency (C) on the percent cover of sessile invertebrates and understory algae. Lines and surrounding shading in B and C are the median \pm 95% CI of linear expectation of the posterior predictive distribution.

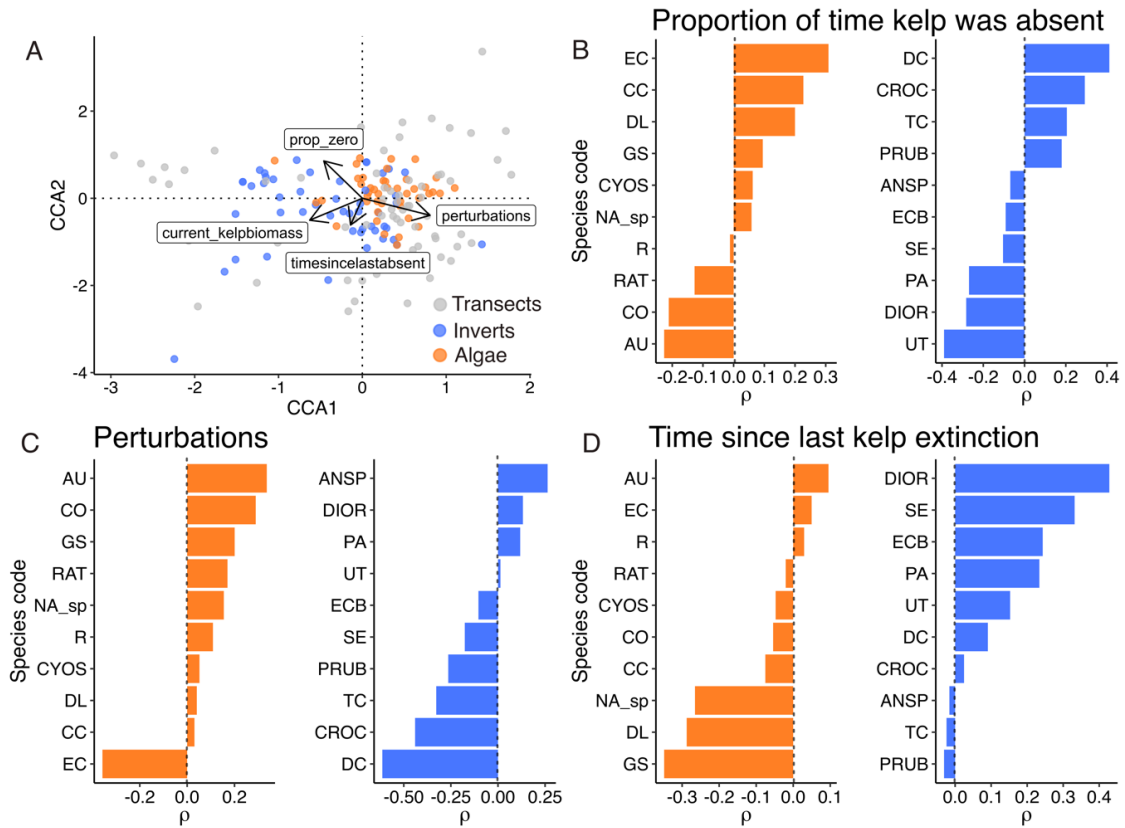


Figure 3.5. (A) Species (colored by functional group) and transect loadings along the first two axis of a canonical correlation analysis demonstrating the impact of metrics of historic kelp canopy variability on the communities in multivariate space. (B-D) Univariate Spearman rank order correlations (ρ) of the top ten understory algae and epilithic sessile invertebrates by percent cover across the full data set. Each bar represents the correlation between a particular species and the proportion of time kelp was absent (B), the number of perturbations in the last 10 years (C), or the time since the last 6-month kelp canopy extinction (D).

5. CONCLUSIONS

Recent decades have seen a rise in calls for ecosystem-based approaches to managing both terrestrial and marine ecosystems (e.g., ecosystem-based management, EBM; Geary et al. 2020). EBM seeks to account for the social, economic, and ecological components of systems, in order to holistically manage species and those who harvest them, not as isolated populations, but as pieces of a broader whole. One component of implementing EBM is understanding how strongly species interact. For example, efforts to restore target predator populations may be hampered if their prey are not simultaneously restored (Samhuri et al. 2017). Therefore, being able to accurately understand when and where species will interact strongly or weakly is important to effectively implementing ecosystem-based approaches to management and restoring ecological communities.

In this dissertation I explored mechanisms that drive variation in species interactions in order to better account for species interactions in management contexts. In Chapter 1, I demonstrated that variation in the size-frequency distributions of lobster and their urchin prey can account for up to ~80% of the variation in interaction strength relative to difference in urchin density. This suggests that two sites in proximity could have equal biomass densities of predators and prey, but could differ dramatically in interaction strength depending on their respective size-frequency distributions. I then showed that relying on canonical relationships grounded in the scaling of metabolism with body size failed to predict the strength of interactions between lobster and urchins by an order of magnitude. Building upon these results, I then tested prevailing theory on the relationships between an animal's size, physiology, and ecology. The results reveal that larger lobster consume disproportionately more than smaller conspecifics, despite declining metabolic requirements, calling into

question the widely held assumption that consumption should scale with body size at an equivalent or slower rate than metabolism. Finally, I zoomed away from specific trophic interactions in kelp forests, to understand how the intense variability in kelp population dynamics could influence community structure. This analysis showed that accounting for the historic dynamics of a foundation species could provide valuable insight into spatial variation in community structure.

Global change is rapidly altering how species interact, and effectively managing ecological communities in the future will require holistic approaches that account for dynamic species interactions. This is a large challenge that will require enormous research on many fronts. The work outlined in this dissertation represents an incremental step towards this goal. Integrating individual-scale variation in body size and accounting for historic contingencies will highlight when and where species interact strongly or weakly, thereby assisting the restoration and management of complex socio-ecological systems.

REFERENCES

- Geary, W. L., M. Bode, T. S. Doherty, E. A. Fulton, D. G. Nimmo, A. I. T. Tulloch, V. J. D. Tulloch, and E. G. Ritchie. 2020. A guide to ecosystem models and their environmental applications. *Nature Ecology & Evolution*.
- Samhouri, J. F., A. C. Stier, S. M. Hennessey, M. Novak, B. S. Halpern, and P. S. Levin. 2017. Rapid and direct recoveries of predators and prey through synchronized ecosystem management. *Nature Ecology & Evolution* 1:1–6.

6. APPENDICES

6.1. CHAPTER 1 – APPENDIX

6.1.1. Modeling

Alternative forms for the size-scaling of attack rates

Previous work has shown that attack rates of predators tend to increase with predator body size to a maximum before declining (e.g., a hump shaped relationship) (Aljetlawi et al., 2004; Barrios-O’Neill et al., 2016; Kalinkat et al., 2013; McCoy et al., 2011; Uiterwaal et al., 2017; Vucic-Pestic et al., 2010; Wahlström et al., 2000). We initially explored the data to determine the relationship between attack rate, predator body size, and prey body size. To estimate the parameters of the functional response for each predator (e.g., α and h), we fit a modified version of the Bayesian model described in the main text. Specifically, we fit a type II functional response (Eq. 1) to each individual predator, where α and h for each individual were drawn from prior distributions for the prey size class that the individual was fed nested within the overall population of lobsters. We assumed that the number of prey consumed in trial i (C_i) was binomially distributed given the number of prey offered (N_i) and the proportion of prey consumed (P_i). Thus,

$$C_i \sim \text{Binomial}(N_i, P_i) \tag{1}$$

$$P_i = \frac{1}{\alpha_{j,k}^{-1} + h_{j,k} N_i}$$

where, $\alpha_{j,k}$ is the attack rate of lobster j (1,2,...46) in treatment k (1,2,3), and $h_{j,k}$ is the handling time of lobster j in treatment k . The model results provided predictions for the functional response for the overall population of lobsters, lobsters preying on each prey size

class, and each individual lobster without assuming any *a priori* relationship between α , h , predator size and prey size.

We then modeled the posterior median estimate of α for each lobster as a function of lobster and urchin body size. Following metaanalyses conducted across taxa (Rall et al. 2012, Uiterwaal and Delong et al. 2020), we fit the following equation to the data:

$$\log(\alpha_j) = \log(\alpha_0) + \beta_{\alpha,c} \log(m_{c,j}) + \beta_{\alpha,r} \log(m_{r,j}) \quad (2)$$

We expected that if α followed a unimodal function of predator mass at a fixed prey mass, then the residuals of the regression would display a hump shaped pattern (*see* Barrios-O'Neill et al. 2016 *for a similar approach*). However, we found no evidence for a pattern in the residuals. To confirm, we included a polynomial term in the regression equation for predator mass, but AIC comparison suggested that the inclusion of the polynomial term did not improve model fit.

We also tested to see if the size-scaling of α and h was dependent on predator size alone, prey size alone, both predator and prey size, or the ratio of predator and prey size. The best fit models for both parameters based on AIC-comparison were models that included both predator and prey size with independent scaling exponents. Uiterwaal and Delong (2020) found a similar a lack of support for body mass ratio-dependence relative to independent effects of predator and prey size.

Model details

Previous studies that examined allometric scaling of the functional response have either fit the functional response and then explored allometric relationships among the parameters sequentially (e.g., Barrios-O'Neill 2016) or fit the allometric functional response in a single step (e.g., McCoy et al. 2011, Kalinkat et al. 2013). A recent simulation analysis suggests that the most accurate and precise method of fitting the functional response is to fit the multivariate response surface directly (Uszko et al., 2020), which also reduces complications in propagating uncertainty between multiple models. Following our preliminary analysis (*see Appendix 6.1.1*), we choose to adopt the approach of Uszko et al. (2020) and fit the size-dependent functional response directly to the data using a Bayesian hierarchical approach.

Specifically, we assumed that α and h for each lobster predator was determined by the lobster's mass and the mass of the urchin size class that it was preying on, where error in α and h between individuals was normally distributed. How many urchins a lobster consumed was dependent on urchin density according to a type II functional response, where the number of urchins eaten followed a Poisson distribution. The model sought to estimate the probability of the parameters given the data and the prior distribution.

Hierarchical, nonlinear models can be fit in a maximum likelihood framework (Bolker, 2008; Oddi et al., 2019). However, we chose to utilize Bayesian approaches because they allow for the incorporation of prior information, and they offer a more direct means of estimating and interpreting parameter uncertainty in hierarchical models (Bolker, 2008; Ellison, 2004). Considering the widespread adoption of $\frac{3}{4}$ scaling of consumption based on metabolic theory (Brown et al., 2004), a Bayesian approach allowed us to include informative prior distributions based on theoretical constants (Table S1.2).

Table S1.1. Summary of prior distributions used to model the body-size dependence of the lobster functional response.

Parameter	Prior
<i>Population-level</i>	
$\log(\alpha_0)$	<i>normal</i> (0, σ)
$\beta_{\alpha,c}$	<i>normal</i> (0.75, σ)
$\beta_{\alpha,r}$	<i>normal</i> (0.5, σ)
$\log(\alpha_0)$	<i>normal</i> (0, σ)
$\beta_{h,c}$	<i>normal</i> (-0.75, σ)
$\beta_{h,r}$	<i>normal</i> (0.5, σ)
<i>Individual-level</i>	
$\mu_{\alpha,j}$	<i>normal</i> (0, σ^*)
$\mu_{\alpha,j}$	<i>normal</i> (0, σ^*)
<i>Variances</i>	
σ	<i>gamma</i> (1,1)
σ^*	<i>gamma</i> (2,1)

Traditional functional response experiments account for prey depletion using Rodger’s random predator equation (Real, 1977). However, we did not account for prey depletion in our analysis because, to our knowledge, there is no practical way to implement Rodger’s random predator equation with hierarchical structure (McCoy et al., 2011).

6.1.2. Mesocosm experiments

To determine the size-dependence of the lobster functional response, we conducted a response-surface experiment where we manipulated prey density, prey size, and predator size. Trained divers collected lobsters and urchins from kelp forests in the Santa Barbara Channel. Experimental lobsters ranged in size from 53 – 160 mm carapace length (n = 45). Each lobster was weighed to the nearest gram (range: 196 - 2736 g; *see Jerde et al. 2019 for methods*). We classified urchins into three size bins (1.0-2.9, 3.0-4.9, 5.0-7.0 cm test diameter; *small, medium, and large*, respectively). For subsequent analyses, we used the center of each urchin size class to estimate urchin mass according to published test-diameter

to length relationships (3.3, 23.9, 76.7 g; Reed et al. 2016). Lobster and urchin sizes used in experiments spanned the range of variation in body size for natural populations based on the observational data (lobsters: 421.3 [88.8 – 897.8] g, urchins: 46.6 [8.1 – 132.2], \bar{X} [95% CI]). Urchins were only collected from sites with kelp present because gonad weight is lower in urchins from barrens and barren urchins are less palatable to predators (Eurich et al., 2014).

In order to determine the relationship between consumption rates, body size, and prey density, we sought to estimate the functional response of each individual lobster. Therefore, we conducted foraging trials in which an individual predator foraged on a single size class of prey at each experimental prey density ($n = 6$). We assigned predators to size bins ($n = 4$), and then randomly assigned each predator a prey size class treatment ($n = 3$), to ensure even replication across the response surface.

We conducted all foraging trials in 400 L laboratory mesocosms with a continuous flow of ambient seawater at $\sim 7 \text{ L min}^{-1}$. Each mesocosm was divided into two foraging arenas by a permeable plastic barrier. We haphazardly assigned predators to foraging arenas, where they remained for the duration of the experiment. Each arena contained a half-round PVC shelter, and three bricks. The area of each mesocosm was 0.52 m^2 . Following capture, we allowed each predator at least three weeks to acclimate to the mesocosms, during which we fed them a mixed diet of urchins and mussels (*Mytilus californianus* or *Mytilus galloprovincialis*) and confirmed that each individual foraged on at least one urchin. Prey were maintained in separate mesocosms and fed giant kelp fronds and stipes (*Macrocystis pyrifera*) for > 1 week.

To initiate a trial, predators were fed mussels *ad libitum* for 48 hours, followed by a 48-hour starvation period. At the start of the trial, we added a given number of urchins within

the predators' assigned prey size class to each arena. Lobsters are nocturnal predators and typically remained sheltered when prey were added to the tanks during the afternoon. We saw no evidence of immediate predation, and urchins moved about the tank freely until nightfall. We allowed predators to forage on prey for 48 hours, after which we counted each remaining prey item to estimate the number of urchins consumed by an individual lobster. No predator consumed all prey in trials with the highest prey density. We conducted trials in consecutive weeks, where predators were randomly assigned a new prey density each week. During the experimental period, ambient water temperatures in the flow-through system were on average $16.1^{\circ} \pm 1.8$ C ($\bar{X} \pm 1$ SD).

We found evidence of non-predation related urchin mortality during trials. When consuming urchins, lobsters pry their prey from the substrate and crack the teste at the vent . By inspecting each urchin for evidence of damage to the test near the vent we discriminated between urchins that died due to predation or natural mortality. We subtracted the number of urchins that experienced non-predation mortality from the total number of urchins available.

6.1.3. Simulation

Estimating predator:prey ratio for observational data

To determine the extent to which lobster and urchin body size varied between sites, we estimated the predator:prey body size ratio for each site in each year. To do this we resampled 1000 draws with replacement from the size-distribution of lobster and urchin at each site/year and calculated the ratio of individual lobster mass to urchin mass. We then

plotted the distributions of lobster:urchin size ratios as a function of site and year (*see* Fig. S1.1).

Simulating plausible distributions of lobster-urchin consumption rates based on observational data

Lobster-urchin interactions are only one feeding link in the complex food web dynamics of the kelp forest (Morton et al., 2021; Tegner & Levin, 1983). Lobsters are opportunistic predators and urchins are preyed upon by other consumers (e.g., *Semicossyphus pulcher*; Hamilton and Caselle 2015). Therefore, we were only interested in estimating consumption rates that accounted for body size variation *relative* to consumption rates that ignore body size. Indeed, estimated consumption rates at any time point are likely different than actual urchin consumption. However, in the absence of spatiotemporal species-specific data on urchin consumption rates, our predictions offer a means of exploring the consequences of body size on estimated variation in consumer-resource interactions.

Partitioning variance between density and body size

Considering the extent of variation in interaction strength between lobsters and urchins, we sought to partition the amount of variation caused by differences in lobster and urchin density between sites/years and the amount of variation driven by differences in the size-distributions of lobsters and urchins. The size-dependent functional response in our experiment depends on the interactive effects of lobster size, urchin size, and urchin density (*see* Eq. 5 in main text). For example, at a particular body size of lobster and urchin, the interaction strength will depend on the density of urchins. Our experimental data suggests

that lobster attack rates are largely invariant with lobster size or urchin size ($\beta_{\alpha,c}, \beta_{\alpha,r} \approx 0$). This means that lobster and urchin body size will have a greater impact on IS when the urchin density is high, compared to when urchin density is low, because at low urchin density predators are constrained by their ability to find new prey (e.g., attack rate, α), which is invariant with body size. Therefore, to partition the variation in interaction strength between body size and density, we fixed the body size of lobster and urchin at different values and estimated interaction strength across variation in density.

Specifically, we selected 625 different values of lobster size and urchin size such that sizes ranged from the max lobster mass and minimum urchin mass to the max urchin mass and minimum lobster mass. We then estimated the distribution of IS assuming only variation in lobster and urchin density for each combination of fixed lobster and urchin size. Finally, we used simple linear regression to estimate the proportion of variance explained (R^2) by the predictions where only density varied, relative to the predictions based on joint variation in body size and density. We reported the full range of resulting $1-R^2$ values to estimate the proportion of variance explained by body size.

Predicting interaction strengths based on previous relationships in the literature

We conducted a non-systematic search of the literature to find estimates for the size-scaling of the functional response. For empirical estimates, we relied on Rall et al. (2012), Barrios-O'Neill et al. (2019), and a recent metaanalysis (Uiterwaal & DeLong, 2020) which represents the largest compilation of functional response data available to date. For the complete data source to Uiterwaal and DeLong (2020), please refer to the FoRAGE database (Uiterwaal et al., 2022).

Each of the three papers we used to generate predictions utilized other covariates to model parameters of the functional response. Barring interactions in these models, the scaling-coefficients on the body mass of resource and consumer should not be affected by the covariates. However, the intercepts will not be directly comparable unless we accounted for the covariates. Therefore, for each manuscript we included the covariates from their models and fixed the values of those covariates at the observed value in our mesocosm trials.

Table S1.2. Summary of the final model structure, units, and fixed values of covariates used to predict interaction strength based on relationships from the literature.

Uiterwaal and DeLong 2020	
Final models	
α	$\ln(\alpha) = \alpha_0 + \beta_{c,\alpha} \ln(m_c) + \beta_{r,\alpha} \ln(m_r) + \beta_T T + \beta_{T^2} T^2 + \beta_A \ln(A) + **$
h	$\ln(h) = h_0 + \beta_{c,h} \ln(m_c) + \beta_{r,h} \ln(m_r) + \beta_T T + \beta_{T^2} T^2 + \beta_A \ln(A) + \beta_D D + **$
Units and fixed values	
$m = \text{mg}$; density = ind. Cm^{-2} ; time = days; $T = 16.1^\circ\text{C}$; $A = 5.206 \times 10^4 \text{ cm}^2$; $D = 2$ (e.g., 2-D)	
** Uiterwaal and DeLong include random effects based on taxonomy. However, we focused only on the population level effect (e.g., across taxa). Therefore, we did not include random effect shifts to the intercept.	
Rall et al. 2012	
Final models	
α	$\ln(\alpha) = \alpha_0 + \beta_{c,\alpha} \ln(m_c) + \beta_{r,\alpha} \ln(m_r) + \beta_T \frac{T - T_0}{kTT_0}$
h	$\ln(h) = h_0 + \beta_{c,h} \ln(m_c) + \beta_{r,h} \ln(m_r) + \beta_T \frac{T - T_0}{kTT_0}$
Units and fixed values	
$m = \text{mg}$; density = ind. m^{-2} ; time = seconds; $T = 289.25 \text{ }^\circ\text{K}$; $T_0 = 293.15 \text{ }^\circ\text{K}$; $k = 8.61733326 * 10^{-5} \text{ eV K}^{-1}$	
Barrios-O’Neill et al. 2019***	
Final models	
α	$\ln(\alpha) = N(\alpha_{0,j} + \beta_{c,\alpha} \ln(m_c) + \beta_{r,\alpha} \ln(m_r) + \beta_T \ln(T) + \beta_{m_r \times T} \ln(m_r) \ln(T) + \beta_{ACstat} I_{ACstat} + \beta_{filit} I_{filit}, \sigma^2)$ $\alpha_{0,j} = N(\mu_{\alpha_0}, \sigma_{\alpha_0,j}^2), \text{ for Taxa } j = 1, \dots, J$ where $I_{ACstat} = 1$ and $I_{filit} = 0$
C_{max}	$\ln(C_{max}) = N(C_{0,j} + \beta_{c,h} \ln(m_c) + \beta_{r,h} \ln(m_r) + \beta_T \ln(T) + \beta_{m_c \times T} \ln(m_c) \ln(T) + \beta_{ACstat} I_{ACstat} + \beta_{filit} I_{filit}, \sigma^2)$ $C_{0,j} = N(\mu_{c_0}, \sigma_{c_0,j}^2), \text{ for Taxa } j = 1, \dots, J$ Where $I_{ACstat} = 1$ and $I_{filit} = 0$
Units and fixed values	
$m = \text{g}$; density = ind. m^{-2} ; time = days; $T = 16.1^\circ\text{C}$	
*** Barrios-O’Neill et al. (2019) included both a categorical fixed effect for encounter strategy and a random effect of taxonomy. We were interested in active predators foraging on static prey (I_{ACstat}) and crustacean predators. Therefore, we estimated the intercept for both models as $I = \mu_x + \beta_{ACstat} + X_{crustacean}$ where x,X is either α_0 C_0 and I is the final intercept used in the simulation	

Table S1.3. Summary of equations and parameter estimates for the size-scaling of the functional response based on theoretical and empirical sources.

Source	$\ln(\alpha_0)$	$\beta_{\alpha,c}$	$\beta_{\alpha,r}$	β_T	β_{T^2}	β_A	$\ln(h_0)$	$\beta_{h,c}$	$\beta_{h,r}$	β_T	β_{T^2}	β_A	β_D	Taxonomic scale
First principles	--	0.58 - 0.92 ¹	0.33 - 0.66 ¹	--	--	--	--	-0.66 to -1 ²	0-1 ³	--	--	--	--	Theoretical
Uiterwaal and DeLong 2020	-8.45 ± 1.05	0.05 ± 0.03	-0.0005 ± 0.02	0.10 ± 0.03	- 0.003 ± 0.001	0.98 ± 0.05	0.83 ± 0.85	-0.25 ± 0.03	0.34 ± 0.02	-0.24 ± 0.04	0.005 ± 0.001	-0.01 ± 0.03	-0.64 ± 0.19	Cross taxa; general estimate
Rall et al. 2012	-21.23	0.85	0.09	0.42	--	--	10.38	-0.76	0.76	-0.30	--	--	--	Marine invertebrates
Barrios-O'Neill 2019	-8.08 + -1.07 + 0 ⁴	0.58	0.59	1.84	--	--	-6.07 ⁵ + 0.55 + 0.48	1.44 ⁵	0.27 ⁵	1.78 ⁵	--	--	--	Active crustaceans that forage on static resources

¹ McGill and Mittlebach 2006; ² Brown et al. 2004, Glazier 2010; ³ Rall et al. 2012, Jescke et al. 2002
⁴ Barrios-O'Neill et al. (2019) report that all random effects on attack rate intersect the group level effect and don't report the random effects therefore we assume they are zero.
⁵ Barrios-O'Neill et al. (2019) fit maximum consumption rates (C_{max}). We converted to handling times when generating predictions.

6.1.4. Supplemental Figures

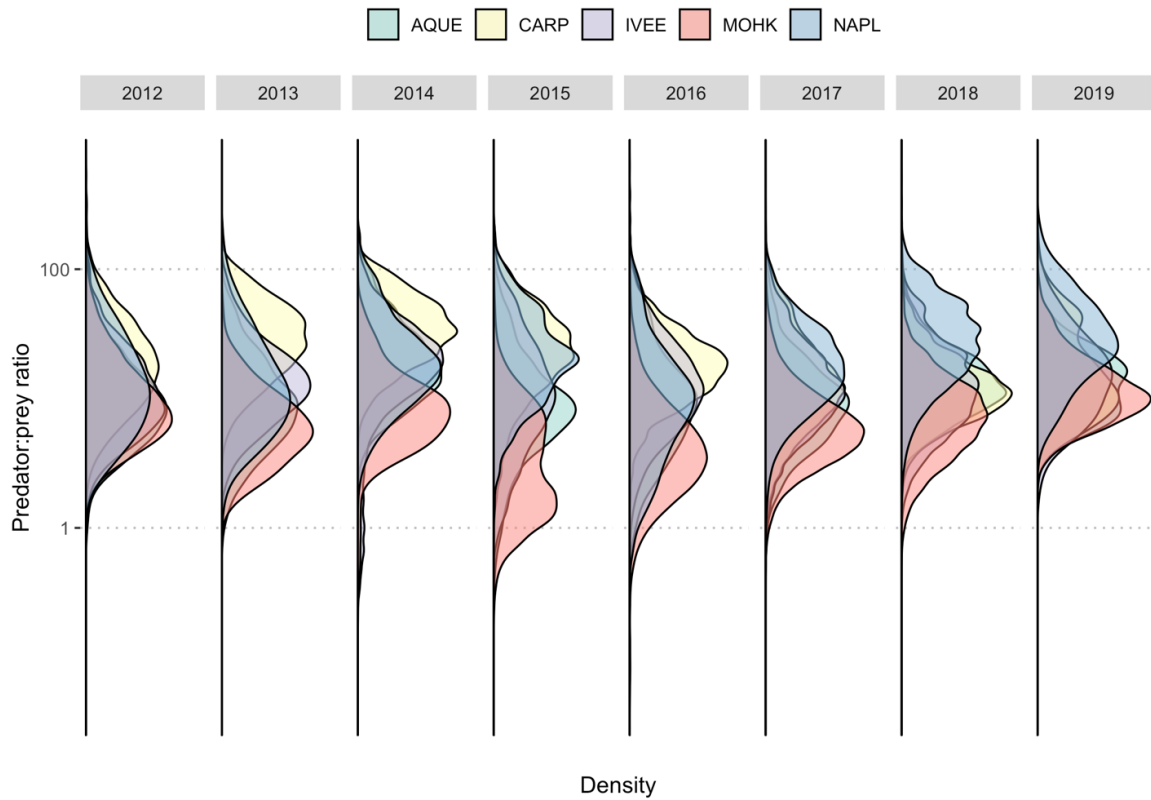


Figure S1.1. Change in the predator (California spiny lobster) to prey (purple urchin) body mass ratio between sites and years. The mean and variance of the predator:prey ratio varies between sites and years. The predator:prey ratio was estimated by resampling from the size distributions of predators and prey with replacement. The y-axis is \log_{10} transformed for visualization purposes.

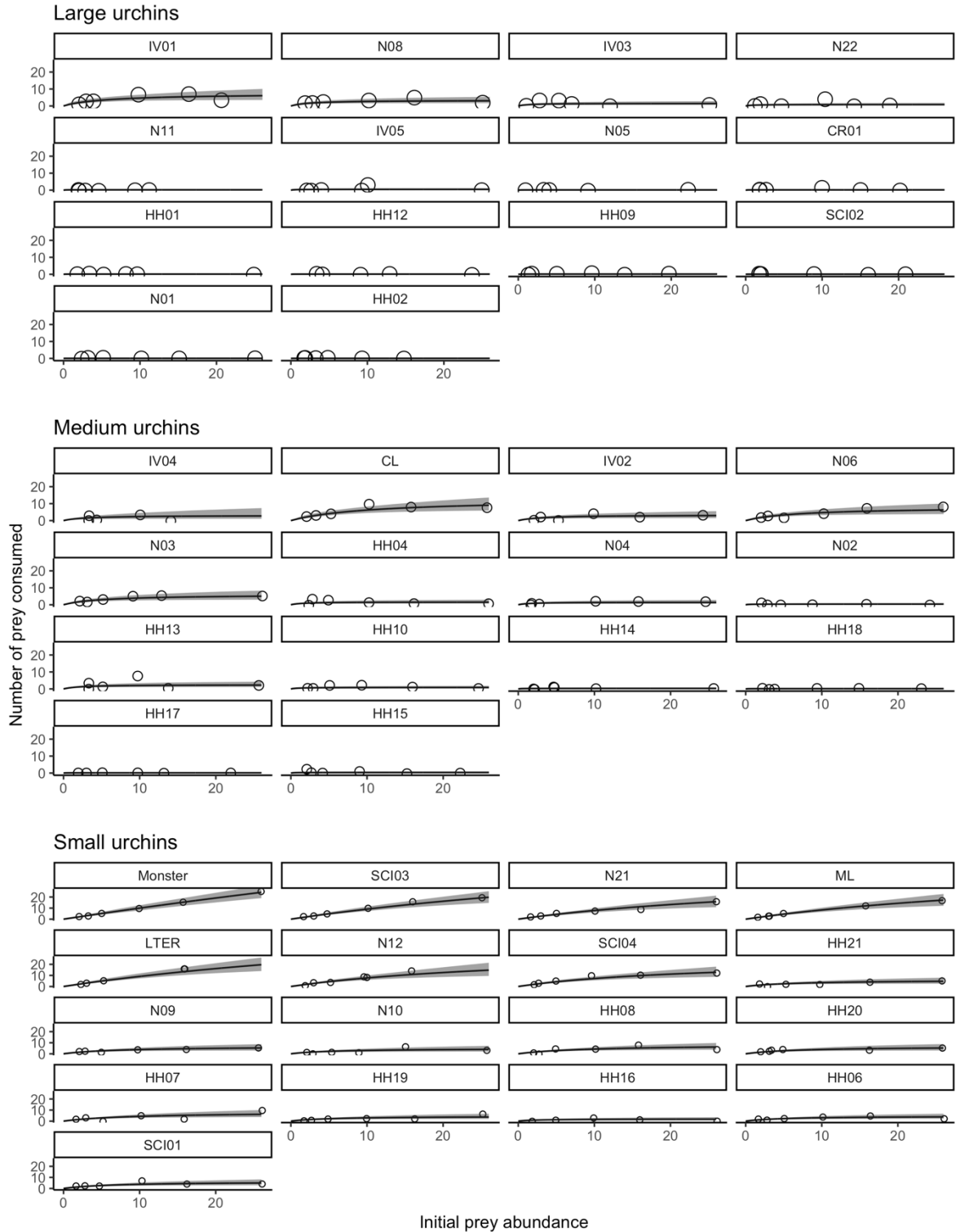


Figure S1.2. The functional responses of individual lobster predators foraging on urchin prey in mesocosms. Lines are median predictions (\pm 95% CI) from a Bayesian hierarchical model that estimated the number of urchins consumed as a function of lobster body size, prey body size, and prey density. Panels are arranged in descending order of lobster body size within a particular prey size class.

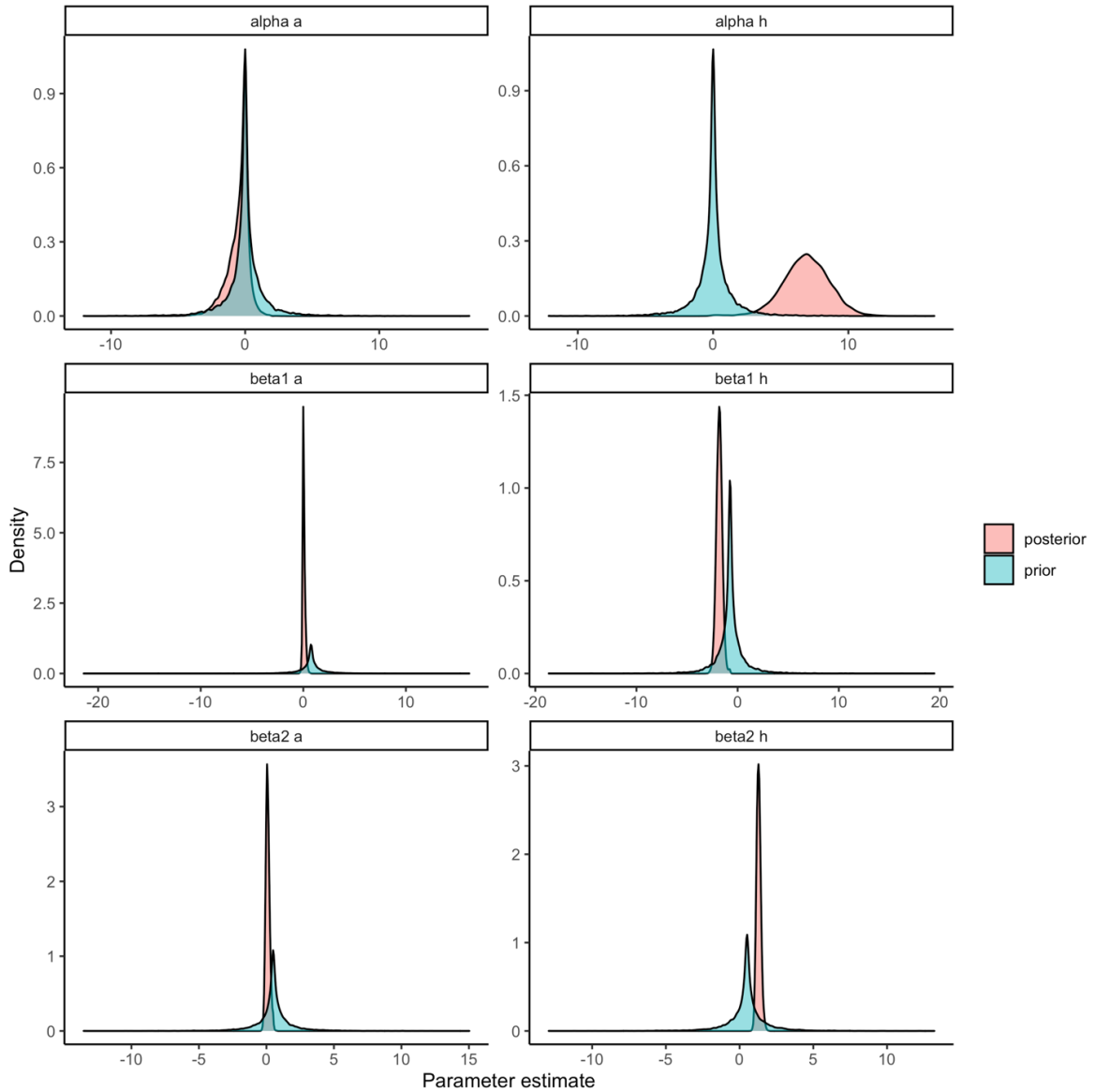


Figure S1.3. Comparison of posterior and prior predictive distributions for population level parameters from a Bayesian hierarchical model. Priors are informed based on theoretical predictions (see Table S2 for details on each prior).

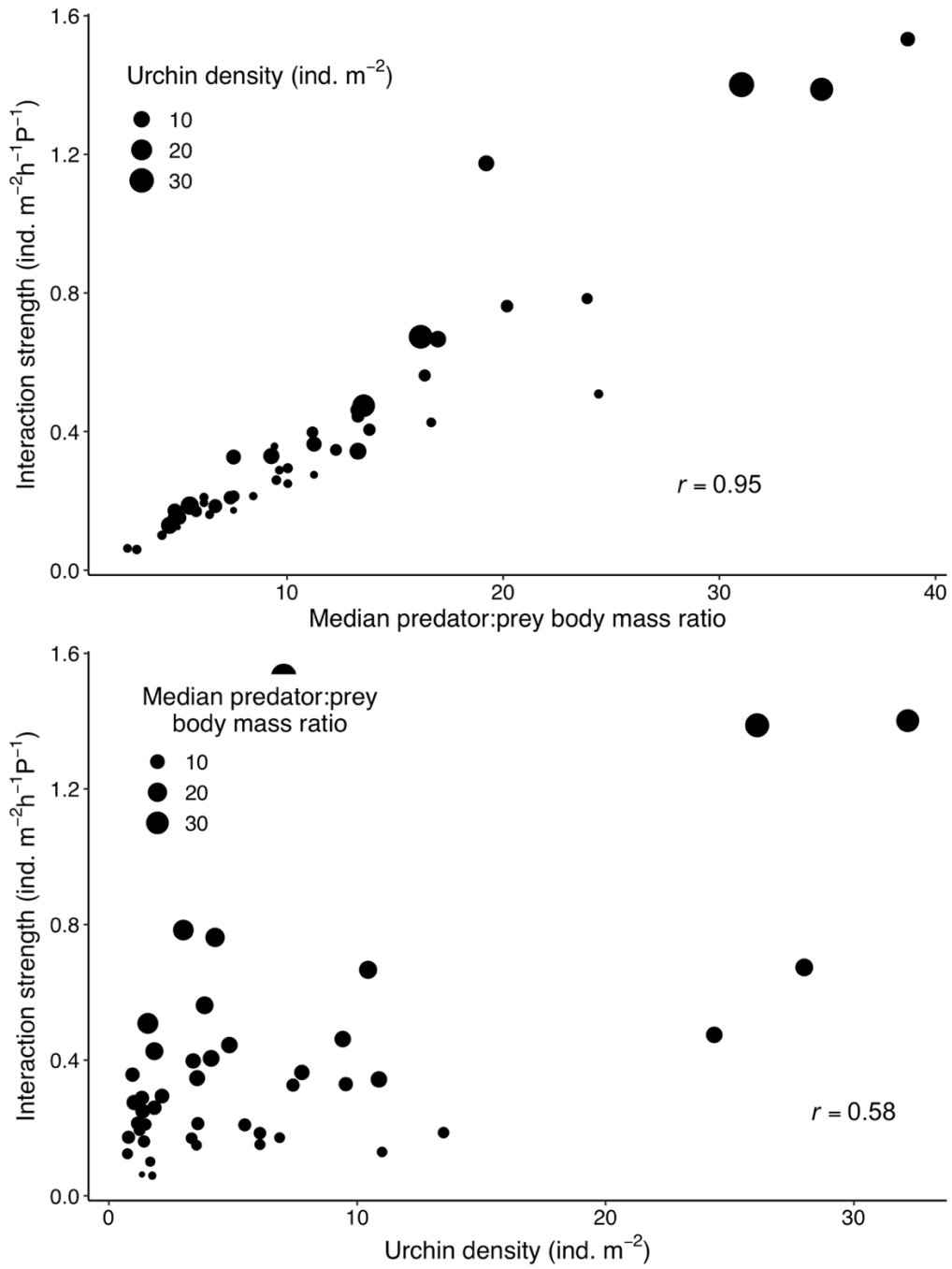


Figure S1.4. The median rate of urchins consumed per lobster predator (e.g., per predator interaction strength) as a function of the median predator:prey body mass ratio (top) and urchin density (bottom). Each point represents a site in a particular year. Sites or times with large lobster, small urchins, and high urchin density were estimated to have the strongest interactions.

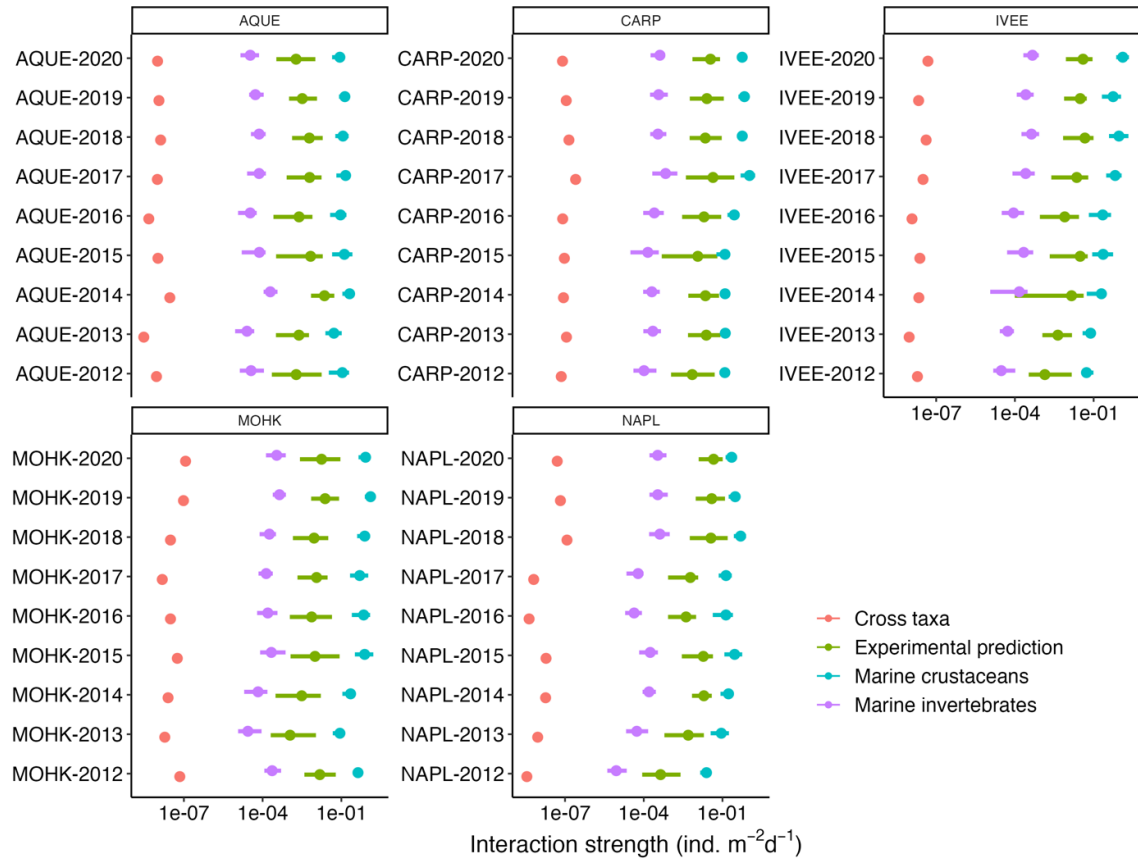


Figure S1.5. Rank order of interaction strength estimated via experimentation and three different predictions from the literature for the size-scaling of consumption rates. Site-year combinations are arranged in decreasing order according to the experimental prediction.

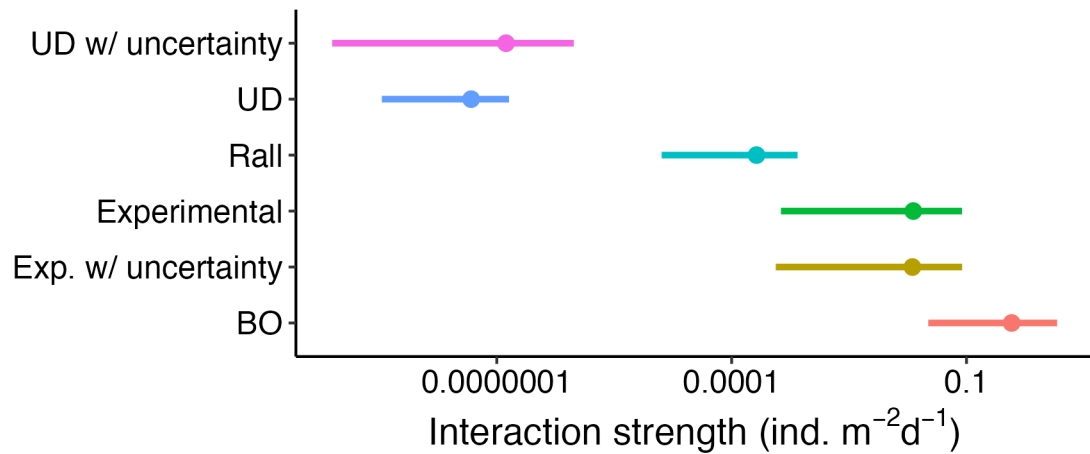


Figure S1.6. Median and 95% CIs of simulated predictions for interaction strength based on our experimental estimates and estimates of the size-scaling of interaction strength from the literature. UD (Uiterwaal and DeLong 2020), Rall et al. (2012), BO (Barrios-O’Neill et al. 2019), and Experimental match the predictions reported in the main text. However, UD w/ uncertainty and Exp. w/ uncertainty incorporate uncertainty in the regression coefficients. For experimental estimates, we sampled from the posterior distribution of each parameter, such that each draw in the simulation paired a unique lobster body size, urchin body size, and parameter set. Uiterwaal and DeLong report mean \pm SE of the regression parameters. To incorporate uncertainty, we sampled from a uniform distribution, where the bounds were defined by the 95% CIs of the mean of each parameter. Rall et al. (2012) and Barrios-O’Neill et al. (2019) do not report confidence intervals on their parameter estimates.

6.1.5. References

- Aljetlawi, A. A., Sparrevik, E., & Leonardsson, K. (2004). Prey–predator size-dependent functional response: Derivation and rescaling to the real world. *Journal of Animal Ecology*, *73*(2), 239–252. <https://doi.org/10.1111/j.0021-8790.2004.00800.x>
- Barrios-O’Neill, D., Kelly, R., Dick, J. T. A., Ricciardi, A., MacIsaac, H. J., & Emmerson, M. C. (2016). On the context-dependent scaling of consumer feeding rates. *Ecology Letters*, *19*(6), 668–678. <https://doi.org/10.1111/ele.12605>
- Bolker, B. M. (2008). *Ecological models and data in R*. Princeton University Press.
- Brown, J. H., Gillooly, J. F., Allen, A. P., Savage, V. M., & West, G. B. (2004). Toward a metabolic theory of ecology. *Ecology*, *85*(7), 1771–1789. <https://doi.org/10.1890/03-9000>
- Ellison, A. M. (2004). Bayesian inference in ecology. *Ecology Letters*, *7*(6), 509–520. <https://doi.org/10.1111/j.1461-0248.2004.00603.x>
- Eurich, J., Selden, R., & Warner, R. (2014). California spiny lobster preference for urchins from kelp forests: Implications for urchin barren persistence. *Marine Ecology Progress Series*, *498*, 217–225. <https://doi.org/10.3354/meps10643>
- Hamilton, S. L., & Caselle, J. E. (2015). Exploitation and recovery of a sea urchin predator has implications for the resilience of southern California kelp forests. *Proceedings of the Royal Society of London B: Biological Sciences*, *282*(1799), 20141817. <https://doi.org/10.1098/rspb.2014.1817>
- Jerde, C. L., Kraskura, K., Eliason, E. J., Csik, S. R., Stier, A. C., & Taper, M. L. (2019). Strong Evidence for an Intraspecific Metabolic Scaling Coefficient Near 0.89 in Fish. *Frontiers in Physiology*, *10*. <https://doi.org/10.3389/fphys.2019.01166>
- Kalinkat, G., Schneider, F. D., Digel, C., Guill, C., Rall, B. C., & Brose, U. (2013). Body masses, functional responses and predator–prey stability. *Ecology Letters*, *16*(9), 1126–1134. <https://doi.org/10.1111/ele.12147>
- McCoy, M. W., Bolker, B. M., Warkentin, K. M., & Vonesh, J. R. (2011). Predicting Predation through Prey Ontogeny Using Size-Dependent Functional Response Models. *The American Naturalist*, *177*(6), 752–766. <https://doi.org/10.1086/659950>
- Morton, D. N., Antonino, C. Y., Broughton, F. J., Dykman, L. N., Kuris, A. M., & Lafferty, K. D. (2021). A food web including parasites for kelp forests of the Santa Barbara Channel, California. *Scientific Data*, *8*(1), 99. <https://doi.org/10.1038/s41597-021-00880-4>
- Oddi, F. J., Miguez, F. E., Ghermandi, L., Bianchi, L. O., & Garibaldi, L. A. (2019). A nonlinear mixed-effects modeling approach for ecological data: Using temporal

- dynamics of vegetation moisture as an example. *Ecology and Evolution*, 9(18), 10225–10240. <https://doi.org/10.1002/ece3.5543>
- Rall, B. C., Brose, U., Hartvig, M., Kalinkat, G., Schwarzmüller, F., Vucic-Pestic, O., & Petchey, O. L. (2012). Universal temperature and body-mass scaling of feeding rates. *Philosophical Transactions of the Royal Society B: Biological Sciences*, 367(1605), 2923–2934. <https://doi.org/10.1098/rstb.2012.0242>
- Real, L. A. (1977). The Kinetics of Functional Response. *The American Naturalist*, 111(978), 289–300.
- Reed, D. C., Nelson, J. C., Harrer, S. L., & Miller, R. J. (2016). Estimating biomass of benthic kelp forest invertebrates from body size and percent cover data. *Marine Biology*, 163(5), 101. <https://doi.org/10.1007/s00227-016-2879-x>
- Tegner, M. J., & Levin, L. A. (1983). Spiny lobsters and sea urchins: Analysis of a predator-prey interaction. *Journal of Experimental Marine Biology and Ecology*, 73(2), 125–150. [https://doi.org/10.1016/0022-0981\(83\)90079-5](https://doi.org/10.1016/0022-0981(83)90079-5)
- Uiterwaal, S. F., & DeLong, J. P. (2020). Functional responses are maximized at intermediate temperatures. *Ecology*, 101(4). <https://doi.org/10.1002/ecy.2975>
- Uiterwaal, S. F., Lagerstrom, I. T., Lyon, S. R., & DeLong, J. P. (2022). FoRAGE database: A compilation of functional responses for consumers and parasitoids. *Ecology*, 103(7), e3706. <https://doi.org/10.1002/ecy.3706>
- Uiterwaal, S. F., Mares, C., & DeLong, J. P. (2017). Body size, body size ratio, and prey type influence the functional response of damselfly nymphs. *Oecologia*, 185(3), 339–346. <https://doi.org/10.1007/s00442-017-3963-8>
- Uszko, W., Diehl, S., & Wickman, J. (2020). Fitting functional response surfaces to data: A best practice guide. *Ecosphere*, 11(4), e03051. <https://doi.org/10.1002/ecs2.3051>
- Vucic-Pestic, O., Rall, B. C., Kalinkat, G., & Brose, U. (2010). Allometric functional response model: Body masses constrain interaction strengths. *Journal of Animal Ecology*, 79(1), 249–256. <https://doi.org/10.1111/j.1365-2656.2009.01622.x>
- Wahlström, E., Persson, L., Diehl, S., & Byström, P. (2000). Size-dependent foraging efficiency, cannibalism and zooplankton community structure. *Oecologia*, 123(1), 138–148. <https://doi.org/10.1007/s004420050999>

6.2. CHAPTER 2 – APPENDIX

6.2.1. Conceptual model

To construct Figure 2.1 (main text), we assumed power law scaling relationships between body size and maximum consumption rate, standard metabolic rate, and maximum metabolic rate in the general form of $y = a_0 m_c^\beta$. We assumed that a_0 for maximum consumption was greater than a_0 for standard metabolic rates, so that even as predator size approaches zero, consumption exceeds standard metabolism ($a_{0,C_{max}} = 0.45$, $a_{0,SMR} = 0.1$). We let the standard metabolic rate scale to the $\frac{3}{4}$ power of predator mass. Under H_0 , β was equal to 0.75 following predictions from the metabolic theory of ecology (Brown et al. 2004). Ontogenetic growth models often assume that maximum consumption increases with body size slower than metabolism increases with body size (West et al. 2001). Therefore, we set $\beta = 0.65$ for H_1 . Finally, maximum consumption rates may increase with body size faster than metabolism (Marshall and White 2019), so we set $\beta = 1.1$ for H_2 . Similarly, maximum metabolic rate may increase with body size faster than SMR ($\beta_{MMR,H5} = 0.9$), slower than SMR ($\beta_{MMR,H4} = 0.6$), or at the same rate as SMR ($\beta_{MMR,H3} = 0.75$). We set the $a_{0,MMR} = 0.8$.

6.2.2 Modeling details

Table S2.1. Summary of prior distributions for all parameters in the Bayesian hierarchical model used to fit the functional response for lobster foraging on mussels.

Parameter	Prior
<i>Population-level</i>	
$\log(a_0)$	$normal(0, \sigma_1)$
$\beta_{\alpha,c}$	$normal(0.75, \sigma_1)$
$\beta_{\alpha,r}$	$normal(0.5, \sigma_1)$
$\log(h_0)$	$normal(0, \sigma_1)$
$\beta_{h,c}$	$normal(-0.75, \sigma_1)$
$\beta_{h,r}$	$normal(0.5, \sigma_1)$
<i>Individual-level</i>	
$\mu_{\alpha,j}$	$normal(0, \sigma_2)$
$\mu_{h,j}$	$normal(0, \sigma_2)$
<i>Variiances</i>	
σ_1	$gamma(1,1)$
σ_2	$gamma(2,1)$

Table S2.2. Prior distributions for all parameters used in Bayesian model to test differences in metabolic rates with lobster body size. We fit the model using the `stan_glm()` function in the `rstanarm` package (Goodrich et al. 2020). Specifically, we fit

$$\text{metabolic rate} \sim \text{Normal}(\bar{y}, \sigma) \quad (1)$$

$$\log(\bar{y}) = \alpha_0 + \beta_1 \log(m_c) + \beta_2 \text{type} + \beta_3 \log(m_c) \text{type}$$

where m_c is lobster mass (g) and *type* was a categorical predictor for either maximum metabolic rate or standard metabolic rate. The interaction allowed us to test for differences in the scaling of maximum and standard metabolic rates (see inlay in Fig. 2.3 in main text). We used a similar modeling procedure to test how absolute aerobic scope (AAS), factorial aerobic scope (FAS), and factorial energy acquisition (FEA) varied with body size. However, these univariate models did not include an interaction term and assumed normally distributed priors with mean = 0 and SD = 10 on the β coefficient.

Parameter	Prior
α_0	<i>normal</i> (0, 10)
β_1	<i>normal</i> (0.75, 1)
β_2	<i>normal</i> (0, 10)
β_3	<i>normal</i> (0, 1)
σ	<i>exponential</i> (1)

Table S2.3. Summary of scaling exponents and intercepts for response variables. Standard metabolic rate (SMR) and maximum metabolic rate (MMR) were modeled with an interaction (not displayed here) to test for differences in scaling exponents. Factorial aerobic scope (FAS), absolute aerobic scope (AAS), and factorial energy acquired (FEA) were modeled as univariate relationships. Maximum consumption rate (C_{\max}) was estimated from a more complex Bayesian hierarchical model (see Table S1). Estimates are the median \pm 95% CIs from the posterior distribution of each parameter. Credible intervals are not included for FEA because they would depend on the number of draws from the posterior distributions of each individual lobster's maximum consumption rate.

Response	$\log(\alpha_0)$	β	Units
SMR	-6.74 [-9.7,-3.8]	0.85 [0.4 - 1.3]	mg O ² min ⁻¹
MMR	-4.26 [-5.5,-2.9]	0.78 [0.6-1.0]	mg O ² min ⁻¹
FAS	2.55 [0.8, 4.3]	-0.09 [-0.3,0.2]	–
AAS	-4.33[-5.9,-2.8]	0.76 [0.5-1.0]	mg O ² min ⁻¹
C_{\max}	0.38 [-0.3,1.7]	1.50 [1.1, 1.9]	ind. day ⁻¹
FEA	-1.06	0.51	–

6.2.3. Supplemental figures

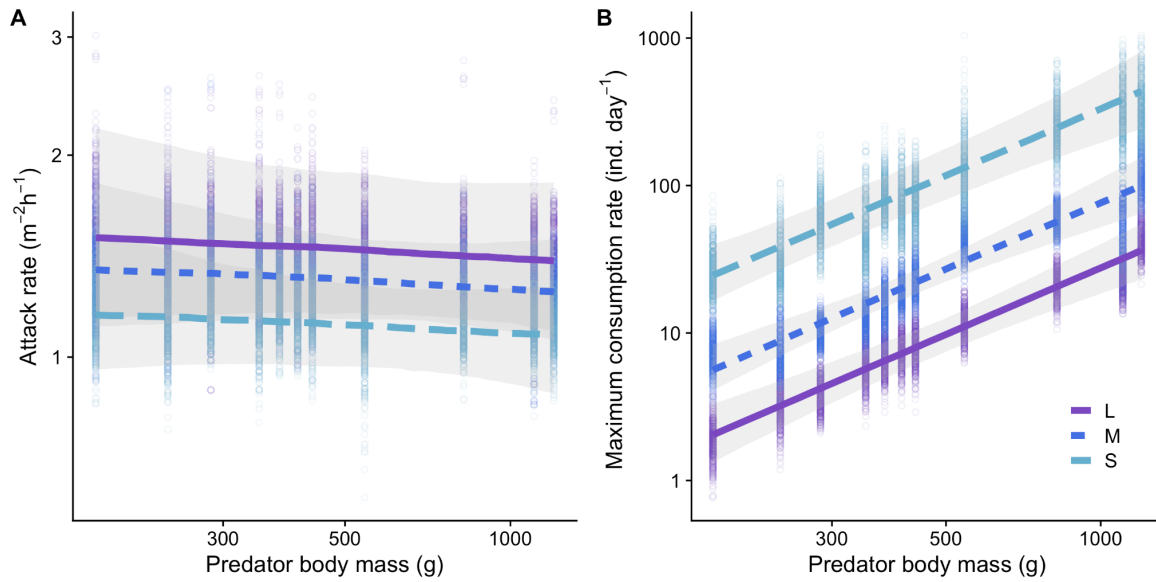


Figure S2.1. Variation in attack rate (A) and maximum consumption rate (1/handling time) (B) with body size of lobster foraging on mussels of three different mussel size classes. Points are 100 samples from the posterior distribution of each parameter for individual lobster predators foraging on each size class of mussel. Lines are the median \pm 95% CIs of the posterior distribution for lobsters foraging on each mussel size class.

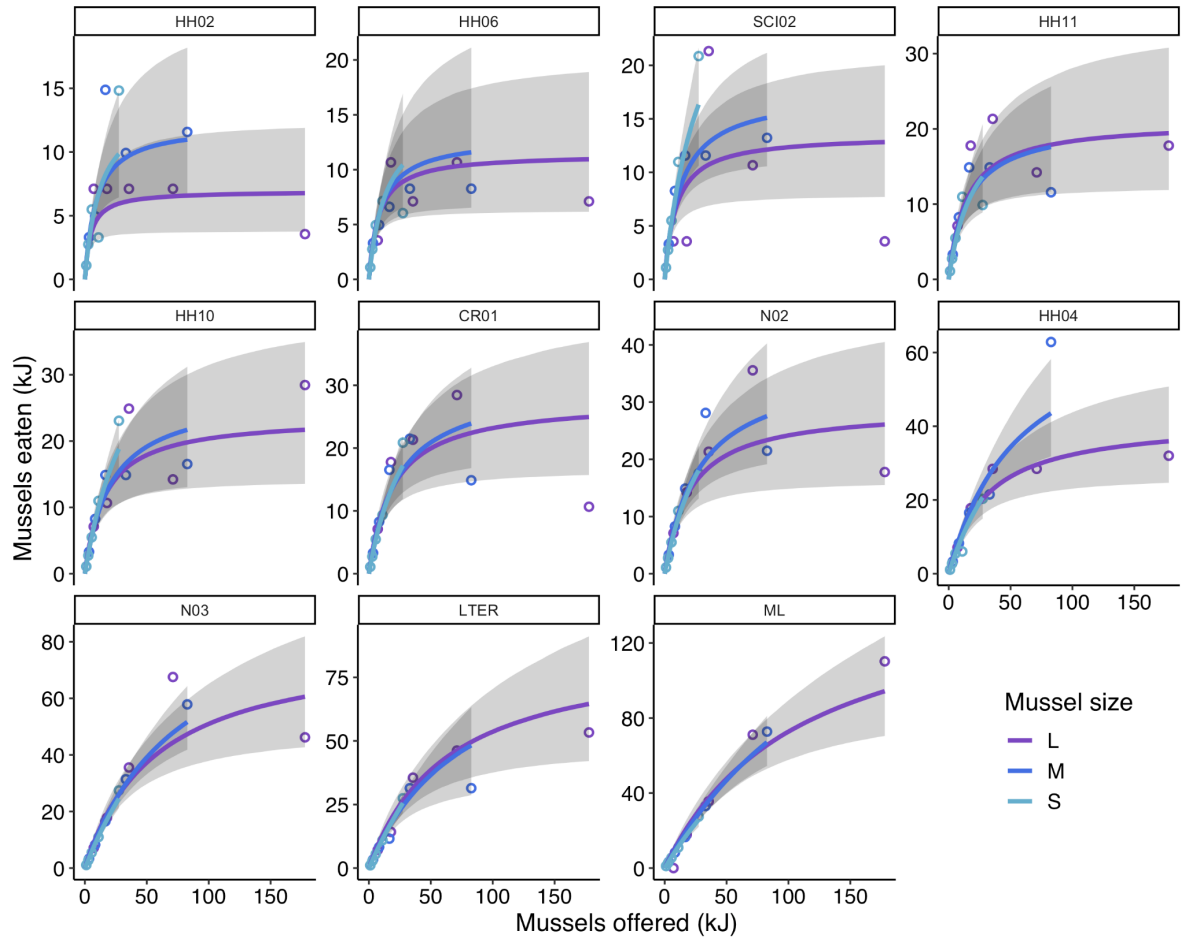


Figure S2.2. Functional response of individual lobsters foraging on mussels of three size classes. Lines and surrounding shading are median \pm 95% CIs of the posterior distributions for the individual level parameters. Units of mussel prey offered (ind.) and consumed (ind.) were converted to units of energy (kJ) based on the conversion described in the main text. Once converted to units of energy, lobsters appeared to consume similar kJ of mussel regardless of mussel size class across the range of kJ of mussels offered in the experimental trials. Panels are arranged in order of increasing lobster size. Note the changes in the y-axis between panels.

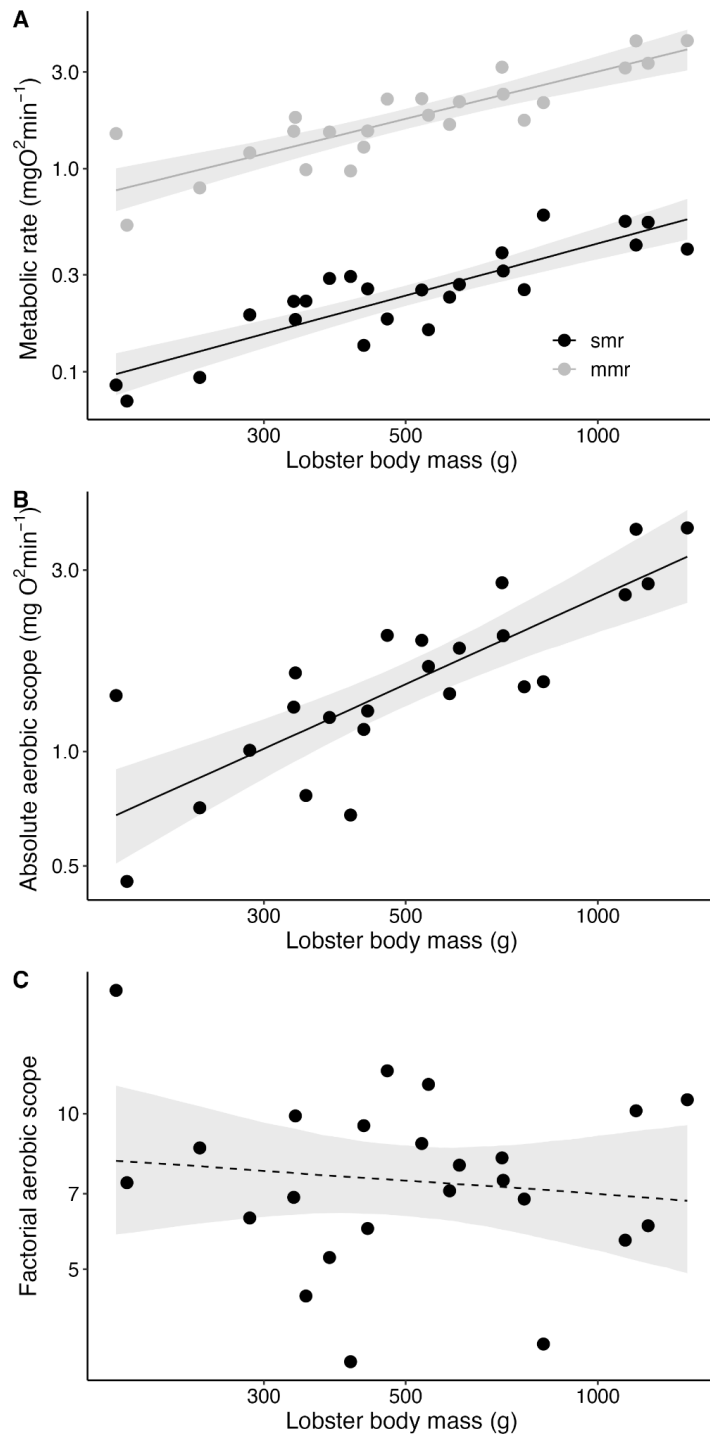


Figure S2.3. Relationship between maximum (MMR) and standard (SMR) metabolic rates (A), absolute aerobic scope (B), and factorial aerobic scope (C) with lobster body size. Points are the observed data in the original units of measurement. Lines and surrounding shading are model predictions (median \pm 95% CI's) from Bayesian regression models. SMR and MMR were modeled simultaneously to test for differences in slopes, while AAS and FAS were modeled as univariate responses.

6.2.3. References

- Brown, J. H., Gillooly, J. F., Allen, A. P., Savage, V. M., & West, G. B. (2004). Toward a metabolic theory of ecology. *Ecology*, *85*(7), 1771–1789. <https://doi.org/10.1890/03-9000>.
- Goodrich, B., J. Gabry, I. Ali, and S. Brilleman. 2023. rstanarm: Bayesian applied regression modeling via Stan.
- Marshall, D. J., and C. R. White. 2019. Have We Outgrown the Existing Models of Growth? *Trends in Ecology & Evolution* *34*:102–111.
- West, G., J. Brown, and B. Enquist. 2001. A general model for ontogenic growth. *Nature* *413*:628–31.

6.3. CHAPTER 3 – APPENDIX

6.3.1. Details of theoretical model

Model structure

To explore the effects of disturbance history on kelp community dynamics we adapted a stage-structured kelp community model developed by Detmer et al. (2021). Specifically, we modeled three stages of kelp (*Macrocystis pyrifera*): gametophytes, juvenile sporophytes, and canopy-forming adult sporophytes. Kelp gametophytes (G) grow from external populations at rate σ_{ext} and from adult kelp at rate σ_A . Recruitment to the juvenile sporophyte stage is dependent on an intrinsic growth rate r_G and the amount of light reaching the benthos ($L_{benthos}$), and experience density dependent mortality at rate m_G :

$$\frac{dG}{dt} = \sigma_{ext} + \sigma_A A - r_G L_{benthos} G - m_G G^2 \quad (1)$$

Juvenile sporophytes (J) arise from the recruitment of gametophytes. For consistency with observational data collected by the Santa Barbara Coastal long-term research program (SBC LTER), we considered juvenile kelp to be < 1 m tall. Juvenile kelp experiences density dependent mortality at rate m_J and mature at rate r_J which depends on light availability.

$$\frac{dJ}{dt} = r_G L_{benthos} G - r_J L_{benthos} J - m_J J^2 \quad (2)$$

Adult kelp (A) grows logistically from the maturation of juveniles and from the growth of existing adults to a carrying capacity K_A . We set $K_A = 1$, so that A represents the proportion of kelp relative to its carrying capacity. Explicitly, we tracked A as changes in the number of adult fronds per unit area. However, frond number is strongly correlated with biomass (Rassweiler et al. 2018) and can be interpreted as a relative metric of kelp biomass

density. Adult frond increased at intrinsic rate (r_A) which was modified by the amount of light reaching the surface. Kelp senesced according to a time dependent function s_A .

$$\frac{dA}{dt} = r_J L_{benthos} J + r_A A L_{surface} \frac{K_A - A}{K_A} - s_A(t) A \quad (3)$$

For full details on the function s_A , refer to Detmer et al. (2021). Briefly, the senescence function allows for disturbance events to synchronize frond initiation following a time lag after which fronds senesce according to a sinusoid function. However, fronds that survive disturbance are assumed to senesce asynchronously at a flat baseline rate.

The mechanism by which kelp influences competitive dynamics on the benthos is by altering the amount of light that reaches the seafloor. We modeled light using an exponential decay function, where light on the seafloor was modified by adult kelp abundance:

$$L_{benthos} = L_{surface} e^{-k_l A} \quad (4)$$

Based on previous work and analysis of seafloor irradiance, we assumed that when adult kelp was at its carrying capacity 10% of light reached the seafloor. Therefore, we set $k_l = 2.3$.

Understory algae (M) and sessile invertebrates (I) competed for space on the seafloor. We assumed that physical space was taken up by sessile invertebrates or understory algae, and we did not explicitly account for space occupied by kelp holdfasts, or other kelp stages. M and I competed according to classic Lotka-Volterra competition equations with competition coefficients α and β :

$$\frac{dM}{dt} = r_M M L_{benthos} \frac{(S_T - M - \alpha I)}{S_T} - m_M M + \sigma_M \quad (5)$$

$$\frac{dI}{dt} = r_I I \frac{(S_T - I - \beta M)}{S_T} - m_I I + \sigma_I \quad (6)$$

where r_M and r_I are intrinsic growth rates, m_M and m_I are senescence rates, S_T is total space on the seafloor (assumed to be equal to 1, such that M and I represent proportional cover), and σ_M and σ_I represent a constant supply of external propagules.

Simulating disturbance

We simulated pulse disturbances by triggering reductions in the state variables. We assumed that disturbances could only happen annually (e.g., 1 per year), and simulated severe disturbances by reducing adult kelp 100% ($\psi_A = 1$). Severe disturbances, like large wave events, may also impact organisms on the seafloor, which we term benthic scouring (ψ_B). However, the extent of damage to the benthos is unclear. Therefore, we ran simulations where we manipulated the level of benthic scouring ($0 > \psi_B > 1$). Benthic scouring occurred at the same time point as the severe disturbance to adult kelp, and affected kelp gametophytes, juvenile kelp sporophytes, understory algae, and sessile invertebrates equally.

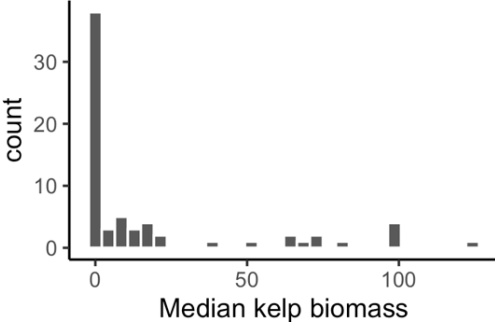
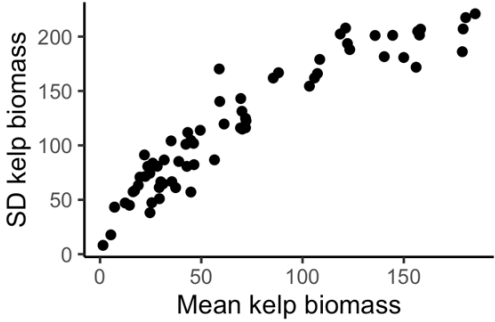
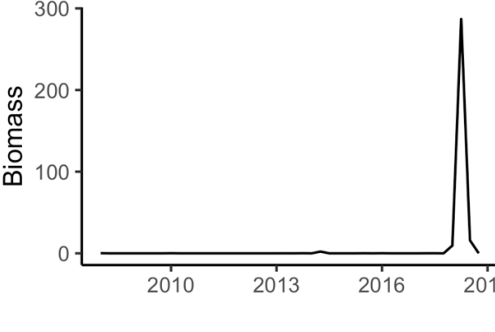
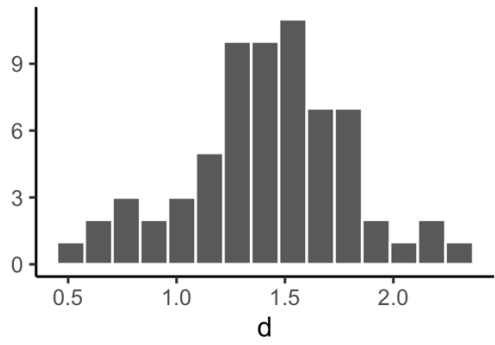
We were interested in understanding how the impacts of historic disturbances to kelp on community structure might be impacted by differences in the life-history parameters of sessile invertebrates relative to understory algae. Therefore, we ran simulations where we:

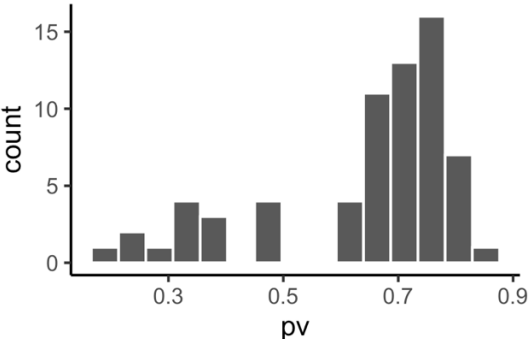
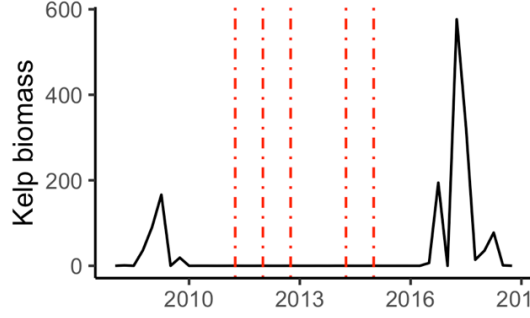
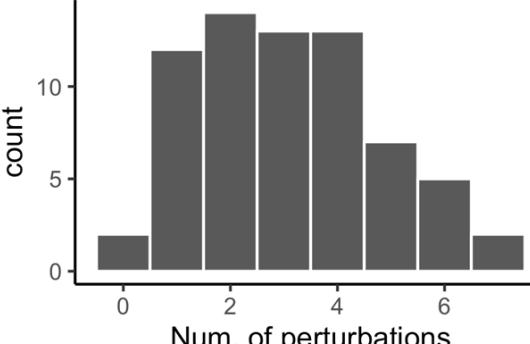
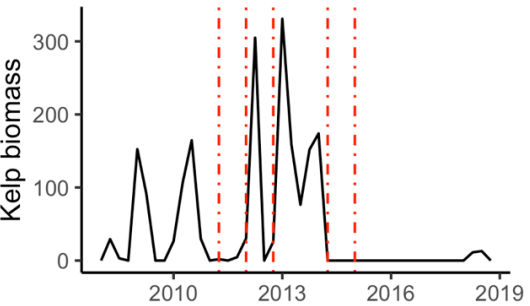
- a) reduced the external supply of sessile invertebrate propagules by 50 and 10% of defaults.
- b) reduced sessile invertebrate growth rates by 75 and 50% of defaults.
- c) Altered parameters to make invertebrates more k-selected ($0.75 * r_I, 0.1 * \sigma_I$) and stronger competitors ($\alpha = 0.125, \beta = 0.8$).

Table S3.1. Summary of state variables, parameters, and simulation values for theoretical model. Notation follows Detmer et al. (2021).

Symbol	Description	Units	Simulation values
Variable			
G	Kelp gametophytes	ind. m ⁻²	
J	Juvenile kelp sporophytes	ind. m ⁻²	
A	Adult kelp sporophytes	ind. m ⁻²	
M	Proportional cover understory macroalgae	--	
I	Proportional cover sessile invertebrates	--	
t	Time	d	
Parameter			
$L_{surface}$	Surface irradiance	mol m ⁻² s ⁻¹	1000
k_I	adult kelp frond extinction coefficient	m ² frond ⁻¹	2.3
σ_{ext}	external supply of kelp gametophytes	ind. m ⁻² d ⁻¹	0.0001
σ_A	rate of gametophyte production by adult kelp	ind. frond ⁻¹ d ⁻¹	0.01
σ_M	external supply of understory algae propagules	d ⁻¹	0.001
σ_I	external supply of sessile invertebrate propagules	d ⁻¹	(0.0005, 0.00025, 0.00005)
r_G	rate of recruitment of kelp gametophytes to juvenile sporophytes	m ² s mol ⁻¹ d ⁻¹	10 ⁻⁸
r_J	rate of maturation of juvenile sporophytes to adult sporophytes	m ² s mol ⁻¹ d ⁻¹	0.00001
r_A	kelp frond growth rate	m ⁴ s mol ⁻¹ d ⁻¹ fronds ⁻¹	0.00009
r_M	understory algae growth rate	m ² s mol ⁻¹ d ⁻¹	0.00006
r_I	sessile invertebrate growth rate	d ⁻¹	(0.008, 0.006, 0.004)
m_G	kelp gametophyte mortality rate	m ² ind. ⁻¹ d ⁻¹	1
m_J	juvenile kelp sporophyte mortality rate	m ² ind. ⁻¹ d ⁻¹	1
m_M	understory algae senescence rate	d ⁻¹	0.009
m_I	sessile invertebrate senescence rate	d ⁻¹	0.002
K_A	carrying capacity of adult kelp	max. proportion of fronds m ⁻²	1
S_T	total substrate space available for sessile invertebrates and understory algae		1
α	competition coefficient for sessile invertebrates on understory algae		(0.8, 1.25)
β	competition coefficient for understory algae on sessile invertebrates		(1.25, 0.8)
ψ_A	proportion of adult kelp removed by disturbance		1
ψ_B	proportion of gametophytes, juvenile kelp, sessile invertebrates, and understory algae removed by disturbance		[0,1]

Table S3.2. Summary of all metrics of historic disturbance explored.

Description	Comments	Example
Mean kelp canopy biomass over the last 10 years	There are many ways in which a time series can vary and still have the same mean.	--
Median kelp canopy biomass over the last 10 years	Because of the zero-inflated nature of the data, the median was often zero, making it not very useful for representing variation across sites.	 <p>A histogram showing the distribution of median kelp biomass. The x-axis is labeled 'Median kelp biomass' and ranges from 0 to 100. The y-axis is labeled 'count' and ranges from 0 to 30. The distribution is highly right-skewed, with a very high count (around 35) at zero biomass, and a few smaller counts at higher biomass values up to 100.</p>
Standard deviation in kelp canopy biomass over the last 10 years	SD scales with the mean making it challenging to compare across sites with very different mean biomass	 <p>A scatter plot showing the relationship between mean kelp biomass (x-axis, 0 to 150) and standard deviation kelp biomass (y-axis, 0 to 200). The data points show a strong positive correlation, indicating that as the mean biomass increases, the standard deviation also tends to increase.</p>
Coefficient of variation (mean/sd)	CV is highly affected by rare events and is dependent on the mean. For example, sites that were consistently zero, but had one large spike in kelp had the highest CV. The timeseries of kelp to the right had the highest CV of all site/transects.	 <p>A line graph showing biomass over time from 2010 to 2019. The y-axis is labeled 'Biomass' and ranges from 0 to 300. The x-axis shows years 2010, 2013, 2016, and 2019. The biomass remains near zero until 2018, where it spikes sharply to approximately 280 in 2019.</p>
Consecutive dissimilarity index	Proposed by Fernandez-Martinez et al. 2018 <i>Ecosphere</i> . Estimates a metric of variability in time series that is not dependent on the mean and insensitive to rare events. Despite its normal distribution across sites/transect, we could find little pattern of the metric with the biomass of either UA or SI.	 <p>A histogram showing the distribution of the consecutive dissimilarity index (d). The x-axis is labeled 'd' and ranges from 0.5 to 2.0. The y-axis is labeled 'count' and ranges from 0 to 9. The distribution is roughly bell-shaped and centered around 1.5, with counts ranging from 1 to 10.</p>

<p>Proportional variability index</p>	<p>Proposed by Heath (2006), pv ranges from 0-1, with zero being low variability and 1 being high variability. The pv is independent of the mean but does not consider the chronological order of the time series.</p>	 <p>A histogram showing the distribution of the proportional variability index (pv). The x-axis is labeled 'pv' and ranges from 0 to 0.9 with major ticks at 0.3, 0.5, 0.7, and 0.9. The y-axis is labeled 'count' and ranges from 0 to 15. The distribution is unimodal and right-skewed, with the highest frequency (count of 16) occurring between 0.7 and 0.8.</p>
<p>Number of times kelp canopy biomass was >0 and then declined to 0 for two quarters.</p>	<p>By not using a threshold value at time t, this metric identified many “extinction” events when in fact kelp was exceptionally low but not zero at time t, and then zero for the next two quarters. See example at right, where extinction events are coded in red.</p>	 <p>A line graph showing kelp biomass from 2010 to 2019. The y-axis is labeled 'Kelp biomass' and ranges from 0 to 600. The x-axis shows years from 2010 to 2019. The biomass fluctuates, with a major peak near 600 in 2017. Four vertical red dashed lines indicate extinction events, occurring around 2011, 2012, 2014, and 2015.</p>
<p>Number of times kelp was greater than or equal to 10% of its 10-year maximum, then declined by >80% for two quarters.</p>	<p>At no site/transect was kelp always zero. By estimating the threshold at 10% of the max, the threshold was always greater than zero. While 10% of the max may seem low, the distribution of kelp biomass was log-normally distributed, with rare high biomass events. We used a decline of 80% to ensure there was enough variability among sites, as increasing this value above 95% resulted in few events that typically occurred across most sites at the same time.</p>	 <p>A histogram showing the number of perturbations. The x-axis is labeled 'Num. of perturbations' and ranges from 0 to 6 with major ticks at 0, 2, 4, and 6. The y-axis is labeled 'count' and ranges from 0 to 10. The distribution is roughly bell-shaped, peaking at 2 perturbations with a count of approximately 13.</p>
<p>Amount of time (in years) since the last kelp canopy extinction, where an extinction is identified as described in the metric “extinction”.</p>	<p>This metric identified the time since the last canopy extinction event, rather than the time since the last period when kelp was zero. This resulted in long times since last extinction even when kelp had been zero for many consecutive quarters (see example at right w/ extinction events coded in red).</p>	 <p>A line graph showing kelp biomass from 2010 to 2019. The y-axis is labeled 'Kelp biomass' and ranges from 0 to 300. The x-axis shows years from 2010 to 2019. The biomass shows several peaks, with the highest near 300 in 2012. Four vertical red dashed lines indicate extinction events, occurring around 2011, 2012, 2014, and 2015.</p>

<p>Amount of time (in years) since the last 6-month period kelp canopy biomass was zero for a 6-month period, regardless of whether kelp was zero or greater than zero in the previous quarter.</p>	<p>Our hypothesis was focused on the fact that when kelp biomass was zero, then understory algae should be able to outcompete sessile invertebrates and take space on the benthos. Thus, the time since the last period when kelp was zero for 6 or more months seemed like the most biologically relevant metric.</p>	<table border="1"> <caption>Data for Time since last absent histogram</caption> <thead> <tr> <th>Time since last absent</th> <th>count</th> </tr> </thead> <tbody> <tr><td>0.0</td><td>20</td></tr> <tr><td>0.5</td><td>15</td></tr> <tr><td>1.0</td><td>10</td></tr> <tr><td>1.5</td><td>14</td></tr> <tr><td>2.0</td><td>2</td></tr> <tr><td>2.5</td><td>3</td></tr> <tr><td>3.0</td><td>0</td></tr> <tr><td>3.5</td><td>0</td></tr> <tr><td>4.0</td><td>0</td></tr> <tr><td>4.5</td><td>0</td></tr> <tr><td>5.0</td><td>1</td></tr> <tr><td>5.5</td><td>0</td></tr> <tr><td>6.0</td><td>0</td></tr> <tr><td>6.5</td><td>0</td></tr> <tr><td>7.0</td><td>0</td></tr> <tr><td>7.5</td><td>0</td></tr> <tr><td>8.0</td><td>0</td></tr> <tr><td>8.5</td><td>1</td></tr> <tr><td>9.0</td><td>0</td></tr> <tr><td>9.5</td><td>2</td></tr> </tbody> </table>	Time since last absent	count	0.0	20	0.5	15	1.0	10	1.5	14	2.0	2	2.5	3	3.0	0	3.5	0	4.0	0	4.5	0	5.0	1	5.5	0	6.0	0	6.5	0	7.0	0	7.5	0	8.0	0	8.5	1	9.0	0	9.5	2
Time since last absent	count																																											
0.0	20																																											
0.5	15																																											
1.0	10																																											
1.5	14																																											
2.0	2																																											
2.5	3																																											
3.0	0																																											
3.5	0																																											
4.0	0																																											
4.5	0																																											
5.0	1																																											
5.5	0																																											
6.0	0																																											
6.5	0																																											
7.0	0																																											
7.5	0																																											
8.0	0																																											
8.5	1																																											
9.0	0																																											
9.5	2																																											
<p>Proportion of time in the last 10 years that kelp canopy biomass was zero.</p>	<p>See hypothesis in “time since last absent”.</p>	<table border="1"> <caption>Data for Proportion of time kelp absent histogram</caption> <thead> <tr> <th>Proportion of time kelp absent</th> <th>count</th> </tr> </thead> <tbody> <tr><td>0.0</td><td>4</td></tr> <tr><td>0.1</td><td>8</td></tr> <tr><td>0.2</td><td>7</td></tr> <tr><td>0.3</td><td>10</td></tr> <tr><td>0.4</td><td>6</td></tr> <tr><td>0.5</td><td>10</td></tr> <tr><td>0.6</td><td>6</td></tr> <tr><td>0.7</td><td>8</td></tr> <tr><td>0.8</td><td>6</td></tr> <tr><td>0.9</td><td>2</td></tr> </tbody> </table>	Proportion of time kelp absent	count	0.0	4	0.1	8	0.2	7	0.3	10	0.4	6	0.5	10	0.6	6	0.7	8	0.8	6	0.9	2																				
Proportion of time kelp absent	count																																											
0.0	4																																											
0.1	8																																											
0.2	7																																											
0.3	10																																											
0.4	6																																											
0.5	10																																											
0.6	6																																											
0.7	8																																											
0.8	6																																											
0.9	2																																											
<p>Proportion of time in the last 10 years that kelp canopy biomass was greater or equal to 50% of its maximum.</p>	<p>It was challenging to understand where to set this threshold. At 50% of the maximum, there was little variation across sites because kelp biomass was rarely above 50% of its maximum.</p>	<table border="1"> <caption>Data for Proportion of time kelp >50% of max histogram</caption> <thead> <tr> <th>Proportion of time kelp >50% of max</th> <th>count</th> </tr> </thead> <tbody> <tr><td>0.0</td><td>11</td></tr> <tr><td>0.02</td><td>4</td></tr> <tr><td>0.04</td><td>7</td></tr> <tr><td>0.06</td><td>0</td></tr> <tr><td>0.08</td><td>6</td></tr> <tr><td>0.10</td><td>3</td></tr> <tr><td>0.12</td><td>0</td></tr> <tr><td>0.14</td><td>1</td></tr> <tr><td>0.16</td><td>3</td></tr> </tbody> </table>	Proportion of time kelp >50% of max	count	0.0	11	0.02	4	0.04	7	0.06	0	0.08	6	0.10	3	0.12	0	0.14	1	0.16	3																						
Proportion of time kelp >50% of max	count																																											
0.0	11																																											
0.02	4																																											
0.04	7																																											
0.06	0																																											
0.08	6																																											
0.10	3																																											
0.12	0																																											
0.14	1																																											
0.16	3																																											

6.3.2. Supplemental figures

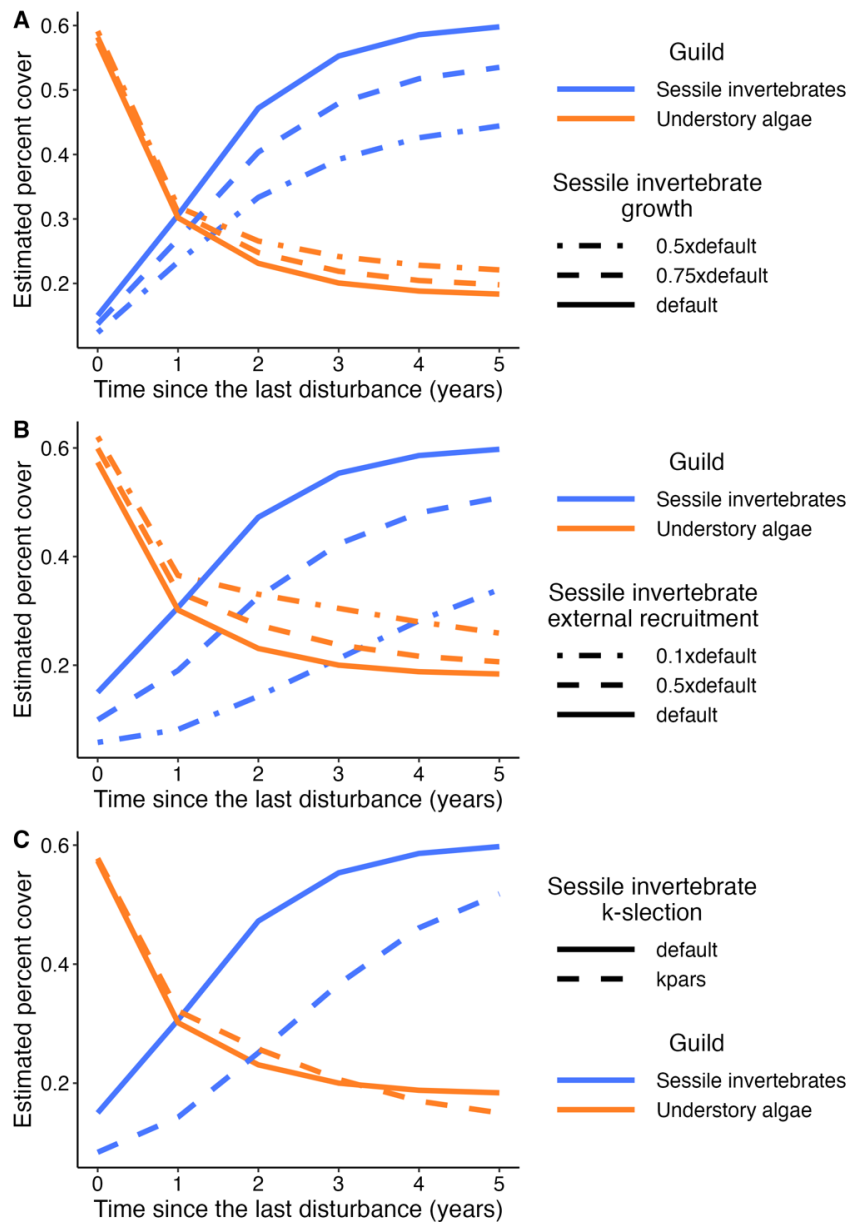


Figure S3.1. Effects of changing life-history parameters of sessile invertebrates relative to understory algae on community structure recovery following a single disturbance. Decreasing the growth rate (A) or external recruitment rate (B) of sessile invertebrates slowed the recovery time on the community relative to default parameters. Similarly, making sessile invertebrates more k-selected [slower growth ($0.75 * r_I$), lower external recruitment ($0.1 * \sigma_I$), but higher competitive ability ($\alpha = 0.125, \beta = 0.8$)] altered equilibrium abundances and slowed the recovery of the community following a disturbance. In all simulations, we assumed that 90% of the benthos was removed with each disturbance ($\psi_B = 0.9$).